Investigations on optimal planning of Distributed Generators in distribution system considering uncertainties using multi-objective optimization approaches

Submitted in partial fulfillment of the requirements

for the award of the degree of

DOCTOR OF PHILOSOPHY

in

Electrical Engineering

By

Thunuguntla Vinod Kumar

Roll No: 718127

Supervisor:

Dr. Injeti Satish Kumar

Assistant Professor

Department of Electrical Engineering

NATIONAL INSTITUTE OF TECHNOLOGY WARANGAL

HANUMAKONDA-506004, TELANGANA STATE, INDIA

April - 2023

Approval

This Thesis work entitled **"Investigations on optimal planning of Distributed Generators in distribution system considering uncertainties using multi-objective optimization approaches"** by **Thunuguntla Vinod Kumar**, bearing **Roll No: 718127**, is approved for the degree of **Doctor of Philosophy** in **Electrical Engineering** from **National Institute of Technology, Warangal**.

Examiners

_____

_____

_____

Supervisor

_____

Dr. Injeti Satish Kumar

Assistant Professor

Department of Electrical Engineering

NIT Warangal

Chairman

_____

Dr. Narasimharaju B. L

Professor

Department of Electrical Engineering

NIT Warangal

Date: _____

Place: NIT Warangal

DEPARTMENT OF ELECTRICAL ENGINEERING

NATIONAL INSTITUTE OF TECHNOLOGY WARANGAL

HANUMAKONDA-506 004, TELANGANA, INDIA

CERTIFICATE

This is to certify that the thesis entitled "**Investigations on optimal planning of Distributed Generators in distribution system considering uncertainties using multi-objective optimization approaches"** which is being submitted by **Thunuguntla Vinod Kumar**, bearing **Roll No.718127**, is a bonafide work submitted to **National Institute of Technology, Warangal** in partial fulfillment of the requirements for the award of the degree of **Doctor of Philosophy** in **Department of Electrical Engineering**. To the best of my knowledge, the work incorporated in this thesis has not been submitted elsewhere for the award of any degree.

Dr. Injeti satish kumar

(Supervisor)

Assistant Professor
Department of Electrical Engineering

NIT Warangal

Date:

Place: NIT Warangal

DECLARATION

This is to certify that the work presented in the thesis entitled "**Investigations on optimal planning of Distributed Generators in distribution system considering uncertainties using multi-objective optimization approaches**" is a bonafide work done by me under the supervision of **Dr. Injeti Satish Kumar,** Department of Electrical Engineering, National Institute of Technology,Warangal, India and is not submitted elsewhere for the award of any degree.

I declare that this written submission represents my ideas in my own words and where others' ideas or words have been included, I have adequately cited and referenced the original sources. I also declare that I have adhered to all principles of academic honesty and integrity and have not misrepresented or fabricated or falsified any idea/data/fact/source in my submission. I understand that any violation of the above will be cause for disciplinary action by the Institute and can also evoke penal action from the sources which have thus not been properly cited or from whom proper permission has not been taken when needed.

Thunuguntla Vinod Kumar
(Roll No.718127)

Date:_____

NIT Warangal

ACKNOWLEDGMENTS

I would like to express my gratitude to my supervisor, **Asst Prof. Injeti Satish Kumar**, for providing enough freedom and generating homely feeling throughout the journey, for his patience and valuable suggestions. It is impossible to accomplish this dissertation work without his support, encouragement. Many thanks for his support and encouragement to achieve all my personal life ambitions too. Apart from all these it's an honor for me to associate with a good human being like him.

I would like to thank **Prof. B. L. Narasimharaju,** Head, Department of Electrical Engineering for providing all the required facilities and support.

I wish to express my sincere thanks to **Prof. N. V. Ramana Rao, Director**, NIT Warangal for his official support and encouragement.

I take the privilege to thank all my Doctoral Scrutiny Committee members, **Prof. B. L. Narasimharaju**, Department of Electrical Engineering, **Prof. D.M.Vinod Kumar** (H.A.G), Department of Electrical Engineering, **Dr. B. Nagu**, Associate Professor, Department of Electrical Engineering and **Dr. K. Naga Srinivasarao Batta**, Assistant Professor, Department of Electronics and Communication Engineering for their detailed review, constructive suggestions and excellent advice during the progress of this research work.

I also express my sincere thanks to **Prof. M. Sailaja Kumari** and **Prof. S. Srinivasa Rao**, former heads, Department of Electrical Engineering for their valuable suggestions, support and cooperation.

I also grateful to **Dr. M. Vijaya Kumar**, Assistant professor, former DSC member, Department of Mechanical Engineering for his valuable suggestions, support and cooperation.

I also appreciate the encouragement from teaching, non-teaching members and fraternity of Department of Electrical Engineering, NIT Warangal. They have always been motivating and supportive.

I would like to express my gratitude to my parents **Thunuguntla Anjaneyulu** and **Thunuguntla Giri Raja Kumari**, for introducing engineering life and guiding me by their unconditional support, patience and encouragement throughout my journey, which helped me in completion of this dissertation work.

My sincere thanks to my co-scholars **V S Sandeep Kumar Reddy** and **A Ravi Kumar** for their unconditional support throughout my research period and all co-scholars for their support and valuable suggestions.

Finally, I would like to express my gratitude to National Institute of Technology Warangal for providing me with the opportunity to carry out research and I am indebted to the people of the country for indirectly supporting my work.

(Thunuguntla Vinod Kumar)

ABSTRACT

Centralized generation, which uses traditional generators, is the primary way of electric energy is made available to consumers. But there are a number of obstacles associated with centralized generation, including depletion of fossil fuels, greenhouse gas emissions, rapidly rising load needs, operational constraints, difficulties in expanding the current infrastructure, and high distribution and transmission losses due to long-distance transmission. Distributed generation (DG), a small-scale electric power generation becoming very famous these days due to rapid advancements in their technologies and advantages like quick response time and the ability to connect nearby load centers. Due to an increase in load demand brought by both conventional & plug-in electric vehicle's loads as well as by radial topological structure, distribution networks, the last link in the electric supply chain, are experiencing technical problems like poor efficiency, voltage instability, low reliability, and capacity improvement concerns. Therefore, so much research is going on the efficient making of the existing distribution system by optimal planning of various DG technologies, which provides a solution to the obstacles associated with the centralized generation and rapidly increasing load demand.

This dissertation presents a meta-heuristic-based butterfly optimization algorithm for enhancing distribution network efficiency and loadability using a Ɛ-constraint based multi-objective approach. Enhancement in the network's efficiency is associated with active power loss reduction. In addition, the increase in future load demand can be effectively met by improving the system's loadability which inturn improves the voltage stability margin and loading marginal factor. Therefore, the objective is to find out the injection of how much active power and reactive power by the DGs into the system at optimal locations satisfying operational constraints for the enhancement of the above metrics to the maximum extent.

Further, this dissertation presents optimal planning of non-dispatchable photo-voltaic (PV) & wind-turbine (WT) units, dispatchable PV-BESS & WT-BIOMASS units in the distribution system for the mitigation of the system's energy loss, total voltage deviation and annual economic cost using Pareto-based multi-objective chaotic velocity-based butterfly optimization algorithm (MOCVBOA). The above planning studies consider uncertainties in solar radiance, wind speed and electric load demand. Since PV & WT units are non-dispatchable in nature, the PV unit is assisted

by the BESS unit & WT unit is assisted by the BIOMASS unit to make them dispatchable. Detailed analysis of the outcomes between the optimal planning of non-dispatchable and dispatchable DGs is discussed.

Next, optimal planning of DGs in the presence of plug-in electric vehicles load demand charging under private charging scenario for the improvement of the system's energy loss reduction and total voltage deviation using Pareto-based MOCVBOA is presented. Pareto MOCVBOA generates the final optimal Pareto front, and the most compromised solution is selected using the TOPSIS method. As load due to charging of PHEVs deteriorates the distribution system performance, optimal planning of DGs provides a relief measure due to the above problem.

Finally, optimal planning of PV & PV-BESS units in the distribution system considering both conventional and plug-in electric vehicle loads for improving the system's energy loss reduction and total voltage deviation using MOCVBOA is presented. In this work, the charging of plug-in electric vehicles charging under two charging scenarios: private charging scenario and public charging scenario is considered. The PHEVs electric demand is derived from the probabilistic methods developed in the literature and imposed on the respective distribution system buses. Detailed analysis of the impact of PHEVs load on the distribution system metrics is analyzed, and the optimal planning of PV & PV-BESS units as a solution to the former discussed problem is addressed.

Contents

List of Figures

List of Tables

List of Abbreviations

ABC	Artificial bee colony
AEC	Annual Economic Cost
AI	Annual installation cost
BA	Bat algorithm
BD	Bender's decomposition
BE	Branch Exchange
BESS	Battery energy storage system
BHOA	Black Hole optimization algorithm
BO	Butterfly optimization
CAES	Compressed air energy storage
CRF	Capital recovery factor
CSA	Cuckoo search algorithm
CVBOA	Chaotic butterfly optimization algorithm
DABC	Discrete artificial bee colony
DDG	Dispatchable distributed generation
DE	Differential evolution
DG	Distributed generation
DTATCOM	Distributed static compensator
EENS	Electrical energy not supplied
GA	Genetic algorithm
GSA	Gravitational search algorithm
GWO	Greywolf optimization
HSA	Harmony search optimization algorithm
MINLP	Mixed-integer non-linear problem
MOBOA	Multi-objective butterfly optimization algorithm
MOCVBOA	Multi-objective chaotic velocity-based butterfly optimization algorithm
MT	Micro-Turbine

NIS	Negative ideal solution
NSGA	Non-dominant sorting genetic algorithm
ODNR	Optimal distributed network reconfiguration
OMC	Operation and maintenance cost
OPCS	Off-peak charging scenario
OPDG	Optimal planning of distributed generators
PCS	Peak charging scenario
PDF	probability density function
PFCS	Public Fast Charging Station
PHEV	Plug-in hybrid electric vehicles
PIS	Positive ideal solution
PSO	Particle swarm optimization
PV	Photo-Voltaic
SCS	Stochastic charging scenario
SoC	State of charge
TOPSIS	Technique for order preference by similarity to ideal solution
TVD	Total Voltage Deviation
WT	Wind-Turbine

List of symbols

$\boldsymbol{P_{loss}}$	Active power loss
$\boldsymbol{\lambda_{max}}$	Maximum loadability
$\boldsymbol{\lambda_V}$	Loading marginal factor
$\boldsymbol{J_i}$	Current through the i^{th} branch
$\boldsymbol{R_i}$	Resistance of the i^{th} branch
$\boldsymbol{P_{DG,k}}$	Active power generated by k^{th} DG
$\boldsymbol{pf_k}$	Power factor of k^{th} DG
$\boldsymbol{\lvert V_j \rvert}$	Voltage magnitude of j^{th} bus
nbr	Number of branches
nb	Number of buses
ndg	Number of DGs
$\boldsymbol{P_{sub}}$ & $\boldsymbol{Q_{sub}}$	Active and reactive power generated by substation
I	stimulus intensity
c	Sensor modality
f	Fragrance
p	Probability switch
$\boldsymbol{f_b(s^t)}$	Probability of solar radiance at particular time interval (s^t)
$(\boldsymbol{\alpha^t}), (\boldsymbol{\beta^t})$	Shape parameters of Beta PDF
Γ	Gamma function
$\boldsymbol{f_v(v^t)}$	Probability of wind speed at particular time interval (v^t)
$(\mathbf{k}^t), (\mathbf{c}^t)$	Shape parameters of the Weibull PDF
$\boldsymbol{P_{PV}^t}$	PV unit hourly average output power during the time interval 't'
$\boldsymbol{P_{PV_0}(s_{avg}^g)}$	PV unit output power with average solar radiation in the g^{th} state
$\boldsymbol{N_{PV\,mod}}$	Number of PV modules
FF	Fill factor
$\boldsymbol{I_{MPP}, V_{MPP}}$	PV unit current and voltage at the maximum power point

I_{SC}, V_{OC}	PV unit short circuit current (A) and open-circuit voltage (V)
k_i, k_V	current and voltage coefficients in V/^{o}C, A/^{o}C
P_{WT}^t	WT unit hourly average output power
$P_{WT_0}(v_{avg}^g)$	WT unit output power with average wind speed in the gth state
v_r, v_{cin}, v_{cout}	rated speed, cut-in speed & cut-out speed of WT units respectively
$P_{r,WT}$	Rated speed of WT unit
$E_{BES}(t)$	Energy in the battery in kWh during tth time interval
$P_{BES}^{disch}, P_{BES}^{cb}$	BESS discharging power & charging power
E_{loss}	Energy loss
k_e	Electricity price
$E_{PV+BESS}$	Energy delivered by the PV-BESS unit to the distribution system
E_{PV}^{Grid}	Energy delivered by the PV unit to the distribution system
E_{BESS}^{Disch}	Energy delivered by the BESS unit to the distribution system
$P_{t,(PV+BES)}$	Power delivered by the PV-BESS unit to grid in tth hour
η_{BES}	BESS round trip efficiency
$P_{PV,Max}$	Maximum power output from PV unit
P_{PV}	Final PV unit size
$P_{WT,max}$	Maximum power output from WT unit
P_{WT}	Final WT unit size
$f_n^t(T_a)$	Probability of the arrival of nth PHEV at time 't'
$f_n(d_n)$	Probability of the distance travelled by nth PHEV
AER	All electric range of vehicle
C_{Batt}	Capacity of battery in PHEV
η_{Batt}	Efficiency of the battery in PHEV
$NPHEV(j)$	Total number of vehicles charging through station j
$NC(j)$	Number of connectors in jth PFCS
$CPFCS(j)$	Capacity of jth PFCS

Chapter 1

Introduction

The centralized generation using traditional generators like thermal, hydro & nuclear, is the primary way electricity gets to people's homes. Then, the electricity is sent through a transmission & distribution system to distribution substations, where the voltage is stepped down before it is sent to homes and businesses. But there are problems with centralized generation, such as transmission and distribution losses, the depletion of fossil fuels, the increase in load demand, difficulties in expanding the current infrastructure, the high cost of fossil fuels, and the greenhouse effect.

Distributed generation (DG) is the small-scale generation that usually ranges from a few kW to several MW, typically connected at the customer site or distribution and sub-transmission substations [1]. DG technology can be divided into three categories: non-renewable technologies (traditional), renewable technologies (green or sustainable) and storage technologies [2]. Renewable energy sources include wind, solar (PV and thermal), biomass, geothermal, tidal, and hydropower (small and micro). Micro-turbine, reciprocating engines, gas turbines, and combustion engines are examples of technologies that come under the non-renewable category. Battery energy storage systems, flywheels, supercapacitors, compressed air energy storage (CAES), and pumped storage come under the storage technologies category. Based on their ability to support active and reactive power, DG technologies are divided into four groups [3]. Type-1 DGs support only active power (e.g., Fuel cells & micro-turbines), Type-2 DGs support only reactive power (e.g., Synchronous Compensators), Type-3 DGs support both real & reactive power (e.g., photo-voltaic (PV) systems with voltage source inverters, wind turbines (WT) with doubly fed induction generators, and biomass generators based on synchronous generators) and Type-4 DGs support both active & reactive power but consume reactive power (e.g., wind turbines with induction generators). Based on the sizes of DGs, DG technologies are divided into four groups [3]: micro-DGs (1W – 5 kW), small-DGs (5 kW – 5 MW), medium-DGs (5 MW – 50 MW) & large-DGs (50 MW – 500 MW).

In recent days, distributed generation technologies are becoming increasingly popular as a solution to the problems caused by the depletion of fossil fuels, the increase in electric load demand and the pollution of the environment due to the generation of electric energy

from conventional energy sources. Furthermore, because of their small physical size and ability to be deployed at nearby load centres, the advantages [4] like technological advancements, reductions in installation costs, quick response time, no requirement for government approval for installing DGs, no need to consider the availability of land and the ability to track the changes in loads more closely have triggered the deployment of these technologies in the electricity market by offering a different way to fulfil customer load demand. The application of DG technologies includes as a backup source to provide the required electricity for delicate loads (like hospitals) during grid interruptions, as a standby source in remote locations like isolated and rural areas, to provide electricity for peak loads at peak hours to lower the cost of electricity, to strengthen the grid or power system network in the form of enhancing voltage profile, power quality and efficiency by supplying a portion of the load. As the electrical distribution system is the final stage of the power system, it is the system which is nearer to nearby load centres. Because of the distribution system's radial topological structure, losses in a distribution network [5] account for 70% of all losses in a power system network.

In contrast, losses on transmission & sub-transmission lines made for 30% of the total power losses. Additionally, demand for future load enhancement initially impacts the distribution system. Therefore, much research is going on deploying DGs in the distribution system to improve its efficiency by mitigating network power losses and as a solution for future load demand enhancement. Deploying DG units in the distribution network decreases network losses and raises voltage profiles, strengthens voltage stability, delays network upgrades, and saves money for utilities. However, the output power from some DG technologies like PV & WT units is highly uncertain due to the probabilistic nature of wind speed & solar radiance. Identifying the suitable places and sizes of DG units in the distribution network by considering the uncertainty in their power output determines how well the technical metrics improve. The problem mentioned above is called optimal planning of DGs (OPDGs) in the distribution system. Therefore, the general framework for describing and resolving the issue as discussed above must consider the following factors: the significance and context of the problem; the modelling of DGs output power uncertainties, the modelling of load uncertainties; the choice of objective functions, and the approach for solving the optimization problem.

The shift toward zero-emission plug-in hybrid electric vehicles (PHEVs), which are anticipated to play a significant role in the road transportation system [6], has been prompted

by growing concerns over the depletion of fossil fuels, CO2 emissions and the greenhouse impact. However, the objectives achieved due to the successful transition to plug-in electric vehicles can only be accomplished when non-conventional energy sources like DG technologies provide the required electric power for charging electric vehicles. The PHEVs charge their batteries under two charging scenarios: charging PHEVs at residential homes (private charging) and at public fast charging stations (public charging). Numerous power systems issues, such as economic dispatch, optimal power flow, and OPDG problems in radial distribution systems and microgrids, have been studied extensively in the literature by taking electric vehicle load demand on the system. The authors solved the dynamic economic dispatch issue in [7], [8] by incorporating PHEV load demand into the 24-hour load pattern. Authors in [9] tackled the optimal flow problem by considering the PV, WT and PHEV uncertainties. Due to the proximity of the distribution system to the load centres, it was the first power system to be affected by the demand due to electric vehicle load. Technical metrics of the distribution system, like real power loss and voltage profile, will worsen due to the system's extra electric power demand due to PHEVs. Therefore, several researchers addressed the optimal planning of DGs in the distribution system by considering electric vehicle load demand.

This thesis focuses on the effective planning of various DG technologies in the distribution system to improve its performance. Four kinds of investigations – optimal planning of DGs in the optimal reconfigured distribution system for improvement of its efficiency and loadability - optimal planning of PV, WT, PV-BESS, WT-BIOMASS units in the distribution system for improvement of its efficiency and voltage profile – optimal planning of DGs in distribution system considering the load of PHEVs charging under private charging scenario – optimal planning of PV & PV-BESS units in distribution system considering the load of PHEVs charging under both private and public charging scenarios.

1.1 Investigations on Optimal Planning of Distributed Generators in the Distributed system

As mentioned in the introduction part, the optimal planning of DGs in the distribution system improves several technical metrics, such as the reduction of power loss, the improvement of the voltage profile, the improvement of the system's reliability and security, and the improvement of the system's ability to handle the load and maintain the voltage stability. Additionally, adequate DG planning in the distribution system will have a few

economic and environmental benefits [4]. Economic benefits include reducing operational & maintenance costs, deferrals of infrastructure investments, reduction in fuel costs due to renewable DG technologies, and installation & maintenance costs. Benefits to the environment include decreased health expenses and greenhouse gas emissions. To enhance the technical, economic and environmental metrics indicated above, various researchers have addressed the OPDG problem in distribution systems in many ways. Researchers have tackled the subject of optimal DG planning in the literature by considering different load uncertainties: the system's peak load level, the system's multi-load level, and the system's daily load profile. Researchers addressed several analytical, numerical and meta-heuristic-based optimization algorithms for the OPDG problem in the distribution system. In [10], the authors discussed a detailed review of various analytical techniques for OPDG technologies problems in the distribution system. Analytical methodologies need an explicit model and can produce precise results within a short computational time; however, many simplifications and differentiations of complex equations are required. In [11]–[17], authors addressed the OPDG problem using various analytical methods based on exact loss formulae for distribution system power loss minimization, voltage profile improvement and reliability enhancement. The exact loss formula [10] establishes the overall system real power losses of as a mathematical function of active & reactive power demands at all buses. To lower the distribution network's power losses, the mathematical equation that represents most advantageous DG capacity at a bus is obtained by mathematical simplifications and operations on the exact loss formulae. The detailed step-by-step procedure for finding the optimal DG locations and DG sizes by using the analytical method based on exact loss formulae is found in [3].

In [11], the researchers suggested an analytical method based on an exact loss formula to assess the optimum DG location and size to minimize distribution network reactive & active power losses. The suggested method was efficient in terms of computing because it only needed to repeat the power flow twice. However, this method only applies to the optimal planning of a single DG unit. Due to the bus impedance matrix calculation required by this technique, this technique is computationally inefficient for distribution networks with a greater number of buses. The optimal planning of WT was done by the authors in [12] to reduce active power losses in distribution networks. The wind turbine type based on an induction generator that inject real power and consume reactive power was considered. The bus connected to the WT was first treated as a load bus, and the WT output was represented as mathematical equation. Then, the exact loss formula was employed for finding network power losses. In

[13], an analytical technique developed in [11] is improved that was confined to DG units with real power support and created analytical expressions for optimal DG planning of multiple types of DGs for power loss minimization. The subsequent work in [14] enhanced the analytical method in [13], which determined the various DG unit types for reducing power losses in distribution networks. In both studies [13], [14], the significance of DG operation was examined in terms of real & reactive power injection, and the optimal DG power factor was determined to reduce power losses. The findings revealed that when compared to DG units with real power generation, DG units with both real & reactive power generation dramatically mitigates power losses.

The authors of [15] used an analytical technique to identify the best sizes, positions, and power factors of DG units to lessen power losses while considering the load demand and renewable DGs uncertainties. The results of the above study revealed that dispatchable DG units minimise power losses to significant percentage compared to non-dispatchable DG units. The researchers of [16] proposed an analytical method based on a multi-objective index for the determination of the optimum capacity PV-DG units. A weighted multi-objective function is mathematically formulated, which addresses the minimization of active and reactive power losses and voltage deviation. In [17], the authors combined a PV unit with BESS unit to make PV unit as dispatchable DG and formulated a multi-objective function for reducing power losses and improving voltage profile and developed analytical expressions based on exact loss formulae for the determination of the optimal capacity and power factor of such PV-BESS unit. However, in [16], [17], since optimal sizes of PV & PV-BESS units are determined based on the average load demand, the power loss might not be minimized to the optimal value. From the above discussions, it is observed that analytical methods that rely on the exact loss formula need to calculate bus impedance or Jacobian matrices, results in high computing complexity in the case of distribution networks with greater number of buses.

The OPDG problem was addressed in [18]–[21] using loss sensitivity factor based analytical techniques for minimising distribution system power loss. The loss sensitivity factor based analytical methods decrease the number of viable solutions by limiting the solution search space to a few top-ranked buses. In these methods, at first, a initial load flow is performed without DGs on the system and then mathematically developed analytical expressions are used to determine the sensitivity factors at each bus; then, the buses are prioritised according to their sensitivity factors to create a priority list; Then, by gently increasing the DG capacity at the top priority bus until minimal system losses have been

attained— a process that is done for each priority bus —it is possible to determine the optimum DG size at that bus. Ultimately, the bus with the lowest power losses is selected as the best possible DG location. In [18], the authors presented a combined power loss sensitivity technique to identify the best positions and sizes for DG units operating at unity and fixed power factor. The outcomes showed that DG units running at the 0.9 fixed power factor significantly reduced active and reactive power losses and voltage deviation. In [19], the authors used a combination of the quadratic curve fitting technique and sensitivity analysis to determine the best location and capacity for a DG unit running at a fixed power factor and single capacitor. They subsequently expanded this method to integrate multiple DGs and capacitors, resulting in a more significant loss reduction and improved voltage stability compared to a single DG-capacitor combination. To determine the optimal locations, sizes, and power factors of DG units, the authors of [22] carried out a sensitivity study using an entirely novel formulation of the power flow solution. From the results, it was observed that the power losses could be reduced to the lowest value if the DGs are operating at the optimal power factor. To figure out the optimum capacity of various renewable DG types, a hybrid technique built on sensitivity analysis and continuous power flow was established by the authors in [21]. The suggested technique resulted in significant enhancements in loss reduction and voltage stability. However, as already discussed, analytical methods developed based on loss sensitivity factors requires numerous iterations of power flow calculation, which could lead to computational inefficiencies in the case of large-scale distribution networks.

In [23]–[25], researchers addressed the optimal planning of DGs in distribution systems using analytical methods based on branch current loss formulae and branch power flow formulae. The authors of [23] presented an analytical method based on the branch's current formulae for the allocation of DG units with the objective of minimising network power loss. The authors of [24] evaluated planning of renewable DGs while considering the fluctuations associated with load demand and DGs. To reduce yearly electric energy losses, they determined the optimal locations, sizes and power factors of DGs. With the aim of minimising power losses, the authors of [25] presented an equivalent current injection analytical approach to choose the best optimal DG size and position. From the above discussions, the following drawbacks are associated with the optimal planning of DGs by using analytical methods. The analytical methods with exact loss formulae [11]–[17] and loss sensitivity factors [18]–[21] are inefficient for large scale distribution systems and there are few literature papers on optimal planning of DGs by using analytical methods based on branch

current loss formulae and branch power flow formulae. As previously mentioned, optimal DG planning enhances several technical, financial, and environmental factors. However, the majority of research focused on optimal DG planning by utilising analytical techniques for power loss mitigation and voltage profile improvement only.

Therefore, several researchers addressed the OPDG problem using meta-heuristic optimization algorithms to overcome the drawbacks associated with analytical methods. The advantage of meta-heuristic algorithms is that they can efficiently solve very complicated tasks. The meta-heuristic algorithms use an iterative generation process that effectively locates near-optimal solutions using learning methodologies and intelligently integrating various concepts to explore and examine the search space. These algorithms employ randomized operators to look for the best outcomes based on exploration and exploitation [5]. The advantage of meta-heuristic algorithms is that they are problem independent. Another benefit of utilising meta-heuristic optimization algorithms is that they allow the use of any multi-objective optimization technique instead of analytical techniques that only allow the use of the weighted sum approach for multiple objectives optimization. Meta-heuristics optimization algorithms can be broadly divided into two categories: population-based algorithms and single solution-based (or) trajectory-based algorithms. In single solution-based algorithms, a solution is randomly generated, and the solution is improved until they achieve the best outcome. In population-based algorithms, a collection of random solutions in a specified search space are generated first, and solutions are updated with the help of heuristics & intelligence gained during iterations until the best solution is produced. Population-based algorithms can escape local optima because of the presence of many searching agents. Population-based algorithms are divided into several categories: algorithms based on the theory of evolution (e.g., Genetic algorithm (GA), Differential Evolution (DE)), algorithms based on physical laws (e.g., Gravitational search algorithm (GSA), Black Hole optimization algorithm (BHOA)) , algorithms that take inspiration from swarms of particles (e.g., Artificial Bee Colony (ABC), Particle Swarm Optimization (PSO)), and algorithms that mimic biological behaviour (e.g., Cuckoo search algorithm (CSA), Bat algorithm (BA)) [26]. In literature, several researchers addressed optimal DG planning using several meta-heuristic optimization algorithms for improving distribution system metrics using several single and multi-objective optimization techniques.

Authors in [27] used loss-sensitive indexes to identify the best locations for DGs, and then a simulated annealing optimization algorithm was used for DGs sizing to reduce the

distribution system's power loss. The outcomes revealed that the greatest reduction in power loss is observed when DGs are operating with a 0.866 power factor rather than DGs operating with a unity power factor. [28] used the artificial bee colony algorithm to identify the optimal DG size, location, and power factor for the minimization of the system's power loss. However, the authors of [28] only discussed the optimal planning for a single DG unit. In [29], firefly and backtracking search algorithms are implemented for optimal planning of multi-DG units and determined optimal DGs' locations, sizes and power factors for the minimization of the system's power loss. From the outcomes, it was observed that DGs operating with optimal factor yield the most significant reduction in power loss compared to those operating with fixed power factor. From the articles [27]–[29] mentioned above, it has been observed that utilizing optimization algorithms to determine the optimal locations and sizes of DGs yields the most significant gain in power loss reduction. However, based on the complexity involved in the problem, researchers have been using both methods. In [30], the authors discussed the optimal planning for Type-3 DGs using the PSO algorithm for DGs generation cost reduction. From the results mentioned in [27]–[30], it has been found that multiple-DG unit planning in the distribution system, as opposed to single-DG unit planning, results in the highest reduction in distribution system power loss because of the significant changes in line power flows in the distribution system. In [31], authors addressed optimizing system maximum loadabilty using the HPSO algorithm. The authors of [32] addressed the hybrid genetic dragonfly optimization algorithm for minimization of the distribution system's EENS (electrical energy not supplied) technical metric's reliability index through the optimal planning of Type-I, Type-II, and Type-III DGs.

Several researchers have solved the OPDG problem and optimal network reconfiguration problem simultaneously for the improvement of distribution system metrics. Distribution networks are generally employed with two types of switches: section switches and tie switches. The tie switches are usually used for line reconfiguration. Meanwhile, the section switches are generally used to confine the fault damage. Therefore, these switches assist in isolating faulty subsystems from the original network and prevent disruption in the significant system's functionality [5]. In addition to the functionality mentioned above, several researchers have discussed network reconfiguration in the literature to improve technical distribution system metrics such as load balancing between feeders and branches, voltage profile improvement, and power loss reduction. Optimal distributed network reconfiguration (ODNR) problem is the process of finding the best topological structure of the network by

finding the network's switch states, which could either be usually open (for tie switches) or closed (sectionalizing switches) while maintaining the radiality of the network for the improvement of distribution system metrics by satisfying the several operational constraints. In the literature, authors tackled the network reconfiguration problem using various mathematical optimization approaches, heuristic optimization algorithms, and meta-heuristic optimization algorithms for enhancing distribution system metrics.

The ODNR problem was initially solved in [33] using a branch and bound (B&B) algorithm. Even though the proposed method discovered an effective solution, its convergence was a sluggish process. Distribution feeders were divided into various networks as part of a binary integer programming strategy introduced in [34] for solving the ODNR problem. The proposed method, however, encountered computational issues with large-scale distribution systems. The Benders decomposition (BD), which separates separating the problem into a "master problem" and a "slave problem", was introduced in [35] to address the ODNR problem. The slave problem was used to examine these radial solutions' viability, while ideal radial topological structures with the lowest losses were determined in the master problem while considering power flows limits. The performance of BD decreases with a rise in nonlinear variables of the model, despite the findings showing the efficacy and robustness of the suggested methodology for ODNR problem. A MILP model with a two-stage decomposition approach was presented in [36] to address an ODNR problem. However, the piecewise linear approximations utilised in [36] diminish the accuracy of solutions for reconfiguring large distribution systems. From the above discussions, it was observed that solving the ODNR problem using mathematical approaches [33]–[36] typically takes a long time, and this problem worsens when more integer decision variables are considered. In [37], authors introduced the branch exchange (BE) heuristic method to address an ODNR problem. In BE, new radial topologies are produced by closing an open switch and opening a switch that is already closed on each planar loop until the best configuration is reached. Unfortunately, the time-consuming nature of BE's point-to-point searching process makes it a slow way to reconfigure big distribution systems. a heuristic approach based on the fundamental ideas of network partitioning for solving an ODNR problem was introduced in [38] to overcome the size limitations. In this method, the distribution network was separated into bus groups, and the power losses between these groups were reduced. A novel BE-based heuristic strategy was proposed in [39] to solve the ODNR problem. The algorithm's precision was respectable despite the lengthy computation time. In [40], a dual-stage heuristic technique

for solving ODNR was proposed. In the first stage, switches with the least loss increase are opened, and BE chooses the best proposals in the second stage. Despite the proposed technique's high accuracy and simplicity, this process takes a lot of time due to repetitive load flows and checking all promising solutions. In place of BE in the second step of the suggested heuristic algorithm, [41] used the neighbour-chain updating process (NCUP) to boost the precision of the method described in [40]. Because heuristic algorithms must be developed for a particular application and time-consuming procedures, several authors solved the ODNR problem using meta-heuristic optimization algorithms. The genetic algorithm (GA), a well-known metaheuristic technique, was used in [42] to solve the ODNR problem.

However, reconfiguring large distribution networks using the usual GA is time-consuming. Authors suggested an meta-heuristic evolutionary optimization algorithm (EA) in [43] to reduce network real power losses through ODNR problem. However, due to a subpar tree representation of the distribution network's graph, non-radial topological structures occur during algorithm search, severely reducing the algorithm's efficiency. In order to reduce the system's active power loss, a more effective selective BPSO algorithm [44] is used for the ODNR problem. Few researchers addressed ODNR problem with multi-objective optimization. To reduce active power loss and the system's voltage deviation index, authors in [45] addressed the ODNR problem using cuckoo search algorithm (CSA). To reduce active power loss, load balancing between branches and feeders, and the quantity of switching operations, a multi-objective Max-Min multi-objective strategy using runner root algorithm is suggested in [46] optimal network reconfiguration problem. A fuzzy adaptation of the evolutionary programming algorithm, the Discrete Artificial Bee Colony (DABC) algorithm, and a second-stage employee-improved harmony search algorithm, respectively, were used by the authors of [47], [48], and [49] to address the ODNR problem to maximise the network's maximum loadability.

Researchers in [50] and [51] addressed the optimal network reconfiguration problem and optimal allocation of Type-1 DGs to minimize the active power loss of the system by considering different scenarios. Harmony search and adaptive cuckoo search algorithms have been used to find the optimal DG sizes, DG locations and open switch positions to achieve the desired result. Authors in [52] addressed the optimal allocation of Type-3 DGs with optimal power factor to minimize the network active power loss using the UVDA-based heuristic method. From the outcomes observed in [50]–[52], it can be concluded that the most

significant improvement in technical metrics of the distribution system is obtained when DGs are optimally planned in the optimal reconfigured network.

As mentioned earlier, optimal DG integration allows for improving several technical distribution system aspects. The works mentioned above, however, considered single-objective optimization only. As a result, the improvement in the other objectives is not up to par owing to the conflicting nature between the objectives. Numerous studies have employed multi-objective optimization techniques to find the solution (i.e., determining the best locations and sizes for DGs) that optimally balances several objectives. In [53], the authors discussed a weighted multi-objective technique employing the Harmony search optimization algorithm (HSA) for minimising network power loss and total hormonic distortion, improving the system voltage profile, and enhancing system security. The optimal placement of DGs in the distribution system was discussed in [54] using a weighted multi-objective particle swarm optimization technique to reduce power loss and increase reliability. Using a weighted multi-objective genetic algorithm, authors of [55] discussed the optimal way to plan DGs for minimising system power loss, maximising system loadability, and enhancing voltage profile. The authors of [56] discussed inertia-weighted PSO for maximising system loadability and minimising power loss through optimal DG planning utilising a weighted multi-objective method. In [57], authors discussed a hybrid sequential Monte Carlo simulation analytical hierarchical approach for the optimal DG planning in a distribution system to reduce system power loss, voltage variation, SAIDI, CAIDI, and EENS utilising a weighted-based multi-objective technique. In [58], authors discussed the weighted-based multi-objective hybrid SFLA (shuffled frog leap algorithm) and DE (differential evolution) algorithms for the optimal placement of DGs in distribution systems to reduce power loss, operational power costs, and emission costs. To optimize power loss, voltage deviation, and voltage stability technical metrics, researchers used a multi-objective weighted technique-based quasi-oppositional teaching learning-based optimization algorithm [59]. To reduce power loss and improve loadability, epsilon artificial bee colony optimization [60] and multi-objective techniques are employed. In [61], an analytical hierarchy weighted based multi-objective hybrid multiverse optimization algorithm is used to improve four distribution system technical metrics: reduction of system's energy loss & node voltage deviation metrics, enhancement of voltage stability and reliability metrics. With the intent to decrease loss and increasing reliability, authors in [62] implemented a hybrid multi-objective TLBO-GWO optimization algorithm for optimal planning of DGs in distribution system.

The Pareto-based Harris hawk optimization algorithm is implemented in [63] to improve the system's technical parameters. Numerous researchers have considered economic factors while planning of DGs in distribution networks to reduce DGs' installation, maintenance, and operational expenses. Authors in [64] addressed improving technical and economic objectives using a Pareto-based muti-objective differential evolution optimization algorithm. The authors of the studies mentioned above [27-32], [53-62] used numerous single- and multi-objective strategies to handle the OPDG problem in the distribution system at its peak load level to improve various technical & economic metrics. The idea behind addressing the OPDG issue at the system's peak load level is that DGs have to inject how much active and reactive power into the system at optimal locations for the improvement of systems technical & economic metrics to the maximum extent. Then similar system performance is achieved at other load levels other than system's peak load if DGs adjust its power output following load changes. The above methodology works only if optimal planning of dispatchable DGs like BIOMASS, Micro-Turbine and DSTATCOM in the distribution system is addressed. However, optimal planning of non-dispatchable units like PV & WT units should be done by taking load data of a particular time frame.

Several researchers addressed the optimal planning of non-dispatchable renewable-based PV and WT units in the distribution system by considering the system's p.u typical daily load profile. The average p.u. daily load profile is generated using historical load demand. Probabilistic approaches that consider the intermittency nature of solar radiance & wind speed must first be explored for the optimal design of PV and WT units in the distribution system. Authors in [65] concluded that the Beta & Weibull probability distribution functions were the most fitted distributed function in coping with the probabilistic nature of solar radiance & wind speed. Based on this, a few researchers developed [66],[67]–[70] various probabilistic methods using beta PDF. However, dealing with the uncertainty involved in PV unit output power is made simpler by applying the probabilistic method developed in [70], which determines the typical p.u PV output power curve from historical solar irradiance data. To enhance system performance, authors in [66], and [71] addressed the optimal integration of PV (Photo-Voltaic) and WT (Wind Turbine) units in electrical distribution networks by taking daily load demand, solar radiance, and wind speed uncertainty into consideration. However, if DGs dispatch/inject power into the system optimally during each hour of the day, the system's performance (energy loss reduction, enhancement of the system's voltage profile, etc.) would be improved more. Therefore, to overcome the non-dispatchable nature of PV, the

PV unit is assisted by BESS so that the combined PV-BESS would act like dispatchable DG. Similarly, in the case of the WT-Biomass unit, the difference of power between the required power from the WT-Biomass unit and the WT unit will be supplied by the Biomass unit. Optimal integration of PV-BESS units is addressed in [72], [73] for the mitigation of distribution network energy loss, and in [74], optimal integration of either PV-BESS or WT-Biomass units in the distribution system for the mitigation of energy loss is addressed.

1.2 Investigations on optimal planning of Distributed Generators in the distribution system in the presence of plug-in hybrid electric vehicles load demand

Numerous studies have focused on the appropriate planning of DGs in the distribution system to reduce the impact of PHEVs load demand and enhance its performance. Few researchers [75], [76] handled optimal planning and scheduling of RDGs in the distribution system by integrating PHEVs load demand with the 24-hour load demand of the system. In the previous works, PDFs address the probabilistic nature of arrival time and trip distances of PHEVs. However, the methodology considered in the earlier papers addressed night-time charging of electric vehicles at residential buses, i.e., charging of electric cars at home, which is coined as private charging. However, the effective transfer of car owners from conventional to electrical vehicle technology depends on creating an adequate public charging infrastructure. Because in Public Fast Charging Station (PFCS), an electric vehicle's battery can be charged in 20 to 30 minutes. Many countries worldwide are developing regulations and providing incentives to encourage the installation of charging stations.

Therefore, few researchers addressed the optimal placement of PFCS in radial distribution systems. In [77], the authors proposed investment, operation, maintenance, and network loss costs as the objectives for problem formulation that were gained by the modified primal-dual interior-point algorithm for the optimal placement of PFCS. Considering the costs of PFCS equipment, land, PFCS electrification, electric grid loss, and EV loss for charging, a mixed-integer nonlinear problem (MINLP) is described in [78], and the MINLP optimization problem was addressed using GA. In [79], the genetic algorithm (GA) technique is used to solve the suggested model of the optimal placement for PFCS, which includes two objective functions, such as the cost of PFCS construction and the cost of charging station access. The fuzzy-based multi-objective grasshopper optimization algorithm is implemented in [80] for optimal planning of RDGs and PFCS to improve the technical metrics of the distribution

system. In [81], the authors discussed the best location for PFCS and RDGs utilizing the HPSO-GWO optimization algorithm in the distribution system, taking land costs and the population of electric vehicles. In [82], the authors examined the optimal placement for parking lots by maximising parking lot revenue, considering the cost of parking lots, reliability, power loss, and voltage improvements as the objective functions. The GA was then used to determine the best outcomes. The authors in [83] proposed land cost, station equipment cost, operating and maintenance cost, real power loss cost, and voltage profile improvement as objective functions for the placement of CS, and the proposed problem is resolved by an advanced GA and PSO algorithm. In [84], the authors used the investment cost of CS, operation and maintenance costs, electricity cost for battery charging, electricity cost for travelling to charge the battery, time cost for driving, waiting time cost, and charging time cost as the objective for problem formulation. The integrated planning problem was solved by the PSO algorithm. The placement of the PFCS is studied in [85] with the goal of minimising power loss and maximising the stability of the distribution system, with APSO solving the optimization problem. A multi-objective mixed integer nonlinear problem (MINLP) with FCS development costs, EV specific energy consumption costs, electrical network power loss costs, DGs costs, and voltage deviation was developed by the authors in [86], [87]. The NSGA-II & SFL-TLBO was used in this study to address the formulation problem for placing PFCSs and DGs in the distribution network. The 118-bus distribution system served as an evaluation system for the suggested technique. But authors have not considered the optimal placement of PV or WT-based RDGs. Using a Pareto-based WOAGA algorithm, authors in [88] examined the best way to connect RDG, PFCS, and BESS to improve distribution systems' technical, fiscal, and environmental metrics.

1.3 Motivation and dissertation objectives

As discussed in the introduction, due to the advantages of DG technologies like compact in size, advancements in DG technologies and reduction in installation costs, so much research is going on how an electrical distribution system should be made efficient by the deployment of DGs optimally. From the literature review on optimal planning or deployment of DGs in the distribution system at its peak load level, several researchers addressed the improvement of several metrics using single and multi-objective optimization techniques by various analytical and meta-heuristic optimization algorithms. However, the literature does not discuss employing a suitable multi-objective method to bring the balanced solution in improving power loss reduction and lodability technical metrics. And also, from the literature

review on optimal deployment of PV, WT, PV-BESS and WT-BIOMASS units in the distribution network, it was observed that researchers addressed the minimization of systems' energy loss only and not considered other technical metrics & economic aspects. From the literature review on optimal planning of DGs in the presence of PHEVs load demand, only a few papers hardly addressed optimal planning of PV & PV-BESS units in distribution systems by considering both private and public charging.

Therefore, the succeeding objectives are deduced based on the observations made from the literature review.

1. To determine the best trade-off solution between the active power loss reduction and maximum loadability enhancement through proper planning of DGs in the distribution system.
2. To obtain the best compromise solution between energy loss reduction, voltage profile improvement and annual installation & maintenance costs of DGs through optimal planning of dispatchable DGs (PV-BESS, WT-BIOMASS) units in the distribution system by considering solar radiance, wind speed and load uncertainties.
3. To look for the optimal planning of DGs in the distribution system for energy loss reduction and voltage profile improvement considering PHEVs load demand charging under private charging scenario.
4. To look for the optimal planning of dispatchable DGs (PV-BESS, WT-BIOMASS) units in the distribution system for energy loss reduction, voltage profile improvement and annual installation & maintenance costs of DGs considering PHEVs load demand charging under both private & public charging scenarios.

By working on the objectives mentioned above, the following contributions are made:

1. Ɛ-constraint-based multi-objective approach for optimal network reconfiguration and optimal allocation of DGs in radial distribution systems using the butterfly optimizer.
2. Probabilistic optimal planning of dispatchable distributed generator units in distribution systems using a Pareto-based multi-objective chaotic velocity-based butterfly optimization algorithm.
3. Optimal integration of DGs into radial distribution network in the presence of plug-in electric vehicles to minimize energy loss and to improve the voltage profile of the system using a pareto-based multi-objective chaotic velocity-based butterfly optimization algorithm.

4. Probabilistic optimal allocation of Solar PV units and Battery Energy Storage System in the distribution system in the presence of plug-in electric vehicles using a multi-objective chaotic velocity-based butterfly optimization algorithm.

1.4 Organization of dissertation

The dissertation is structured as follows:

Chapter 1 briefly overview Distributed Generators (DGs) nomenclature, classification, and applications. Along with a brief overview of PHEVs and their charging behaviour. Investigations on DG planning in distribution systems without and with PHEVs load, their outlines, the thesis's research goals, its contributions, and its structuring are described.

Chapter 2 presents the Ɛ-constraint-based multi-objective approach for optimal network reconfiguration and optimal allocation of DGs in radial distribution systems using the butterfly optimizer with the objective of increasing loadability and reducing power loss.

Chapter 3 presents the probabilistic optimal planning of non-dispatchable PV & WT units and dispatchable PV-BESS, WT-BIOMASS distributed generator units in distribution systems using a Pareto-based multi-objective chaotic velocity-based butterfly optimization algorithm with the objective of reducing energy loss and enhancing voltage profile.

Chapter 4 describes the optimal integration of DGs into a radial distribution network in the presence of plug-in electric vehicles charging under private charging scenarios to minimize energy loss and improve the system's voltage profile using a Pareto-based multi-objective chaotic velocity-based butterfly optimization algorithm.

Chapter 5 details the Probabilistic optimal allocation of Inverter based Solar PV units and Battery Energy Storage Systems in the distribution system in the presence of plug-in electric vehicles charging under private and public charging scenarios using a multi-objective chaotic velocity-based butterfly optimization algorithm.

Chapter 6 presents the conclusions and future scope of the thesis.

Chapter 2

Ɛ-constraint-based multi-objective approach for optimal network reconfiguration and optimal allocation of DGs in radial distribution systems using the butterfly optimizer

2.1 Introduction

This chapter presents the optimal planning of DGs in the distribution system for the improvement of its efficiency and maximum loadability. Maximum loadability (λ_{max}) of the system is defined as the maximum increase in power system load till the voltage instability occurs. Loading margin factor (λ_v) of the system is defined as the maximum increase in power system load until the system buses violate maximum and minimum bus voltage limits. Figure 2.1 shows that the system with better maximum lodability (curve B) has better loading marginal factor and voltage profile at each loading. From the description above, it can be inferred that enhancing the system's maximum loadability also increases its maximum loading factor, allowing for the effective fulfilment of growing load demand without exceeding permitted bus voltage levels.

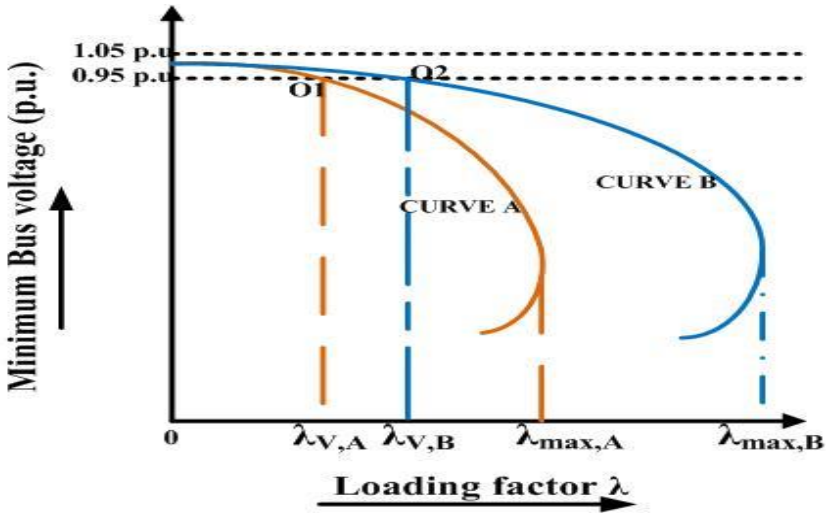

Figure 2.1 Impact of DGs placement and Network reconfiguration on system loadability

In the literature, few researchers addressed enhancing the maximum loadability of the distribution system via optimal planning of DGs and optimal network reconfiguration. Authors in [31] presented a hybrid PSO meta-heuristic algorithm for enhancing maximum

loadability of the distribution system by optimal planning of Type-III DGs. To improve the maximum loadability of the distribution system, authors in [47]–[49] examined the optimal network reconfiguration problem, and findings revealed that the maximum loadability has been improved in the optimal reconfigured network. Authors in [60] discussed simultaneous optimal planning of DGs and optimal network reconfiguration problem for enhancing distribution system maximum loadability using an artificial bee colony (ABC) optimization algorithm, and from the outcomes, it has been revealed that better improvement in system maximum loadability is achieved in case of when DGs are optimally planned in the optimal reconfigured network. From the outcomes in [31], [60], it was observed that even though the system maximum loadability is improved to maximum value but the percentage of active power loss reduction is very less. Based on the description above, it can be concluded that there exists a conflicting nature between the objectives of active power loss reduction and maximum loadability enhancement.

Therefore, this chapter presents Ɛ-constraint multi-objective butterfly optimization algorithm (MOBOA) to bring the balanced solution between the improvement in two metrics of the distribution system (i.e., active power loss reduction and maximum loadability enhancement) by optimal planning of DGs and optimal network reconfiguration. In this work, improvement in above-two mentioned objectives of the distribution system is addressed at the peak load level of the system without considering load and DGs uncertainties. Hence, this work addresses the determination of the injection of how much active & reactive power into the distribution system by identifying the optimal DGs locations, DGs sizes, DGs power factors & optimal switch positions for the improvement of the above-cited metrics.

2.2 Problem Formulation

2.2.1 Active Power Loss of the system

Active power loss (P_{loss}) of the system should be minimized to improve the distribution system efficiency.

$$f_1 = minimize\ (P_{loss}) \tag{2.1}$$

$$P_{loss} = \sum_{i=1}^{nbr} J_i^2 * R_i \tag{2.2}$$

Where, J_i is the ith branch current and R_i is the resistance of the ith branch.

2.2.2 Maximum loadability of the system

Maximum loadability of the system (λ_{max}) should be maximized to meet the future load growth of the system.

$$f_2 = maximize\ (\lambda_{max}) \tag{2.3}$$

To obtain the λ_{max} of the system in [31], [60], [89], the system load level is increased from 0 in step size of 0.01 until the load flow diverges and the corresponding load level at which the load flow has diverged is considered as λ_{max} of the system.

2.2.3 Constraints

The optimal allocation of DGs in the distribution system and optimal network reconfiguration of the distribution system problem needs to satisfy the following constraints:

a. Bus voltage limit constraints: The voltage magnitude of each bus should be within the minimum and maximum limits.

$$|V_{min}| < |V_j| < |V_{max}| \quad j = 1,2 \ldots . . nb \tag{2.4}$$

where *nb* is the number of buses in the distribution system.

b. Thermal limit constraints: The current flowing through each branch should be less than the current rating of the respective branch.

$$J_i \leq J_i^{max} \qquad i = 1,2 \ldots \ldots nbr \tag{2.5}$$

Where, *nbr* is the number of branches in the system.

c. Active power limit of DGs: Active power generated by each DG ($P_{DG,k}$) should be less than the maximum active power limit of DGs.

$$P_{DG,k} \leq P_{DG,k}^{max} \qquad k = 1,2 \ldots . ndg \tag{2.6}$$

Where, *ndg* is the number of DGs to be placed in the system.

d. The power factor of DGs: power factor of each DG should be within the minimum (pf_k^{min}) and unity power factor limits.

$$pf_k^{min} \leq pf_k \leq 1 \qquad k = 1,2 \ldots ndg \tag{2.7}$$

e. Total active power ($P_{T,DG}$) and reactive power generated ($Q_{T,DG}$) by DGs should be less than the total active (P_{load}) and reactive power (Q_{load}) demand of the system respectively.

$$\sum_{k=1}^{ndg} P_{DG,k} = P_{T,DG} \leq P_{load} \tag{2.8}$$

$$\sum_{k=1}^{ndg} Q_{DG,k} = Q_{T,DG} \leq Q_{load} \tag{2.9}$$

f. Active Power and Reactive power balance constraints.

$$P_{sub} + P_{T,DG} = P_{load} + P_{loss} \tag{2.10}$$

$$Q_{sub} + Q_{T,DG} = Q_{load} + Q_{loss} \tag{2.11}$$

where P_{sub}, Q_{sub} are the active and reactive power generated by substations.

g. The optimal network reconfiguration problem requires checking of radiality of the reconfigured network. In this work, spanning tree technique is utilized for checking the radiality of the reconfigured network [89].

2.2.4 Multi-objective optimization- Ɛ-constraint method

Ɛ-constraint method [90] is one of the methods to optimize two or more objectives at a time. In the Ɛ-constraint method, multi-objective optimization is redeveloped as taking one of the objectives as an objective function and other objectives are limited within the specified limits by converting them into constraints. The mathematical formulation of the multi-objective Ɛ-constraint method is formulated as follows

Minimize $f_\mu(x)$ (2.12)

subjected to $f_m(x) \leq \varepsilon_m \quad m = 1,2,\ldots\ldots, M \; and \; m \neq \mu$ (2.13)

$g_j(x) \geq 0 \quad j = 1,2,\ldots\ldots J$ (2.14)

$h_k(x) = 0 \quad k = 1,2,\ldots\ldots K$ (2.15)

$x_i^L \leq x_i \leq x_i^U \quad i = 1,2\ldots\ldots n$ (2.16)

Where, ε_m is the upper bound limit of the m[th] objective function $f_m(x).g_j(x)$, $h_k(x)$, $x_i$are the j[th] inequality constraint, k[th] equality constraint, and i[th] decision variable. x_i^L,$x_i^U$are lower bound and upper bound limits of the decision variables.

2.3 Butterfly Optimization Algorithm

In the literature, various researchers have taken several optimization algorithms for the OPDG and ODNR problems. According to the "No Free lunch theorem," no optimization algorithm gives exceptional results for all optimization problems. An optimization algorithm may give admirable results for some set of optimization problems and may give inferior results for another set of optimization problems. Performance-wise, all optimization algorithms are indistinguishable while solving a whole set of optimization problems. However, while choosing an optimization problem of, few things are considered like since finding the loadability of the distribution system is a very tedious process, authors try to avoid optimization algorithms with a two-stage evolutionary process like in cuckoo search algorithm, TLBO algorithm, etc., and algorithm should be easy in implementation. Since the Butterfly optimization (BO) algorithm is a new one and advantages like ease in implementation have driven the authors to use this algorithm [91], [92].

Butterfly optimization (BO) algorithm is a new meta-heuristic optimization algorithm developed by Sankalap Arora and Satvir Singh in 2018 [93]. The BO algorithm is developed based on the food foraging behaviour and mating behaviour of the butterflies. In the real world, butterflies use their sense of smell to find food and mating partner. During the search

process for food, each butterfly will emit fragrance with some intensity, and the intensity of the fragrance is proportional to the quality or quantity of food sources at the neighbourhood of that butterfly. The fragrance emitted by the butterfly will propagate over some distance. If the other butterflies in the group were able to sense the fragrance, they would move towards it. In this way, butterflies will move in the real world until they find a good food source position.

In developing the BO algorithm, all butterflies are treated as searching agents. Each agent has a position and associated fragrance. The fragrance of each agent is correlated with the fitness of the objective function. The mathematical modelling of the fragrance is given in Eq.2.17.

$$f = cI^a \tag{2.17}$$

where f is the perceived magnitude of the fragrance, I is the stimulus intensity, c is the sensor modality and a is the power exponent. In BO algorithm, I is the fitness of the searching agent or butterfly. In BO algorithm c and a are the control parameters of the algorithm and the detailed analysis of the algorithm control parameters were given in [93].

All agents will move to the new positions in the search space based on the global best agent, magnitudes of the fragrances of all the agents and a switch probability p. The switch probability p decides whether the agent to go for local search or global search. The equations for position updating are given below.

Perform a global search using Eq. 2 if $rand < P$

$$x_i^d(t+1) = x_i^d(t) + \left(r^2 * gbest - x_i^d(t)\right) * f_i \tag{2.18}$$

or local search using Eq. 2 if $rand > P$

$$x_i^d(t+1) = x_i^d(t) + \left(r^2 * x_j^d(t) - x_k^d(t)\right) * f_i \tag{2.19}$$

Where $x_j^d(t)$and $x_k^d(t)$are Jth and kth butterflies from the solution space which belongs to the same swarm and r is a random number in [0, 1]. The detailed flowchart is given in APPENDIX-A.

The detailed steps for implementation of BO algorithm are as follows

Step 1: Initialize algorithm parameters such as the number of agents *N*, the dimension of the problem *d*, the maximum number of iterations $Iter_{max}$, probability switch *P*, power exponent *PE* and sensor modality *SM*.

Step 2: Generate initial random solution x_i between minimum ($x_{\min}$) and maximum

(x_{max}) limits.

$$x_i = x_{min} + (x_{max} - x_{min}) * rand \quad (2.20)$$

Where, $x_i$represent the position of the i^{th} agent or butterfly.

For optimal allocation of DGs unit's problem, the x_i constitute

$$x_i = \left[L_i^1, L_i^2 \ldots\ldots L_i^d \;\; P_{DG_i}{}^1, P_{DG_i}{}^2, \ldots\ldots P_{DG_i}{}^d pf_i^1, pf_i^2, \ldots\ldots pf_i^d\right] \; i = 1,2 \ldots . N \quad (2.21)$$

Where *N* is the number of agents and *d* is the number of DGs to be placed, L_i^d , $P_{DG_i}{}^d$, pf_i^drepresents location (integer number), size (real value) and power factor (real value) of N^{th} agent of $d^{th\ DG}$ unit. During the simulation, location value is round-off to the nearest integer value.

For optimal network reconfiguration problem, the x_i constitute

$$x_i = \left[SW_i^1, SW_i^2 \ldots\ldots SW_i^d \;\right] \; i = 1,2 \ldots . N \quad (2.22)$$

Where *N* is the number of agents and *d* is the number of tie switches in the distribution system,SW_i^d represents the d^{th} switch position of N^{th} agent.

Step 3: Evaluate the fitness (objective functions) of agents using Eq. 2.1, Eq. 2.3 & Eq. 2.12. Record the best solution as *gbest*.

Step 4: Set iteration count *t* as zero.

Step 5: Calculate the fragrance f_N for each agent or butterfly using Eq. 2.17.

Step 6: Update the positions of the agents using the equations Eq. 2.18 and Eq. 2.19.

For optimal network reconfiguration problem, the updated position is rounded to the nearest integer value.

Step 7: Evaluate the fitness of each agent in the new population using Eq. 2.1, Eq. 2.3 & Eq. 2.12.

Step 8: Update the *gbest* vector

Compare each new solution with the previous solution. If the new solution is better than the previous solution, record the new otherwise discard the new solution and preserve the previous solution as it is. Find out the gbest vector from updated population.

Step 9: Stopping criterion

Increment the iteration count by 1. If the iteration count reaches the maximum number of iterations ($iter_{max}$) computation is terminated. Otherwise, Step 5 to Step 9 is repeated.

Step 10: Print out the results.

2.4 Results and Discussion

In this section, the proposed BO algorithm for improving the λ_{max} and active power loss reduction is applied on standard 33 and 69 bus test systems for the following scenarios.

1. Single objectives optimization, i.e., Minimization of active power loss of the system and maximization of Maximum loadability of the system, are discussed in scenario-1.
2. Ɛ-constraint MOBOA (Multi-objective butterfly optimization algorithm) approach: Taking λ_{max} as objective function and active power loss as a constraint.

Each scenario consists of two cases: Optimal placement of DGs in the initial configured network (Case-1) and Optimal Network reconfiguration followed by DGs allocation (Case-2). The tuned parameters of the BO algorithm are given in Table 2.1. Distribution systems with DGs installed at more than two buses have been found to have significant changes in power flows, which is responsible for the more significant improvement in technical parameters. Additionally, it was noted that there was little improvement in technical metrics between DGs put at 3 buses and 4 buses. This may have been because we used the 33 & 69 bus systems as our test systems. Therefore, it is assumed that number of DGs to be placed is fixed 3. The lower and upper bound limits for location decision variables are 2 & 33 for 33 bus system, 2 & 69 for 69 bus system respectively. The lower and upper bound limits for DGs are 200 kW & 3000 kW respectively for both the test systems.

Table 2.1 BO Algorithm Parameters

Parameter Description	Assigned Value
Number of Agents (N)	80
Dimension (dim)	Scenario and Case dependent
Maximum number of iterations (*maxit*)	50
Modular modality ‘c’	0.01
Power exponent ‘a’	0.1 to 0.3
Probability switch ‘P’	0.5

2.4.1 33 Bus System

The network data of the system is given in [31]. The system consists of 33 buses, 37 branches and 5 tie switches. The nominal voltage rating of the system is 12.66 kV. The nominal load

on the system is 3715 kW and 2300 kVar. Initial open tie switch positions are 33,34,35,36 and 37. Single line diagram of 33-bus system is depicted in Figure 2.2. The base case active power loss and maximum loadability of an uncompensated system are 210.98 kW and 3.4 respectively. For optimal network reconfiguration problem, the switch positions given by BO algorithm for active power loss minimization are 7,9,14,32 and 37, the active power loss of the system is reduced to 138.5513 kW and maximum loadability of the system is improved to 4.87. The switch positions given by BO algorithm for maximization of λ_{max} are 7,9,14,28 and 32, the maximum loadability of the system is improved to 5.23 and active power loss of the system is reduced to 139.9782 kW. Since both objectives are improved in the case of λ_{max} maximization, the switch positions obtained for loadability maximization are taken for case-2 in all scenarios.

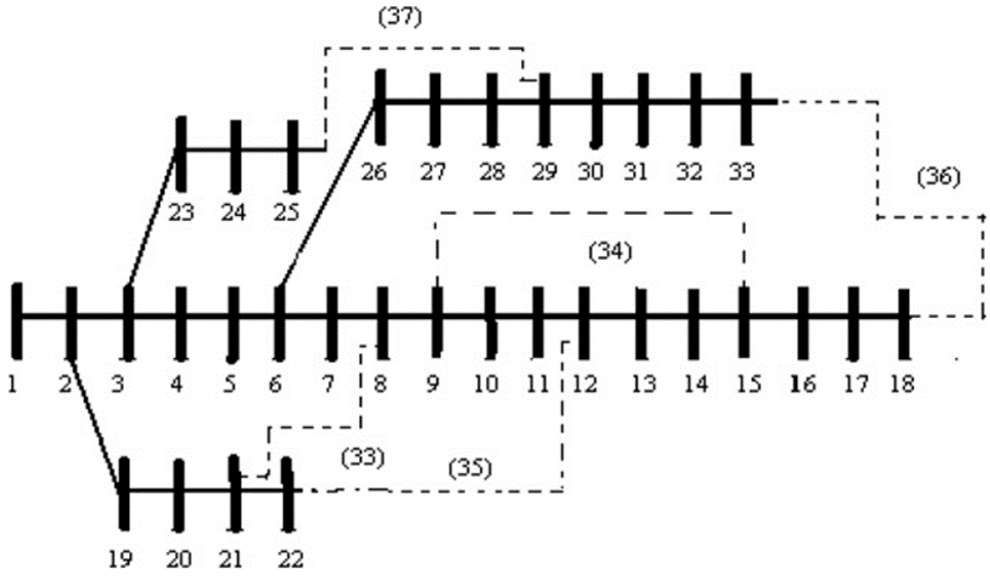

Figure 2.2 Single line diagram of 33-Bus system

Table 2.2 shows the various technical parameters of the system, DGs locations, DGs sizes, DGs power factors for optimal planning of DGs in scenario-1. In this work number of DGs to be placed in the 33-bus system is fixed to three due to the maximum enhancement in technical parameters of the system is observed in when Three DGs are placed optimally in the system. From Table 2.2, the following points are observed. In the case of active power loss minimization, the active power loss of the system is reduced to 12.74 kW (accounts 93.95 % of active power loss reduction), 18.75 kW (accounts 91.11 % of active power loss reduction with respect to the base case) when DGs are placed in case-1 and case-2 respectively. In the case of maximization of maximum loadability of the system, λ_{max} improved to 5.1, 7.23 in case-1 and case-2, respectively. And it is also observed that in the case of maximization of

maximum loadability of the system, the active power loss of the system is reduced to 86.5804 kW, 91.8943 kW in case-1 & 2 respectively accounts 58.96%, 56.44% reduction only. Therefore, from scenario-1 it is concluded that a multi-objective approach is needed to improve both the objectives, i.e., active power loss reduction and λ_{max}.

Table 2.2 Simulation results of 33-bus system for scenario-1

Parameters	**Initial configured network**		**Optimal Reconfigured Network**	
	Power Loss Minimization	**Maximum Loading Maximization**	**Power Loss Minimization**	**Maximum Loading Maximization**
Active power loss (in kW)	12.7458	86.5804	18.7531	98.8904
$\boldsymbol{\lambda_{max}}$	4.4	5.1	6.15	7.23
Minimum and Maximum voltage (in p.u)	0.9916 & 1.0007	0.9853 & 1.0498	0.9884 & 1.001	0.978 & 1.0495
% KVA DG INJECTION	79.17	84.97	68.4	99.6
% PLR	93.95	58.96	91.11	53.12
% MLI	29.41	50	80.88	112.64
DGs sizes (in kW)/Bus/ power factor	0737/14/0.88 1044/24/0.88 1156/30/0.80	0792/14/0.82 0550/17/1.00 1832/31/0.80	0573/12/0.88 1520/29/0.80 0414/33/0.92	2519/30/0.83 0356/32/0.80 0828/33/0.93

According to Ɛ-constraint method, the Ɛ value has to be chosen in such a way that it should be lies within the minimum and maximum values of the individual objective function [90]. Therefore, in scenario-2, Ɛ value has to choose between 12.12 kW, 86.5804 kW for case-1 and between 17.4779 kW, 91.8943 kW for case-2. In this work, to keep the active power loss reduction of the system to more than 70% (i.e., to reduce the active power loss of the system to below 63.29 kW) and to analyze the impact of different values of Ɛ on both objectives, we have chosen Ɛ values of 60 kW, 50 kW and 40 kW in scenario-2. The simulation outcomes of Ɛ-constraint MOBOA for different values of Ɛ is depicted in Figure 2.3. From the outcomes depicted in Figure 2.3, it can be concluded that both objectives are conflicting in nature.

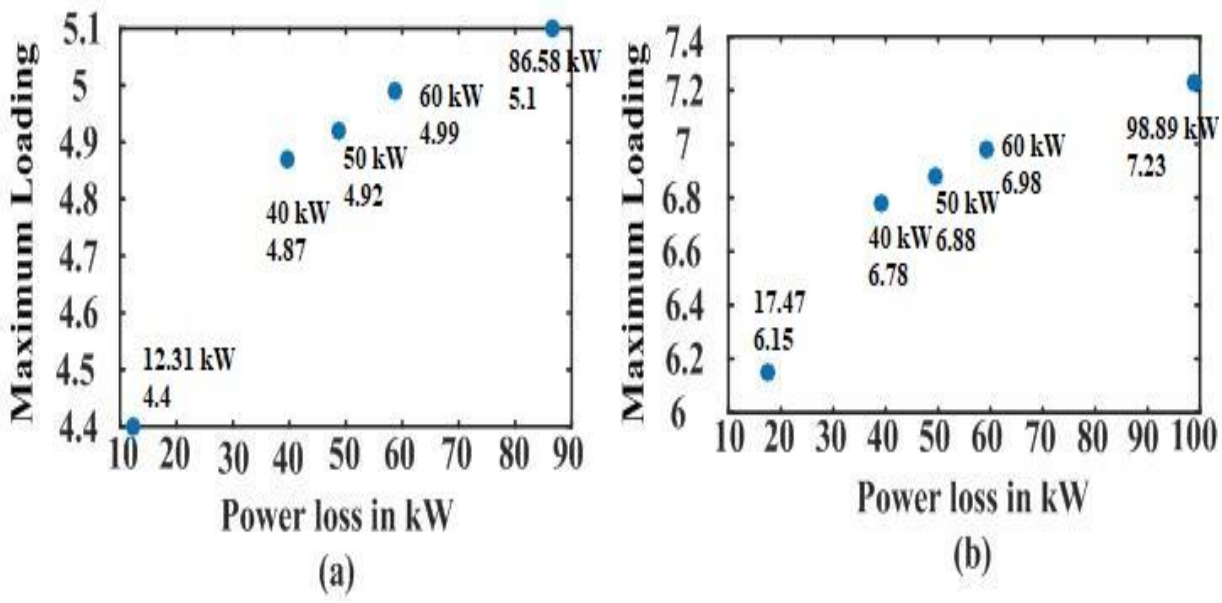

Figure 2.3 Simulation outcomes of 33-bus system for scenario-2 cases (Ɛ-constraint MOBOA) (a) Without reconfiguration (b) With reconfiguration

Due to the importance of minimization of active power loss to the lowest value, the value of Ɛ is taken as 40 kW is chosen to determine the optimal DGs locations, DGs sizes & DGs optimal power factors. Table 2.3 shows the various technical parameters, DGs locations, DGs sizes, DGs power factors for optimal placement of DGs in scenario 2.

Table 2.3 Simulation outcomes of 33-bus system for scenario-2 (Ɛ-constraint MOBOA)

Parameters	**Initial reconfigured network**	**Optimal Reconfigured Network**
	Ɛ= 40 kW	**Ɛ= 40 kW**
Active power loss (in kW)	39.6135	39.1406
λ_{max}	4.87	6.78
λ_V	1.9	2
Min voltage (in p.u)	0.9944	0.9917
Max voltage (in p.u)	1.042	1.028
DGs sizes (in kW)/ DGs location/ DGs power factor	1187/15/0.90 0739/25/0.86 1542/30/0.78	0583/12/0.93 0567/16/0.90 2138/30/0.78

From Table 2.3 shows a remarkable improvement of λ_{max} and active power loss reduction is observed in case-2 rather in case-1, i.e., λ_{max} is improved from 3.4 to 6.78, the active power

loss of the system is reduced to 39.1406 kW. The voltage profile graphs and the maximum loading curve for both cases in scenario-2 are shown the Figure 2.4 & Figure 2.5 respectively.

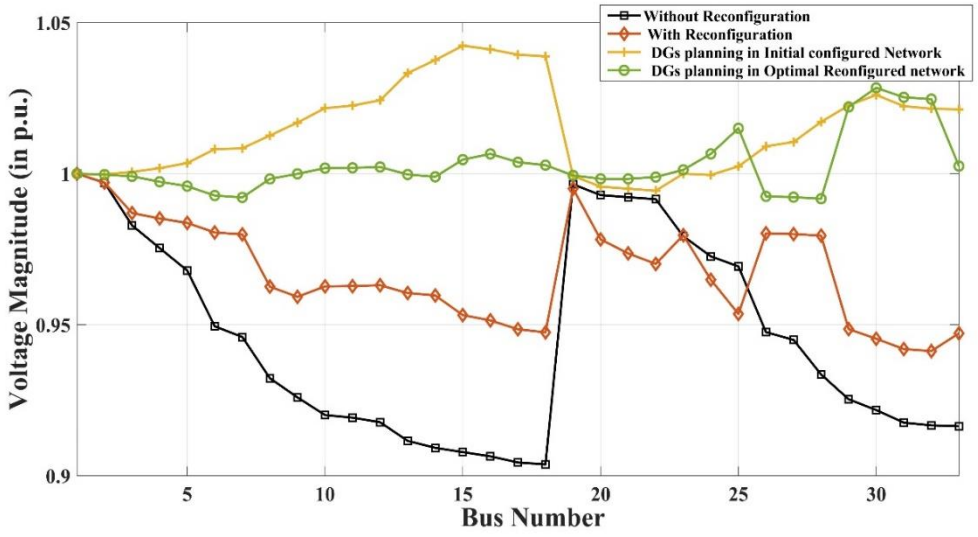

Figure 2.4 Voltage profiles of 33-bus system for Scenario-2

(Ɛ- Constraint MOBOA method when Ɛ = 40 kW)

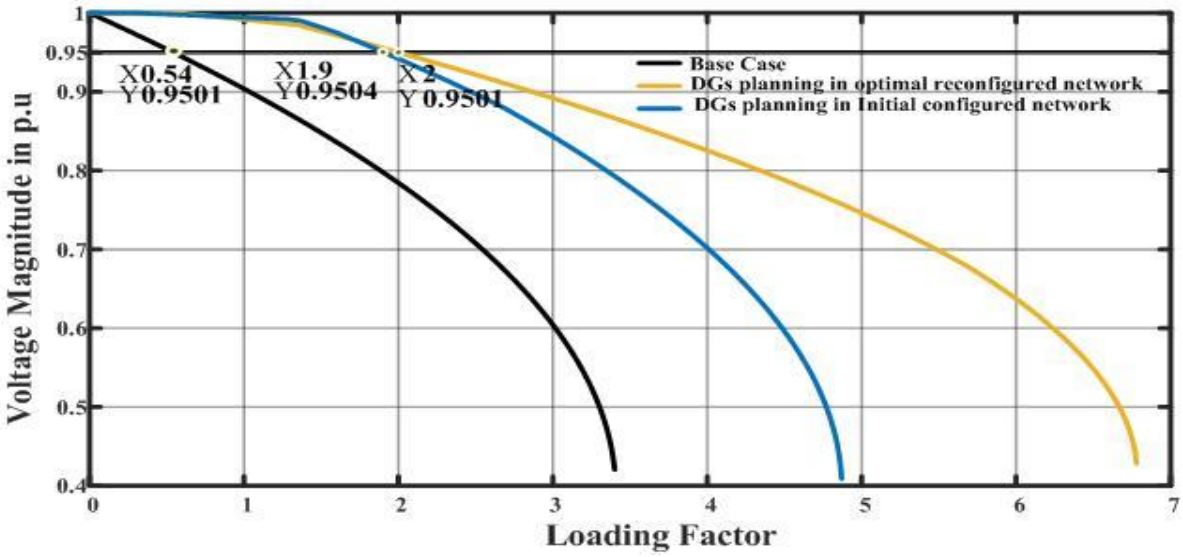

Figure 2.5 Maximum Loading curves of 33-bus system for Scenario-2

(Ɛ- Constraint MOBOA method when Ɛ = 40 kW)

From Figure 2.5, due to the consideration of maximum loadability as one of the objectives, it is observed that the loading marginal factor of the system is improved to 2, which indicates system bus voltages are within the permissible limits even though the system load increased by 100%.

To check the effectiveness of the proposed algorithm, the results of scenario 1 are compared in Table 2.4 with the suitable results available in the literature. And also, to get a greater number of comparisons, simulations for optimal placement of one DG & two DGs placement have been carried for scenario-1 and the comparisons are given in Table 2.4. Table 2.4 shows that the proposed methodology, i.e., the concept of using DGs with optimal power factor, gives better results than DGs with fixed power factor. And also, it is observed that the Proposed BO algorithm performs in achieving the desired objectives compared to HLTBO-GWO, HPSO and DABC algorithms in respective cases.

2.4.2 69 Bus System

The network data of the system is given in [31]. The system consists of 69 buses, 73 branches and 5 tie switches. The nominal voltage rating of the system is 12.66 kV. The nominal load on the system is 3801.4 kW and 2693.6 kVar. Initial tie switch open positions are 69,70,71,72 and 73. Single line diagram of the 69-bus system is depicted in Figure 2.6. The base case active power loss and maximum loadability of an uncompensated system are 224.9515 kW and 3.21, respectively. For optimal network reconfiguration problem, the optimal switch positions given by BO algorithm for active power loss minimization and loadability maximization are 14,58,61,69 and 70, the active power loss of the system is reduced to 98.55 kW and the maximum loadability of the system is improved to 5.49 from 3.21.

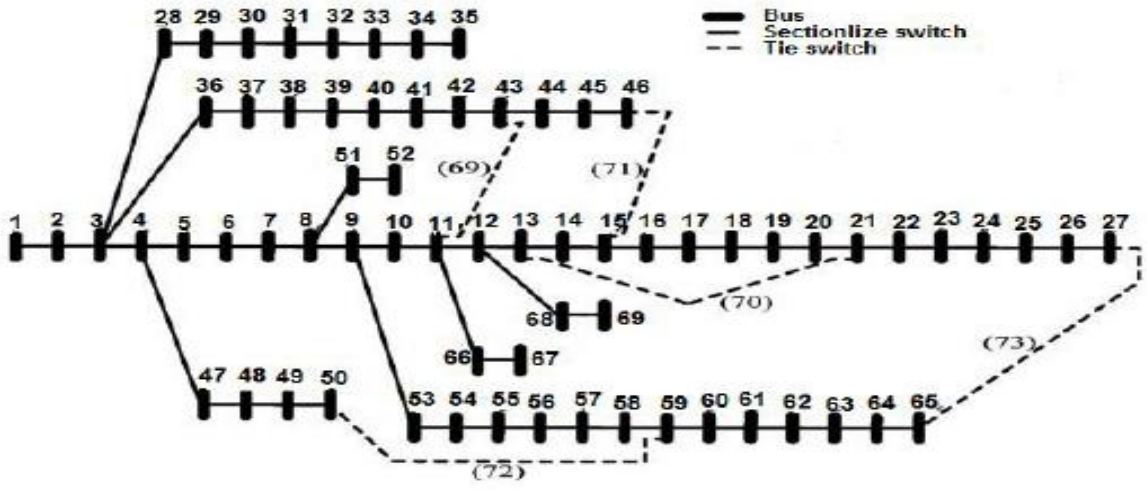

Figure 2.6 Single line diagram of 69-Bus system

Table 2.4 Comparison results of 33 bus system

Scenarios	Method	Open switch Positions	DGs sizes in kW/BUS/ p.f	Active power loss (kW)	λ_{max}
Scenario-1 (Power loss Minimization)					
Case-1	Proposed BO Algorithm	33,34,35,36,37	0737/14/0.88 1044/24/0.88 1156/30/0.80	12.75	4.4
	HTLBO-GWO[62]	33,34,35,36,37	997/30/0.8659 1000/13/0.8122 789/24/0.8726	13.68	---
	HSA-PABC[94]	33,34,35,36,37	862/12/0.85 1159/30/0.85 816/25/0.85	15.91	---
Case-2	Proposed Algorithm	7,9,14,28,32	0573/12/0.88 1520/29/0.80 0414/33/0.92	18.753	6.25
	UVDA Heuristic Method[52]	7,9,14,32,37	1.125+j1.034/30 0.592+j0.252/15 0.526+j0.280/12	25.346	----
Scenario-1 (Loadability Maximization)					
Case-1	Proposed BO Algorithm	33,34,35,36,37	3353/8/0.9	141.71	4.31
	HPSO Algorithm[31]	33,34,35,36,37	3080/8/0.85	131.85	4.31
	MOCTLBO Algorithm[89]	33,34,35,36,37	3017/8/3017	130.86	4.31
	Proposed BO Algorithm	33,34,35,36,37	347/15/0.9594 2100/30/0.7800	94.64	5.07
	HPSO Algorithm[31]	33,34,35,36,37	1117/16/0.85 1880/22/0.85	98.65	5.00
	CTLBO Algorithm[89]	33,34,35,36,37	1373/15/0.959 1944/30/0.7569	86.57	5.06
	DABC Algorithm[60]	33,34,35,36,37	1968/32/0.95 1555/14/0.95	90.63	4.99
	Proposed BO Algorithm	33,34,35,36,37	1832/31/0.7998 550/17/1 792/14/0.8201	86.5804	5.1
	HPSO Algorithm[31]	33,34,35,36,37	377/29/0.85 1159/15/0.85 1677/31/0.85	84.16	5.04
	CTLBO Algorithm[89]	33,34,35,36,37	938/13/0.9692 522/16/0.9265 1936/30/0.7729	83.39	5.07
Case-2	Proposed BO Algorithm	7,9,14,28,32	843/17/0.8309 2275/31/0.800	92.7889	7.06
	DABC Algorithm[60]	7,10,14,28,32	2962/25/0.95 909/9/0.95	58.86	6.31

Table 2.5 shows the various technical parameters, DGs locations, DGs sizes, power factors for optimal placement of DGs in scenario 1. From Table-2.5, the following points are observed. In the case of active power loss minimization, active power loss of the system is reduced to 4.2657 kW (accounts for 98.10 % of active power loss reduction), 5.2978 kW (accounts for 97.64 % of active power loss reduction with respect to the base case) when DGs are placed in case-1 and case-2 respectively. In the case of maximization of maximum loadability of the system, λ_{max} improved to 4.91 and 7.73 in case-1 and case-2, respectively. And it is also observed that in the case of maximization of maximum loadability of the system, active power loss of the system is reduced to 89.8601 kW and 93.9651 kW in case-1 & 2, respectively, accounts for 60 % & 58.52 % reduction only. Therefore, from scenario-1, it is concluded that a multi-objective approach is needed to improve both the objectives, i.e., active power loss reduction and λ_{max}.

Table 2.5 Simulation results of 69-bus system for scenario-1

Parameters	**Initial configured network**		**Optimal reconfigured network**	
	Power loss Minimization (f1)	**Maximum Loading Maximization (f2)**	**Power loss Minimization (f1)**	**Maximum Loading Maximization (f2)**
Active power loss (in kW)	4.2657	89.8601	5.2978	93.9651
$\boldsymbol{\lambda_{max}}$	4.21	4.91	6.49	7.73
Minimum and Maximum voltage (in p.u)	0.9943 & 1.0047	0.9818 & 1.0497	0.9938 & 1	0.9899 & 1.05
% KVA DG INJECTION	68.79	93.56	64.45	98.58
% PLR	98.10	60.05	97.64	58.22
% MLI	30.84	52.95	102.18	140.18
DGs sizes (in kW)/Bus/power factor	0495/11/0.81 1675/61/0.81 0378/18/0.83	2292/61/0.80 0500/36/0.80 0724/62/0.84	1418/61/0.81 0488/64/0.82 0536/11/0.81	0214/69/0.83 0378/62/0.80 3207/61/0.83

The simulation outcomes of Ɛ-constraint MOBOA for different values of Ɛ is depicted in Figure 2.7.

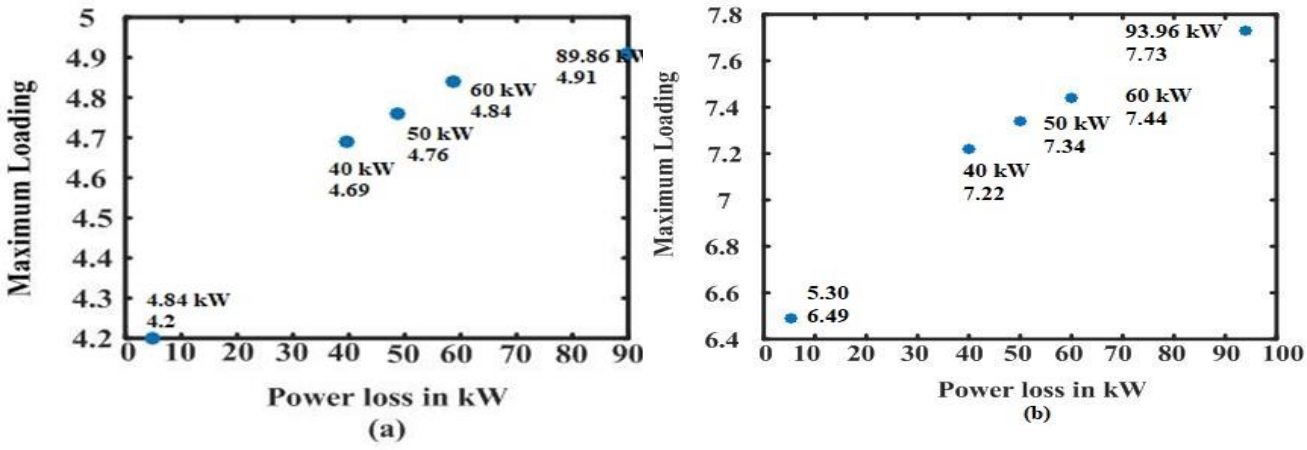

Figure 2.7 Simulation outcomes of 69-bus system for scenario-2 cases (Ɛ-constraint MOBOA) (a) Without reconfiguration (b) With reconfiguration

From the outcomes depicted in Figure 2.7, it can be concluded that both objectives are conflicting in nature. Due to the importance of minimization of active power loss to the lowest value, the value of Ɛ is taken as 40 kW is chosen to determine the optimal DGs locations, DGs sizes & DGs optimal power factors. Table 2.6 shows the various technical parameters, DGs locations, sizes and power factors for optimal placement of DGs in scenario 2.

Table 2.6 Simulation results of 69-bus system for scenario-2

Parameters	**Initial reconfigured network**	**Optimal Reconfigured Network**
	Ɛ = 40 kW	**Ɛ = 40 kW**
Active power loss (in kW)	37.62	38.87
λ_{max}	4.69	7.22
Min voltage (in p.u)	0.9943	0.9921
Max voltage (in p.u)	1.0348	1.0293
DGs sizes (in kW)/ DGs location/ DGs power factor	0211/64/0.78 0481/18/0.80 2433/61/0.86	0309/68/0.87 2436/61/0.81 0539/25/0.78

From Table 2.6, it is observed that a remarkable improvement of λ_{max} and active power loss reduction is observed in case-2 instead in case-1, i.e., λ_{max} is improved from 3.21 to 7.22, the active power loss of the system is reduced to 38.87 kW. The voltage profile graphs and the maximum loading curve for both cases in scenario-2 are shown the Figure 2.8 & Figure 2.9, respectively.

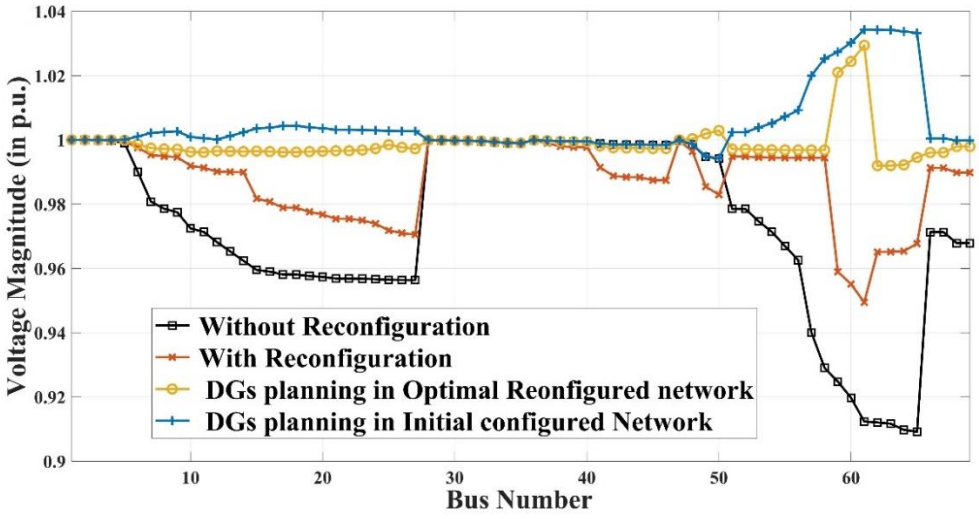

Figure 2.8 Voltage profiles of 69-bus system for Scenario-2

(Ɛ- Constraint MOBOA method when Ɛ = 40 kW)

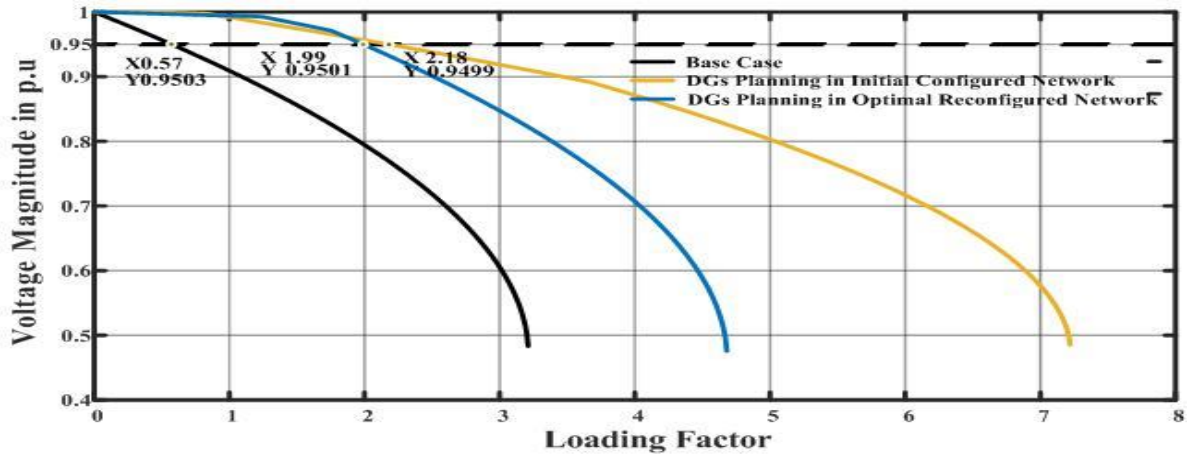

Figure 2.9 Maximum Loading curves of 69-bus system for Scenario-2

(Ɛ- Constraint MOBOA method when Ɛ = 40 kW)

From Figure 2.9, due to the consideration of maximum loadability as one of the objectives, it is observed that the loading marginal factor of the system is improved to 2.18, which indicates system bus voltages are within the permissible limits even though system load increased by

118%. To check the effectiveness of the proposed algorithm and proposed methodology, the results of scenario-1 are compared in Table 2.7. The BO algorithm performs well in compassion to other HTLBO-GWO, DABC and HPSO algorithms.

Table 2.7 Comparison results of 69 Bus system

Scenarios	**Method**	**Open switch Positions**	**DGs sizes in kW/BUS/ p.f**	**Active power loss (kW)**	λ_{max}
Scenario-1 (Power Loss Minimization)					
Case-1	Proposed BO Algorithm	69,70,71,72,73	0495/11/0.81 1675/61/0.81 0378/18/0.83	4.2657	4.21
	HLTBO-GWO[62]	69,70,71,72,73	523/18/0.8294 1000/61/0.8191 723/62/0.8020	7.27	---
	UVDA Heuristic Method[52]	69,70,71,72,73	1.41+j1/61 0.604+j0.432/11 0.417+j0.27/17	7.676	---
Case-2	Proposed BO Algorithm	14,58,61,69,70	1418/61/0.81 0488/64/0.82 0536/11/0.81	5.2978	---
	UVDA Heuristic Method[52]	14,58,61,69,70	1.378+j0.984/61 0.62+j0.443/11 0.722+j0.514/64	9.3493	---
Scenario-2 (Loadability maximization)					
Case-1	Proposed BO Algorithm	69,70,71,72,73	2878/61/0.75	103.3991	4.92
	HPSO Algorithm[31]	69,70,71,72,73	3161/61/0.85	104.86	4.91
	DABC Algorithm[60]	69,70,71,72,73	3453/61/0.95	86.56	4.83
	Proposed BO Algorithm	69,70,71,72,73	2292/61/0.80 0500/36/0.80 0724/62/0.84	89.8601	4.91
	HPSO Algorithm [31]	69,70,71,72,73	3104/61/0.85 27.3/63/0.85 130/46/0.85	87	4.91
Case-2	Proposed BO Algorithm	14,58,61,69,70	3317/61/0.8553	115.3704	7.73
	DABC Algorithm[60]	13,17,38,57,63	3454/61/0.95	91.85	7.53
	Proposed BO Algorithm	14,58,61,69,70	200/26/0.995 3085/61/0.7994	105.8002	7.73
	CLTBO Algorithm[89]	14,58,61,69,70	382/25/0.99929 3389/61/0.8707	113.961	7.73
	Proposed BO Algorithm	14,58,61,69,70	200/25/0.987 3104/61/0.804 264/11/0.950	102.149	7.73
	CLTBO Algorithm[89]	14,58,61,69,70	122/32/0.8112 3087/61/0.7999 338//65/0.9987	102.149	7.73

Figure 2.10 and Figure 2.11 depicts the convergence graphs given by BO & Ɛ- Constraint MOBOA for scenario-1 & 2 of 33 bus respectively. Figure 2.12 and Figure 2.13 depicts the convergence graphs given by BO & Ɛ- Constraint MOBOA for scenario-1 & 2 of 69 bus respectively.

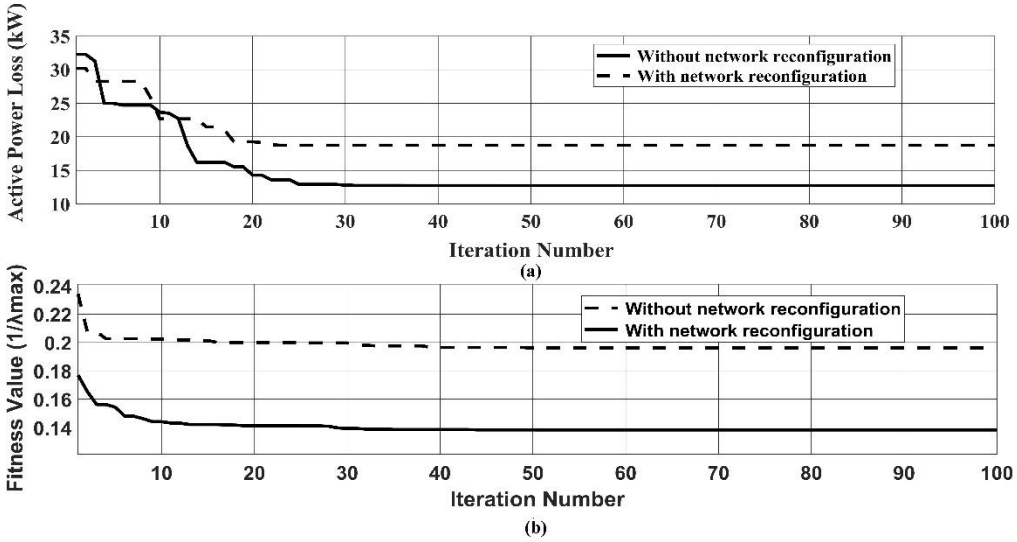

Figure 2.10 convergence graphs given by BO algorithm for 33 bus system simulation outcomes (a) Power loss minimization case (b) Maximum loadability enhancement case

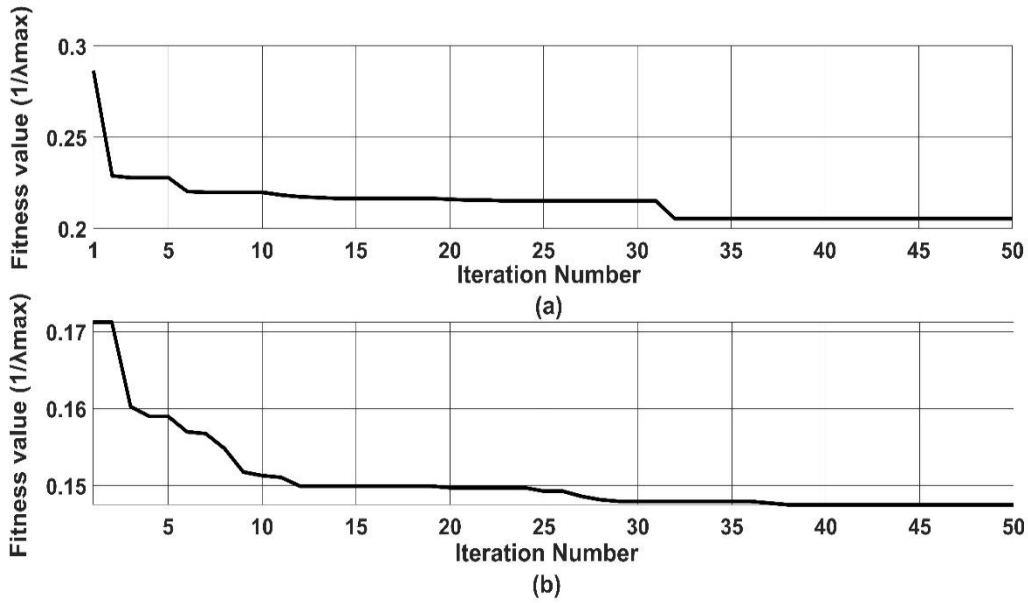

Figure 2.11 convergence graphs given by Ɛ- Constraint MOBOA for 33 bus system simulation outcomes (a) Without reconfiguration case (b) with reconfiguration case

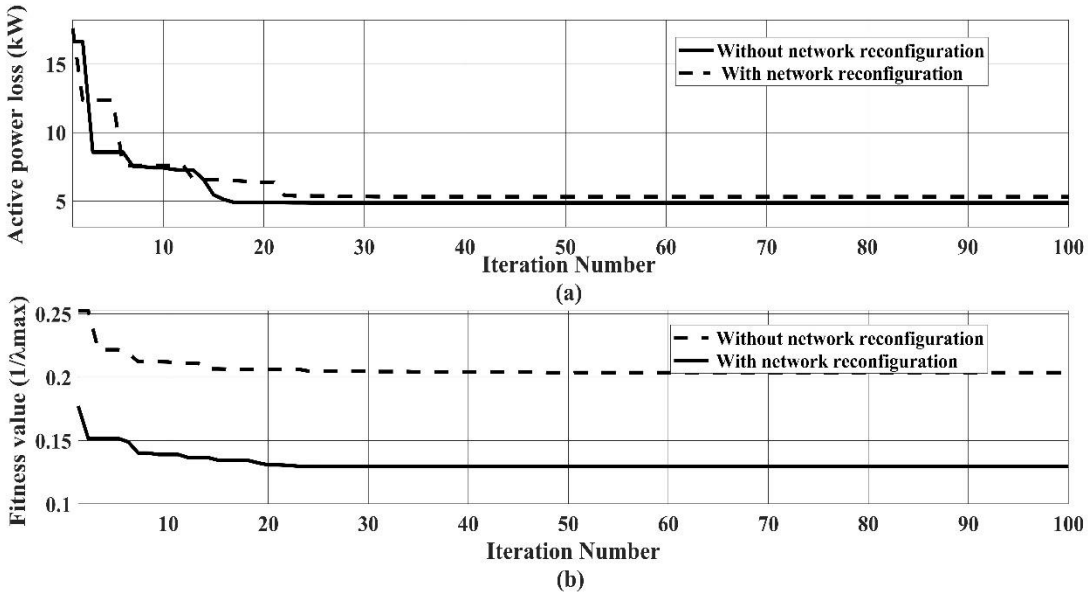

Figure 2.12 convergence graphs given by BO algorithm for 69 bus system simulation outcomes (a) Power loss minimization case (b) Maximum loadability enhancement case

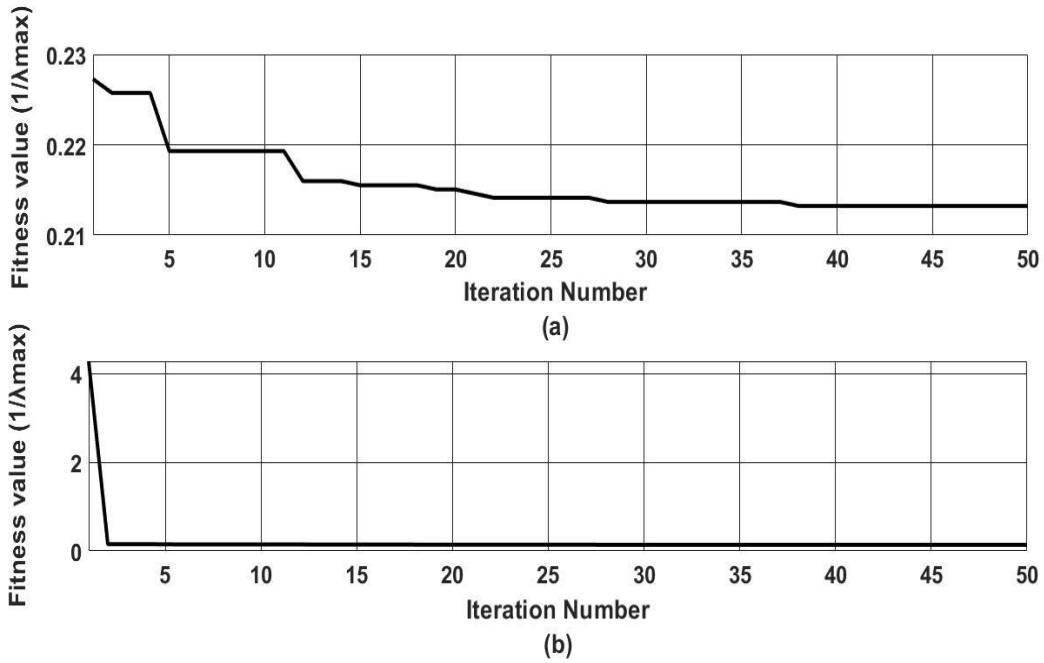

Figure 2.13 convergence graphs given by Ɛ- Constraint MOBOA for 69 bus system simulation outcomes (a) Without reconfiguration case (b) With reconfiguration case

2.5 Summary and comments

This work presented optimal planning of DGs and optimal network reconfiguration of radial distribution network problems for improving network's efficiency and maximum loadability Improvement in above-two mentioned objectives of the distribution system is addressed at peak load level of the system without considering load and DGs uncertainties**.** Therefore, this work corresponds to finding the injection of how much active and reactive power by DGs optimally into the system at optimal locations with respect to systems' peak load level for the improvement of above-two mentioned objectives to maximum extent. To achieve the objectives, two scenarios with two cases per scenario have considered. BO algorithm has been selected to optimize the desired objective functions and implemented on 33 & 69 Bus standard test systems. To optimize both the objective functions, Ɛ-constraint method has been used. obtained results show the improvement in all the objectives i.e., maximum system loadability and active power loss reduction has observed in case-2 of scenario-2 i.e., in case of multi-objective optimization using Ɛ-constraint method by optimal planning of DGs in optimal reconfigured network. The test systems' active power loss is reduced to around 80%, maximum loadability is improved to around (100-120) %. From the outcomes, it is also observed that loading marginal factor of the system is also improved due to the consideration of maximum loadability as one of the objectives which indicates a future load growth can be effectively met by the system without violating system bus voltages permissible limits. However, the improvement in objectives to that extent is due to the (80-85) % of kVA injection by DGs into the distribution system. The above system performance is achieved by the injection of optimal active and reactive powers at optimal locations with the help of single DG unit (or) combination of multiple DG units (Micro-Turbines & synchronous compensators). The similar system performance is achieved at other load levels other than system's peak load if DGs adjust its power output in accordance with load changes provided DGs are dispatchable (BIOMASS, Micro-Turbine etc.) in nature. But, in the case of optimal planning of non-dispatchable PV & WT units, modelling of DGs at peak load level and their adjustment of output power in accordance with load changes is not possible. Therefore, in the next chapter, optimal planning of non-dispatchable PV & WT units & dispatchable PV-BESS & WT-BIOMASS units by considering load and generation uncertainties is discussed.

Chapter 3

Probabilistic optimal planning of dispatchable distributed generator units in distribution systems using a Pareto-based multi-objective chaotic velocity-based butterfly optimization algorithm

3.1 Introduction

This chapter primarily covers the optimal planning of non-dispatchable PV & WT units, dispatchable PV-BESS, and WT-BIOMASS units in the distribution system. In literature, several authors addressed the optimal injection of active & reactive powers at the peak load level of the distribution system for improving the system performance, and the system performs similarly at load levels other than its peak load if DGs adjust their power output in accordance with variations in load, provided DGs are dispatchable. In literature, several researchers addressed optimal planning of non-dispatchable units (usually can't adjust their output power in accordance with the needs, e.g., PV & WT units) by considering load and generation uncertainties. Authors in [66], [71], [95] addressed the optimal integration of PV (Photo-Voltaic) and WT (Wind Turbine) units in electrical distribution networks by considering daily load demand, solar radiance & wind speed uncertainties for the improvement of system performance. From the above papers, it has been observed that both PV and WT units are non-dispatchable, i.e., they don't have complete control over the amount of active power & reactive power injection into the system due to the dependency of DGs output power on solar radiance & wind speed. Better enhancement in system performance (energy loss reduction, enhancement of system's voltage profile etc.) is achieved if DGs dispatch/inject power optimally into the system during each hour of the day. Therefore, to overcome the non-dispatchable nature of PV, the PV unit is assisted by BESS so that during the day time PV unit will supply power to both the grid & BESS, and during nighttime, the battery will supply power to the grid. Similarly, in the case of the WT-Biomass unit, the difference of power between the required power from the WT-Biomass unit and the WT unit at that time will be supplied by the Biomass unit. Authors in [72] addressed the optimal integration of PV-BESS units in the distribution system to mitigate energy loss, and authors in [74] addressed the optimal integration of either PV-BESS or WT-Biomass units in the

distribution system for the mitigation of energy loss. In the above papers, researchers addressed the optimal planning of DGs for energy loss minimization only. And also, it is observed that energy loss of the system is reduced to the utmost value by dispatching more power into the system by DGs (PV-BESS, WT-Biomass), which increases the DGs sizes and the corresponding installation and maintenance costs. Therefore, to create a balance between the amount of power injected by DGs into the system and improvement in technical parameters, in this work, economic aspects of DGs are taken as one of the objectives along with the objective's energy loss reduction & voltage deviation index. Pareto-based multi-objective optimization generates a set of non-dominant solutions between the competing objectives, whereas other multi-objective techniques (such as the weighted sum method and the -constraint method) reduce multi-objective optimisation to single-objective optimisation. Additionally, there is no need to give weights to the objective functions in pareto-based multi-objective optimisation. Therefore, in this work, the above-cited three objectives are optimized with an improved version of BOA, i.e., Pareto-based multi-objective chaotic velocity-based butterfly optimization algorithm.

To summarise, this chapter main contributions are as follows

1. Optimal integration of dispatchable distributed generations (DDG): PV-BESS (Photovoltaic System-Battery energy storage system), WT-Biomass (Wind Turbine) in the distribution system that is optimally restructured.

2. This study's aims include enhancing the voltage profile of the system, lowering the installation & maintenance costs of DGs, and slashing the system's energy loss.

3. A multi-Objective Pareto-based chaotic velocity butterfly optimization algorithm (MOCVBOA) is taken to optimize the objectives.

4. The TOPSIS method, recently becoming a famous method among the other available methods for selecting the most compromised solution from the Pareto front is used in this work.

5. To achieve the desired outcomes, five scenarios are considered in this work and a detailed analysis of the outcomes is presented.

The remainder of this chapter is articulated as follows; Section 2 focuses on PV and WT unit uncertainty modelling, a mathematical description of this work is introduced in Section 3,

Section 4 will give brief insights into the BOA & VBOA optimization technique and specific implementation aspects of it, Section-5 will illustrate the scenarios taken in this work and the associated results.

3.2 Modelling of PV and WT units

Statistical techniques that employ probability density functions (PDFs) are typically used to deal with any random variable's intermittent or probabilistic nature. Authors in [96] concluded that the Beta probability distribution function was the most fitted distributed function in coping with the probabilistic nature of solar radiance. Similarly, researchers concluded that Weibull PDF was the most fitted distributed function in coping with the probabilistic nature of wind speed. Based on this, a few researchers developed [66], [70], [97]–[99] various probabilistic methods using beta & Weibull PDFs. The probabilistic method used in [70], [71] for dealing with the uncertainty involved in PV & WT units output powers is employed in this work, which determines the typical p.u PV & WT output power curves from historical solar irradiance data.

3.2.1 Modelling of solar radiation

Solar irradiance's probabilistic or intermittency nature follows the Beta PDF [71]. The Beta PDF function ($f_b(s^t)$) for calculating the probability of solar radiance at particular time interval (s^t) is given below

$$f_b(s^t) = \begin{cases} \frac{\Gamma(\alpha^t+\beta^t)}{\Gamma(\alpha^t)\Gamma(\beta^t)} s^{t^{(\alpha^t-1)}}(1-S^t)^{(\alpha^t-1)} & , \quad 0 \le S^t \le 1, \alpha^t, \beta^t \ge 0 \\ 0, & otherwise \end{cases} \tag{3.1}$$

where $(\boldsymbol{\alpha^t}), (\boldsymbol{\beta^t})$are the shape parameters of Beta PDF, $\boldsymbol{\Gamma}$ is the gamma function. Shape parameters of the Beta PDF are calculated from the standard deviation (σ^t), mean (μ^t) and their corresponding equations for calculation are given below

$$\boldsymbol{\beta^t} = (1-\mu^t)(\frac{\mu^t\,(1+\mu^t)}{{\sigma^t}^2} - 1) \tag{3.2}$$

$$\boldsymbol{\alpha^t} = \frac{\mu^t * \boldsymbol{\beta^t}}{1-\mu^t} \tag{3.3}$$

3.2.2 Modelling of wind speed

Wind speed's probabilistic or intermittency nature follows the Weibull PDF [71]. The Weibull PDF function $f_v(v^t)$ for calculating the probability of wind speed at particular time interval (v^t) is given below

$$f_v(v^t) = \frac{k^t}{c^t} * \left(\frac{v^t}{c^t}\right)^{k^t-1} * exp\left(-\left(\left(\frac{v^t}{c^t}\right)^{k^t-1}\right)\right) \quad (3.4)$$

Where (k^t), (c^t) are the Shape parameters of the Weibull PDF calculated from the mean (μ^t), standard deviation (σ^t) and their corresponding equations for calculation are given below

$$k^t = \left(\frac{\sigma^t}{\mu^t}\right)^{k^t-1} \quad (3.5)$$

$$c^t = \frac{\mu^t}{\Gamma(1+1/k^t)} \quad (3.6)$$

3.2.3 Modelling of the output power generated by PV and WT units

To determine the PV and WT output power generation for each hour of the day, samples of solar radiance and wind speed for three years are collected from a specific site. Afterwards, from (3*365) samples for every hour, the standard deviation and mean of solar radiance & wind speed for a typical day are determined. After that, each hour is divided into several n_s States. Afterwards, during each interval, an average of solar radiation & wind speed is calculated (Consider the case when the number of states is fixed to 20, then for the first interval, the limits of solar radiation are 0 & 0.05kW/m^{2,} then the average solar radiation for the first state is 0.025 kW/m^2). Then, the hourly average output power from the PV and WT from the above-obtained data is calculated from the following mathematical formulations

The hourly average output power from the PV (P_{PV}^t) [95] during the time interval 't' is obtained from the following equation

$$P_{PV}^t = \sum_{g=1}^{n_s} P_{PV_0}(s_{avg}^g) * f_b(s_{avg}^g) \quad (3.7)$$

where n_s represents the number of states, $P_{PV_0}(s_{avg}^g)$ represents the power generation from the PV unit with average solar radiation in the gth state and the corresponding equations for the calculation of $P_{PV_0}(s_{avg}^g)$ are given below

$$P_{PV_0}(s_{avg}^g) = N_{PV\,mod} * FF * V_g * I_g \quad (3.8)$$

$$FF = \frac{V_{MPP} * I_{MPP}}{V_{OC} * I_{SC}} \quad (3.9)$$

$$V_g = V_{OC} - k_V * T_{cg} \quad (3.10)$$

$$I_g = s_{avg}^{g}[I_{SC} + k_i * (T_c - 25)] \quad (3.11)$$

$$T_{cg} = T_A + s_{avg}^{g} * (\frac{N_{OT}-20}{0.8}) \quad (3.12)$$

where $N_{PV\,mod}$, FF, I_{MPP}, V_{MPP}, I_{SC}, V_{OC}, k_i, k_V, T_{cg}, T_c, N_{OT}, T_A represents the number of PV modules, fill factor, current (A) and voltage (V) at the maximum power point, short circuit current (A) and open-circuit voltage (V), current and voltage coefficients in V/^{o}C, A/^{o}C, PV module temperature, cell temperature, Nominal operating temperature & ambient temperature respectively.

Similarly, the hourly average output power from the WT (P_{WT}^{t}) [95] during the time interval 't' is obtained from the following equation

$$P_{WT}^{t} = \sum_{g=1}^{n_s} P_{WT_0}(v_{avg}^{g}) * f_b(v_{avg}^{g}) \quad (3.13)$$

where (v_{avg}^{g}) represents the WT power generation with average wind velocity in the gth state and the corresponding equations for the calculation of $P_{WT_0}(v_{avg}^{g})$ are given below

$$P_{WT_0}(v_{avg}) = \begin{cases} 0 & v_{avg} < v_{cin} \ \ or \ \ v_{avg} > v_{cout} \\ (A * v_{avg}^{3} + B * P_r) & v_{cin} \leq v_{avg} \leq v_r \\ P_{r,WT} & v_{cin} \leq v_{avg} \leq v_{cout} \end{cases} \quad (3.14)$$

$$A = \frac{P_{r,WT}}{(v_r^3 - v_{cin}^3)} \quad (3.15)$$

$$B = \frac{v_{cin}^3}{(v_r^3 - v_{cin}^3)} \quad (3.16)$$

where $v_r, v_{cin}, v_{cout}, P_{r,WT}$ are the rated speed, cut-in speed, cut-out speed, and rated power of wind turbine respectively.

3.2.4 Modelling of Battery energy storage system (BESS)

The discharging and charging mode of batteries are modelled using the following equations [70]

$$E_{BES}(t+1) = E_{BES}(t) - \Delta t * \frac{P_{BES}^{disch}}{\eta_d} \quad (3.17)$$

$$E_{BES}(t+1) = E_{BES}(t) + \Delta t * P_{BES}^{cb} * \eta_c \quad (3.18)$$

where $E_{BES}(t)$ represents the energy in the battery in kWh during t[th] time interval, P_{BES}^{disch}, P_{BES}^{cb}, η_d, η_c are the discharging power & charging power (kW), discharging & charging efficiency of the batteries, respectively.

BESS must satisfy the following charging power & discharging power constraint limits, and energy storage limit constraints.

$$0 \leq P_{BES}^{disch} \leq P_{BES}^{disch,max} \tag{3.19}$$

$$0 \leq P_{BES}^{cb} \leq P_{BES}^{cb,max} \tag{3.20}$$

$$E_{BES_{min}} \leq E_{BES}(t) \leq E_{BES_{max}} \tag{3.21}$$

where $P_{BES}^{disch,max}$, $P_{BES}^{cb,max}$, $E_{BES_{min}}$&$E_{BES_{max}}$ are the maximum discharge & charge limits of the battery, minimum and maximum energy storage limit constraints.

3.2.5 Modelling of Biomass Output power

Since the output from the Biomass unit is dispatchable in nature, and also in this work biomass unit acts as a backup for WT, the maximum size of the biomass unit and its dispatchable hourly output is determined to form the procedure explained in the latter section of this paper.

3.3 Problem Formulation

Optimal integration of DDGs in the system improves the efficiency, voltage profile, loadability, EENS, Economic aspects etc. In this work, enhancement of the system's maximum loadability is not considered because the improvement of this technical metric to the extent quoted in chapter-2 associated with a huge injection of active & power reactive power into the system, which requires large sizes of DGs and the associated huge annual installation costs of DDGs. Therefore, in this work, the improvement of three objectives is considered: minimization of energy loss for the improvement of system efficiency, minimization of total voltage deviation for the improvement of system voltage profile, and annual economic cost, which deals with the annual & maintenance costs of DDGs.

Apart from that, the following assumptions are made in this work

1) The Optimal integration of DDGs (PV-BESS, WT-BIOMASS) in the 33 & 69 bus distribution systems is considered in this work.

2) The distributed generator will supply reactive power with the help of a grid-connected inverter [100]–[102]. If the kVA rating of the DG Inverter is oversized by the suitable percentage of the maximum kW rating of the distributed generator, then the DG system will have the capability to supply reactive power with a constant power factor. Hence in this work, it is assumed that the DDGs are working at 0.9 power factor by oversizing the DG inverters with a suitable percentage.
3) Distribution network buses are subjected to identical wind and solar irradiance conditions.
4) For load flow studies, DDGs are modelled as negative PQ-Load modelling in the system.

3.3.1 Objective Functions

3.3.1.1 Energy Loss

Optimal integration of DDGs in the system improves the system's efficiency by reducing the system's energy loss (E_{loss}). Energy loss of the system for a 24-hour daily load pattern is obtained by adding all the distribution system active power losses in each hour of that day. The mathematical formulation of the system's energy loss is given below.

$$Minimize\ f_1 = E_{loss} = \sum_{t=1}^{24} \sum_{j=1}^{nb-1} J_{t,j}^2 * R_j \quad (3.22)$$

where nb , $J_{t,j}, R_j$ are the number of buses, branch current and branch resistance, respectively.

3.3.1.2 Total Voltage Deviation

The goal of voltage profile enhancement is to align all the bus voltage magnitudes as closely as possible to offer uniform voltage profiles for the customers. To achieve this, Total Voltage Deviation (TVD), a mathematically formulated function, is used as one of the objectives. At first, for each hour in a day, Voltage Deviation (VD) is obtained by taking the sum of the squares of the voltage deviations of all the buses concerning 1 p.u. After that, the Total Voltage Deviation (TVD) for a day is obtained by adding all the VD's. Therefore, the system's total voltage deviation (TVD) must be decreased to enhance the system voltage profile. Mathematical formulations of the VD and TVD are given below

$$VD_t = \sum_{i=1}^{Nbus} (1 - V_{t,i})^{\,2}\ t = 1,2,\ldots 24 \quad (3.23)$$

$$Minimize\ f_2 = TVD = \sum_{t=1}^{24} VD_t \quad (3.24)$$

3.3.1.3 Annual Economic Cost (AEC)

As the integration of DDGs in the distribution system reduces energy loss, the cost associated with buying that reduced energy loss from the distribution system operator is saved. However, the integration of DDGs in the system is related to annual installation and maintenance costs. And also, the reduction in the system's energy loss due to the integration of DDGs depends on the amount of power injected by the DDGs into the system optimally. Higher penetration of power by DDGs into the system results in higher energy loss reduction but higher annual installation & maintenance costs of DDGs and vice-versa. Therefore, to create a balance between yearly installation & maintenance costs of DDGs and energy loss reduction, an objective function named Annual Economic Cost (AEC) is mathematically formulated as shown below

$$Minimize\ f_3 = AEC = k_e * (E_{loss}) * 365 + (AI_{DDG} + OM_{DDG}) \quad (3.25)$$

where k_e, AI_{DDG}, OM_{DDG} are the electricity price in \$/kW-hr, annual installation costs and maintenance costs in \$ respectively.

$$AI_{DDG} = \left(N_{pv} * INC_{pv} * P_{r,PV} + N_{wt} * INC_{wt} * P_{r,WT} + N_{bio} * INC_{bio} * P_{r,bio}\right) * CRF_{DG} + (N_{BESS} * INC_{BESS}) * CRF_{BESS} \quad (3.26)$$

$$OM_{DDG} = 365 * \sum_{i=1}^{24}(OMC_{pv} * P_{t,PV} + OMC_{wt} * P_{t,wt} + OMC_{bio} * P_{t,bio} + OMC_{bess} * N_{BESS} \quad (3.27)$$

$$CRF_{DG} = \frac{k*(1+k)^{nDG}}{(1+k)^{nDG}-1} \quad (3.28)$$

$$CRF_{BESS} = \frac{k*(1+k)^{nBESS}}{(1+k)^{nBESS}-1} \quad (3.29)$$

Where $N_{pv}, N_{wt}, N_{bio}, N_{BESS}$represents the number of respective DDG units,INC_{pv}, INC_{wt}, INC_{bio}, INC_{BESS} are respective installation costs of individual DDG units, $P_{r,PV}$, $P_{r,WT}$, $P_{r,bio}$ are rated power of respective DDG units, OMC represents the operational and maintenance cost, $P_{t,PV}$, $P_{t,wt}$, $P_{t,bio}$ represents the power dispatched by respective DDGs in the tth hour, CRF represents the capital recovery factor of respective DDGs, k, nDG, nBESS represents the rate of interest, and number of years for the annual payment of respective DDGs.

3.3.1.4 Constraints

i) Power balance constraints: During each hour in a day, Combined power delivered by the substation and DDGs ($P_{t,sub} + P_{t,T,DG}$) must be equal to total system demand and losses ($P_{t,load} + P_{t,loss}$)

$$P_{t,sub} + P_{t,T,DG} = P_{t,load} + P_{t,loss} \quad (3.30)$$

$$Q_{t,sub} + Q_{t,T,DG} = Q_{t,load} + Q_{t,loss} \quad (3.31)$$

ii) The voltage magnitude of the buses in the system must be within the permissible minimum and maximum limits.

$$|V_{min}| < |V_{t,j}| < |V_{max}| \qquad j = 1,2 \ldots\ldots Nbus \quad (3.32)$$

In this paper, $|V_{min}|$ = 0.95 p.u. and $|V_{max}|$ =1.05 p.u. are considered.

iii) Each branch's total current should be less than the branch's maximum current rating.

$$I_{t,J} \leq I_{t,J}^{max} \qquad j = 1,2 \ldots\ldots Nbus - 1 \quad (3.33)$$

iv) Total real power ($P_{t,T,DG}$) and reactive power injected ($Q_{t,T,DG}$) by DDGs in the tth hour must be less than a certain percentage (k_{per}) of distribution system real ($P_{t,load}$) and reactive power ($Q_{t.load}$) demand in that hour.

$$P_{t,T,DG} \leq (k_{per}) * P_{t,load} \quad (3.34)$$

$$Q_{t,T,DG} \leq (k_{per}) * Q_{t,load} \quad (3.35)$$

3.3.2 Sizing of PV-BESS and WT-Biomass units

This work considers the optimal integration of two DDGs (PV-BESS & WT-Biomass) units operating with 0.9 pf in the distribution system. As shown in Figures 3.1 & Figure 3.2, WT & PV units alone cannot deliver power according to the daily load curve because of the intermittency nature of wind speed and solar radiation. If the distributed generators provide power optimally each hour in the day, there is much improvement in the above-mentioned objective functions. Therefore, the PV unit is aided by the BESS unit & the Biomass unit aids the WT unit to make them dispatchable. And both hybrid units will deliver power according to the load curve.

3.3.2.1 Sizing of PV-BESS unit

Figure 3.1 shows the conceptual design of the PV-BESS dispatchable unit [70]. As shown in Figure 3.1, during the daytime (during the abundance of solar radiation), the PV unit will deliver power to both the grid & BESS (charging mode). And during the night-time, the BESS unit (discharging mode) will provide power to the grid. Mathematical formulations for the sizing of PV and BESS are given below.

Let us say the PV-BES unit is installed on bus-q in the system, and the energy delivered by the combination of the PV-BESS unit to the distribution system via bus q ($E_{PV+BESS}$) for the 24 hours is the summation of power delivered by the PV-BESS unit to the grid ($P_{t,(PV+BES)}$) during each hour

$$E_{PV+BESS} = \sum_{t=1}^{24} P_{t,(PV+BES)} \quad (3.36)$$

The total output energy from the PV-BESS unit includes energy supplied by PV and BESS to the system via bus q ($E_{PV}^{Grid}, E_{BESS}^{Disch}$), the total output energy supplied by the PV unit includes energy provided to the system via bus q and BESS ($E_{PV}^{Grid}, E_{BESS}^{Ch}$),

$$E_{PV+BESS} = E_{PV}^{Grid} + E_{BESS}^{Disch} \quad (3.37)$$

$$E_{PV} = E_{PV}^{Grid} + E_{BESS}^{ch} \quad (3.38)$$

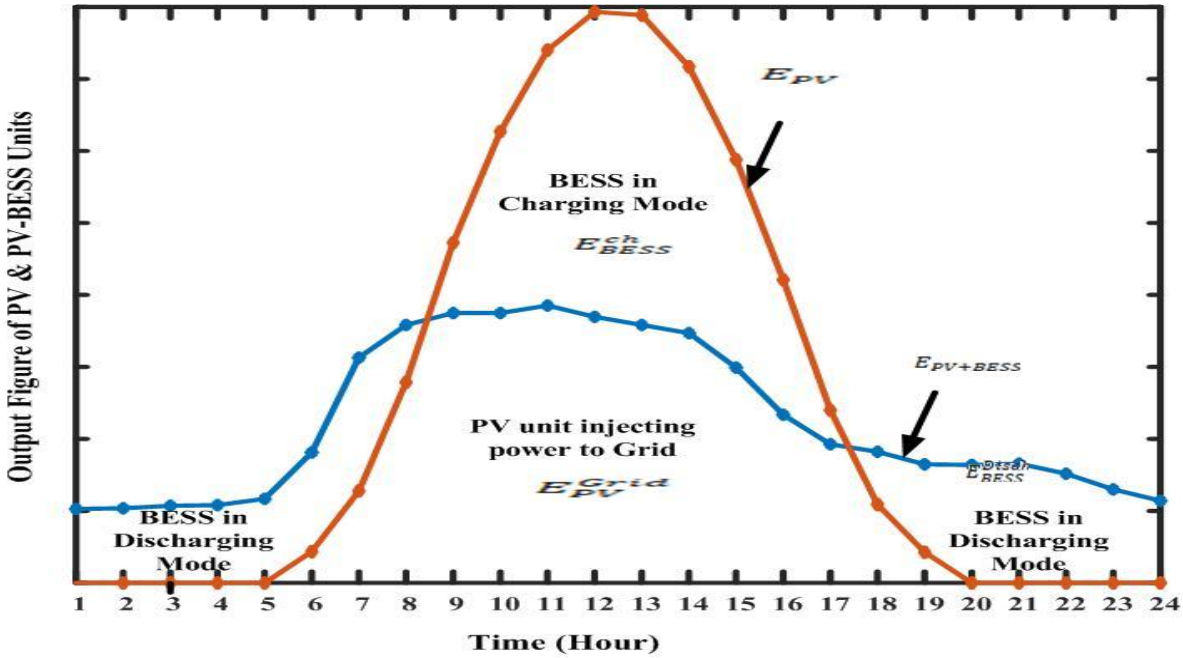

Figure 3.1 Conceptual design of PV-BESS unit

The relation between the total discharging and charging energy of the battery with the round-trip efficiency of η_{BES} is expressed as

$$E_{BES}^{Disch} = \eta_{BES} * E_{BES}^{cb} \quad (3.39)$$

Then from the above three equations, E_{PV} is derived as

$$E_{PV} = \frac{E_{PV+BESS} - (1-\eta_{BES}) * E_{PV}^{Grid}}{\eta_{BES}} \quad (3.40)$$

The maximum PV unit power generation over 24 hours with a PV module maximum power output (P_{PV}^{unit}), energy delivered by PV module over 24 hours (E_{PV}^{unit}) is expressed as

$$P_{PV,Max} = \frac{P_{PV}^{unit}}{E_{PV}^{unit}} * E_{PV} \quad (3.41)$$

To determine the unknown quantity E_{PV}^{Grid} in Eq.3.40, by assuming $\eta_{BES} = 1$,$E_{PV+BESS}$ is determined using Eq.3.36, then E_{PV}=$E_{PV+BESS}$, then the initial maximum PV unit power is determined as $P_{PV,Max}{}^{in} = \frac{P_{PV}^{unit}}{E_{PV}^{unit}} * E_{PV}$, and $E_{PV}^{Grid,in}$ is calculated from Figure 2, then the final maximum PV unit power generation is estimated as

$$P_{PV,Max} = \frac{P_{PV}^{unit}}{E_{PV}^{unit}} * \frac{E_{PV+BESS} - (1-\eta_{BES}) * E_{PV}^{Grid,in}}{\eta_{BES}} \quad (3.42)$$

Then the final PV unit size (P_{PV}) and the number of PV units (N_{pv}) are determined as

$$P_{PV} = \frac{P_{r,PV}}{P_{PV}^{unit}} * P_{PV,Max} \quad (3.43)$$

$$N_{pv} = \frac{P_{PV}}{P_{r,PV}} \quad (3.44)$$

The size of the BESS unit is obtained using Eq .3.45

$$\mathrm{E_{BES}} = \frac{E_{PV+BESS} - E_{PV}^{Grid}}{\eta_{BES}} \quad (3.45)$$

3.3.2.2 Sizing of WT-Biomass unit

Figure 3.2 shows the conceptual design of the WT-Biomass dispatchable unit [70]. As depicted in Figure 3.2, the difference in power between the combined WT-Biomass unit ($P_{t,(WT+Biomass)}$) and WT unit ($P_{t,(WT)}$) will be supplied by the Biomass unit.

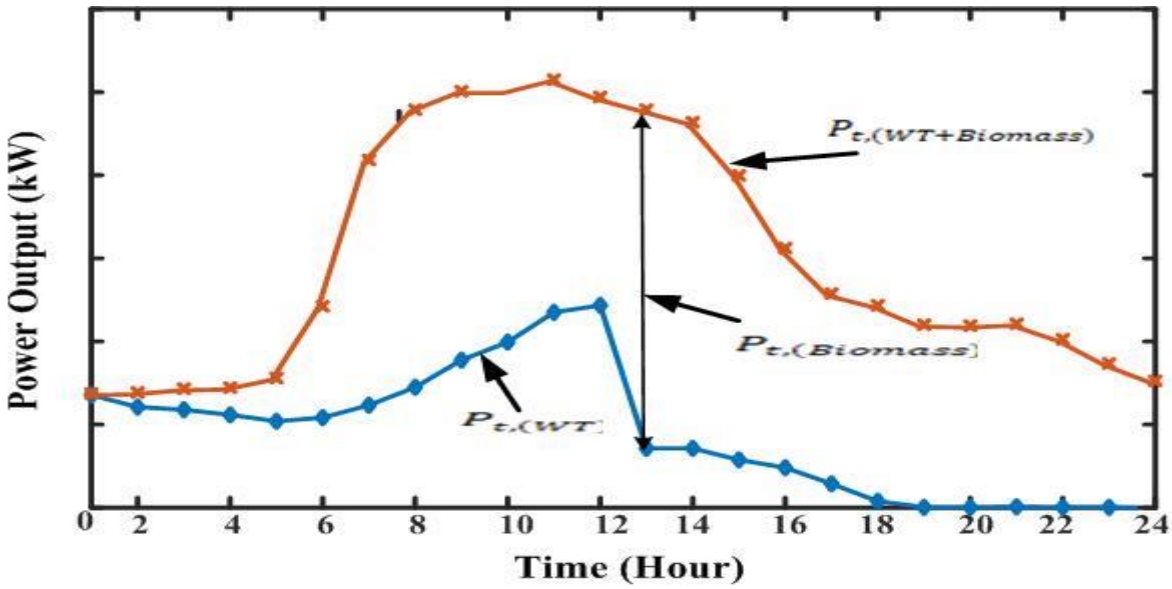

Figure 3.2 Conceptual design of WT-BIOMASS unit

The steps for finding the sizes of WT, Biomass units are

i) Finding the maximum output power of the WT unit ($P_{WT,max}$) from the $hourly\ P_{t,(WT+Biomass)}$ curve on the condition that output power from the wind turbine will never be greater than the power output of the combined WT & Biomass unit.

ii) Then calculate the hourly output power from the wind turbine $P_{t,(WT)}$ from the $P_{WT,max}$& per unit curve of WT turbine.

iii) Then $P_{Biomass,Max}$ is the maximum of difference of all powers between the combined WT-Biomass unit ($P_{t,(WT+Biomass)}$) and WT unit ($P_{t,(WT)}$).

iv) Then the final WT unit size (P_{WT}), the number of WT & Biomass units is determined using

$$P_{WT} = \frac{P_{r,WT}}{P_{WT}^{unit}} * P_{WT,Max} \quad (3.46)$$

$$N_{WT} = \frac{P_{WT}}{P_{r,WT}} \quad (3.47)$$

$$N_{Bio} = \frac{P_{BIo,max}}{P_{r,BIo}} \quad (3.48)$$

3.4 Optimization Algorithm

3.4.1 Chaotic Velocity-based Butterfly Optimization Algorithm (CVBOA)

To overcome BOA's problems during the local and global search phases, the authors in the paper [103] have developed a velocity-based butterfly optimization algorithm by taking inspiration from the velocity update equations in the PSO. The position update equations in the global & local search phases of VBOA are as follows

update the position of ith agent for local search using Eq. 3.49 & 3.50 if $random\ value[0,1] > P$

$$v_i(\mathrm{t}+1) = \mathrm{w(t)} * v_i(\mathrm{t}) + b_3 * r_3 * \left(P_{best}(t) - x_i(t)\right) + \left(r_1 * r_2 * x_j^d(t) - x_k^d(t)\right) * f_i \qquad \mathrm{i} = 1 \ldots\ldots \mathrm{N} \tag{3.49}$$

$$x_i(\mathrm{t}+1) = x_i(\mathrm{t}) + v_i(\mathrm{t}+1) \tag{3.50}$$

where $P_{best}(t)$ is the personal best position of the particle, b_3 is the coefficient factor, r_1, r_2 & r_3 are the uniform random numbers between 0 & 1, w(t) is the inertia weight.

Update the position of ith agent for global search using Eq. 3.51 & 3.52 if $random\ value\ [0,1] < P$

$$x_i(\mathrm{t}+1) = x_i(\mathrm{t}) + \left(r_1 * r_2 * gbest - x_i(\mathrm{t})\right) * f_i \qquad i = 1 \ldots\ldots N \tag{3.51}$$

To avoid the solution getting trapped at local optima, a refraction-based learning strategy is applied to the global best position with a certain probability q.

The equation for RBL strategy on the global best position as follows

$$gbest_i^j = (a_j + b_j) - gbest_i^j \tag{3.52}$$

Where a_j, b_j are the lower and upper bound limits of variable x_i.

Apart from the above modifications made in VBOA, the cubic map chaotic sequence is also applied on the random variable r_2 and r_3 for better exploration capability [104], [105].

$$r_2(t+1) = \rho * r_2(t) * (1 - r_2(t)^2)$$
$$r_3(t+1) = \rho * r_3(t) * (1 - r_3(t)^2) \tag{3.53}$$

where ρ is a control parameter, $r_2(t), r_3(t)$is a chaotic variable at tth step. In this work $\rho, r(0)$ [105] are set to 2.595, 0.315 respectively.

3.4.2 Pareto-based MOVBOA

In multi-objective Pareto-based optimization algorithms, a set of non-dominated solutions are determined from the combined updated & previous iteration population in every optimization

algorithm evolution procedure iteration. A solution $x_1$dominates solution x_2 only if all objectives of x_2 are worse than x_1 and at least one objective of x_1 is better than x_2. Mathematically it can be formulated as [106]

$$\forall k \in \{1, 2, \ldots, N_{obj}\} \rightarrow f_k(x_1) \leq f_k(x_2) \quad (3.54)$$

$$\wedge \exists k \in \{1, 2, \ldots, N_{obj}\} \rightarrow f_k(x_1) < f_k(x_2) \quad (3.55)$$

If the solution $x_1$dominates all the solutions in the merged population, then x_1 enters a non-dominant solution set. Pareto fronts are collections of non-dominant solutions, and the goal of multi-objective optimization is to find the best Pareto front for the given problem.

3.4.3 Cubic Map Chaos Initialization

For the generation of the initial set of solutions in the meta-heuristic optimization algorithms, different types of initialization methods are available in the literature [107]: uniformly random distribution, oppositional-based learning, and chaotic-based initialization. In this work cubic map-based, chaotic initialization method is used for the generation of the initial set of solutions to get a more uniform spreading of initial population positions in the search space.

The mathematical formulation [105] for cubic mapping is given by

$$H(t+1) = \rho * H(t) * (1 - H(t)^2) \quad (3.56)$$

where ρ is a control parameter, $H(t)$ is a chaotic variable at t^{th} step. In this work ρ, $H(0)$ [105] are set to 2.595, 0.315 respectively.

3.4.4 Crowding Distance Metric

The primary goals in pareto based multi-objective optimization are (i) finding the set of solutions as close as possible to Pareto optimal front and (ii) finding set of solutions as diverse as possible. Therefore, to limit the number of solutions in the Pareto front to a predefined number say REP_{max} for preserving the diversity among the solutions, the crowding distance metric is calculated for all the solutions in the Pareto front and the solutions with the highest crowding distance metric are stored in a set called a repository with the size of REP_{max}. The mathematical formulation for crowding distance metric for the nth solution (C_{r_n}) in Pareto front is given as [105], [106]

$$(C_{r_n}) = \sum_{k=1}^{Nobj} \frac{f_k^{n+1} - f_k^{n-1}}{f_k^{max} - f_k^{min}} \quad (3.57)$$

3.4.5 Determination of the most-comprised solution using TOPSIS Method

To obtain the optimal compromised solution from the Pareto front, the fuzzy set theory-based method, game theory max-min method and TOPSIS (Technique for order preference by similarity to ideal solution) method are widely used in the literature. One of the advantages of the TOPSIS method is that there is a provision for assigning weights to the objectives in Pareto solutions for selecting the final compromised solution from the Pareto front. The above-cited advantage of the TOPSIS method motivates the authors of the paper to use this method. The final compromised solution in the TOPSIS method is obtained by measuring the Euclidian distances between the normalized weighted solution of each alternative concerning the positive ideal solution and the negative ideal solution in the Pareto front. The step-by-step procedure for finding the compromised solution using TOPSIS [108] method is as follows.

1. A decision matrix (D) of size $m \times n$ is created.

$$D = \begin{bmatrix} f_1^1 & f_1^2 \ldots\ldots\ldots\ldots f_1^n \\ f_2^1 & f_2^2 \ldots\ldots\ldots\ldots f_2^n \\ & \vdots \\ f_m^1 & f_m^2 \ldots\ldots\ldots\ldots f_m^n \end{bmatrix} \tag{3.58}$$

   where f_m^n represents the n[th] objective function value of the m[th] alternative.

2. A normalized decision matrix (ND) is obtained from the decision matrix (D).

$$ND = \begin{bmatrix} r_1^1 & r_1^2 \ldots\ldots\ldots\ldots r_1^n \\ r_2^1 & r_2^2 \ldots\ldots\ldots\ldots r_2^n \\ & \vdots \\ r_m^1 & r_m^2 \ldots\ldots\ldots\ldots r_m^n \end{bmatrix} \qquad \text{where } r_m^n = \frac{f_m^n}{\sqrt{\sum_{i=1}^{m} f_m^i}} \tag{3.59}$$

3. A weighted normalized decision matrix (WND) is obtained from the decision matrix (ND).

$$WND = \begin{bmatrix} rw_1^1 & rw_1^2 \ldots\ldots\ldots\ldots rw_1^n \\ rw_2^1 & rw_2^2 \ldots\ldots\ldots\ldots rw_2^n \\ & \vdots \\ rw_m^1 & rw_m^2 \ldots\ldots\ldots\ldots rw_m^n \end{bmatrix} \tag{3.60}$$

   where $rw_m^n = (w_1 * r_m^1 + w_{2*} r_m^2 + \ldots\ldots\ldots\ldots + w_{n*} r_m^n)$, w_n represents the assigned weight of the n[th] objective. In this work, equal weight is assigned to three objectives i.e. (Energy loss, Total voltage deviation index, annual economic cost) by meeting the constraint that the sum of all the weights is equal to one.

4. The positive ideal solution (PIS) and negative ideal solution (NIS) are determined from the weighted normalized decision matrix (WND).

$$PIS = \{p_1^+ \;\; p_2^+ \ldots\ldots\ldots\ldots p_n^+\}$$
$$NIS = \{p_1^- \;\; p_2^- \ldots\ldots\ldots\ldots p_n^-\} \quad (3.61)$$

$$where \; p_n^+ = min\{rw_1^n \;\; rw_2^n \ldots\ldots\ldots\ldots rw_m^n\}$$
$$p_n^- = max\{rw_1^n \;\; rw_2^n \ldots\ldots\ldots\ldots rw_m^n\} \quad (3.62)$$

5. Calculation of Euclidian distance of a solution i from the PIS (d_i^+).

$$d_i^+ = \sqrt{\left(\sum_{j=1}^{n} rw_i^j - p_j^+\right)^2}\, i = 1 \ldots . m \quad (3.63)$$

Calculation of Euclidian distance of a solution i from the NIS (d_i^-).

$$d_i^- = \sqrt{\left(\sum_{j=1}^{n} rw_i^j - p_j^-\right)^2}\, i = 1 \ldots . m \quad (3.64)$$

6. Calculation of relative closeness index (RCI) of each solution i, $s_i$is defines as

$$s_i = \frac{d_i^-}{d_i^- + d_i^+} \;\; i = 1 \ldots . . m \quad (3.65)$$

7. A solution with the highest value of RCI is chosen as the most compromised solution.

3.4.6 Implementation of MOCVBOA

The step-by-step procedure for MOCVBOA for optimal integration of DDGs for the improvement of the objectives as mentioned earlier are given below

1. Determination of PV and WT units' p.u. output power curves.

   In this step, P_{WT}^t and P_{PV}^t vector values are determined by reading the three-year solar radiance and wind speed data with the time interval of 10 min, necessary PV unit data & WT data. Then, p.u PV and WT units' output curves are determined from P_{WT}^t and P_{PV}^t.
2. Read the distribution system line and load data, typical p.u 24-hour load curve data.
3. Initialization of parameters of the algorithm such as the population of agents (N), the maximum number of iterations (maxiter), repository size etc.
4. Generation of the initial set of solutions between the minimum and maximum limits.

   In this work, since only the optimal integration of two DDG's considered, four decision variables are there for each agent: DDGs locations ($L_{i,PV-BESS}, L_{i,WT-Biomass}$), DDGs sizes ($P_{i,PV-BESS_{max}}, P_{i,WT-Biomas_{max}}$).
5. Finding objective function values for each agent.

   By using $P_{i,PV-BESS_{max}}, P_{i,WT-Biomas_{max}}$ & typical p.u 24-hour load curve, $P_{i,t,PV-BESS}, P_{i,t,WT-Biomass}$ vector data for 24-hour data is determined and then objective functions are determined by the load-flow run.

6. Set iteration count =0.
7. Update the aroma/fragrance of butterflies.
8. Update the solutions of each agent using Eq.3.49, Eq.3.50, Eq..51 & Eq.3.52.
9. Calculate each updated agent's objective function or fitness value using the sequential process followed in Step 5.
10. Merge updated agents and previous iteration agents and find the non-dominated solutions using the techniques explained in sections 3.4.2 & 3.4.3 and update the solutions in the repository set using the methods explained in section 3.4.4.
11. Find the gbest solution using the fuzzy-based technique from the repository set. i.e., $L_{gbest,PV-BESS_{max}}, L_{gbest,WT-Biomass_{max}}, P_{gbest,PV-BESS_{max}}, P_{gbest,WT-Biomass_{max}}$.
12. Repeat steps 6-11 when iterations fall below the maximum number; otherwise, print out results like the global best solution and objective function values.

    The detailed flowchart is given in APPENDIX-B.

3.5 Results and Discussion

This section applies the MOCVBOA technique for minimization of the system energy loss, total voltage deviation, and annual economic cost using the proposed method on IEEE 33 & 69 bus distribution test systems. The tuned algorithm parameters are given in Table 3.1.

Table 3.1 MOCBOA parameters

Parameters	Value
Number of searching Agents (N)	100
Repository size	60
Maximum number of iterations	300
Modular modality 'c'	0.01
Power exponent 'a'	0.3
Probability switch 'P'	0.7

The wind speed and solar radiance data are taken from [70]. In this work PV module with the characteristics [95] of V_{MPP}=28.36 V, I_{MPP} =7.76 A, V_{OC}=36.96 V, I_{SC}=8.38 A, N_{OT}=43 °C, k_V=0.1278 V/°C, k_i=0.00545 A/°C and PV unit with $N_{PV\,mod} = 600$, rated capacity of 132 kW is considered in this paper, WT unit with a rated capacity [95] of 250 kW, $v_{cin} = 3\ m/s$,

v_{cout} =25 m/s and v_r = 12 m/s is considered. And, battery unit size [109] of 400 kWh, maximum charging and discharging power of 133.33 kW is considered. The typical daily load curve, p.u PV & WT output power curves obtained from the respective units' data are depicted in Figure 3.3. Installation and operational costs of PV, WT, BESS & Biomass units [110], [111] are given in Table 3.2. The line & load data of 33 & 69 bus systems are taken from [31]. The 33-bus system total load demand is (3715+j*2300), 69-bus system total demand is (3801.5+j*2694.6). The base MVA & kV of both systems are 100 & 12.66. The hourly load demand at each bus in the system is obtained from the daily load curve [70]. In this work, to optimize the proposed objectives, four scenarios are considered; in each scenario, two cases are considered: optimal integration of DGs in the initial configured system/network and optimal integration of DGs in the optimal restructured system/network. All the simulations are implemented in MATLAB R2017a platform and carried out on a computer having Core i7 7200U 3.10 GHz, 16GB RAM. The lower and upper bound limits for DGs sizes are 500kW and 2000kW respectively.

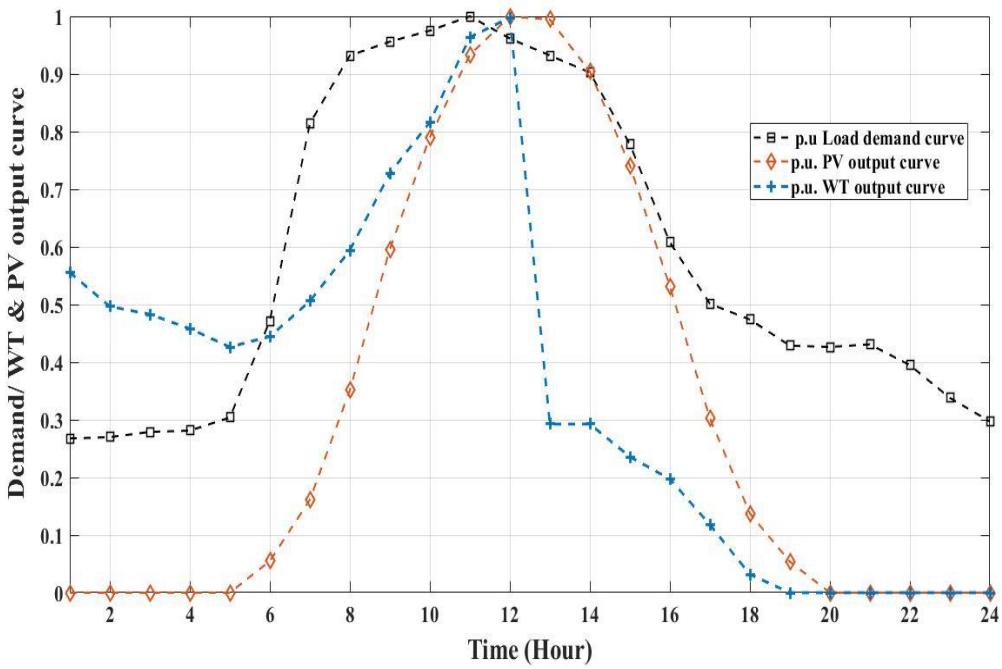

Figure 3.3 Typical p.u daily load curve, p.u. PV and WT output power curves

The base case energy loss and total voltage deviation of the 33-bus system without integration of DDGs are 2044 kWh,1.2936 p.u., for 69 bus system are 2173 kWh,0.9603 p.u. And for the optimal restructured network of 33 bus systems without DGs, energy loss & total deviation index are 1372 kWh, 0.4325 p.u. and for 69 bus system, energy loss & total deviation index are 967.59 kWh, 0.2069 p.u. Table 3.3 shows the best-compromised solution and the

corresponding PV & WT sizes given by the MOCVBOA algorithm for the scenario-1 outcomes.

Table 3.2 Installation Costs and Operational Costs of DGs

Parameters	**Value**
Installation cost of PV unit (INC_{pv}) in \$/kW	1100
Operational & Maintenance cost of PV unit (OMC_{pv}) in \$/kWh	0.01
Installation cost of WT unit (INC_{wt}) in \$/kW	1100
Operational & Maintenance cost of WT unit (OMC_{wt}) in \$/kWh	0.01
Installation cost of Biomass unit (INC_{bio}) in \$/kW	3000
Operational & Maintenance cost of Biomass unit (OMC_{bio}) in \$/kWh	0.012
Installation cost of 400 kWh BESS unit (INC_{BESS}) in \$	128000
Operational & Maintenance cost of BESS unit (OMC_{bess}) in \$/year	10666.67
Number of years for DG planning (nDG)	20
Number of years for BESS planning (nBESS)	8
Rate of interest in % (k)	10
Electricity price in \$/kWh (k_e)	0.2

Table 3.3 Simulation outcomes of scenario 1

Parameters	**Without Network restructuring**		**With Network restructuring**	
	33 Bus System	**69 Bus system**	**33 Bus System**	**69 Bus system**
Energy Loss in kWh	**835.227**	**823.11**	**662.63**	**374.28**
TVD in p.u	**0.3589**	**0.2951**	**0.1742**	**0.076**
Minimum Voltage in p.u	0.9507	0.9411	0.9614	0.9653
$P_{PV,Max}$ in kW/Bus No	945/32	1327/64	1186/30	1250/61
$P_{WT,max}$ in kW/Bus No	841/15	500/23	600/33	578/64
P_{PV} in kW	1560	2190	1942	2025
P_{WT} in kW	1236	735	897	883

3.5.1 Scenario-1: Minimization of E_{loss} & TVD (PV & WT units)

To observe the difference between the integration of non-dispatchable & dispatchable units in the distribution system on the improvement of proposed objectives, in scenario-1, the minimization of E_{loss} & TVD of the test systems by optimal integration of non-dispatchable WT, PV units are addressed. Figure 3.4 depicts the optimal Pareto front given by the MOCVBOA technique for case-1 & case-2 of 33 & 69 bus test systems, respectively. For case-1 of 33 bus system, the system's energy loss is reduced to 835.227 kWh (accounts for 59% loss reduction), TVD reduced to 0.3589 & for case-2, energy loss is reduced to 662.63 kWh (accounts for 67.6 % loss reduction), TVD is reduced to 0.1742 p.u. For case-1 of 69 bus system, energy loss is reduced to 823.11 kWh (accounts for 62% loss reduction) & TVD reduced to 0.2951 p.u and for case-2, energy loss is reduced to 374 kWh (accounts for 82% loss reduction) & TVD reduced to 0.0767 p.u. From the outcomes, it is noticed that both the objectives are well improved by optimal integration of non-dispatchable PV & WT units in the optimal reconfigured case, i.e., in case-2.

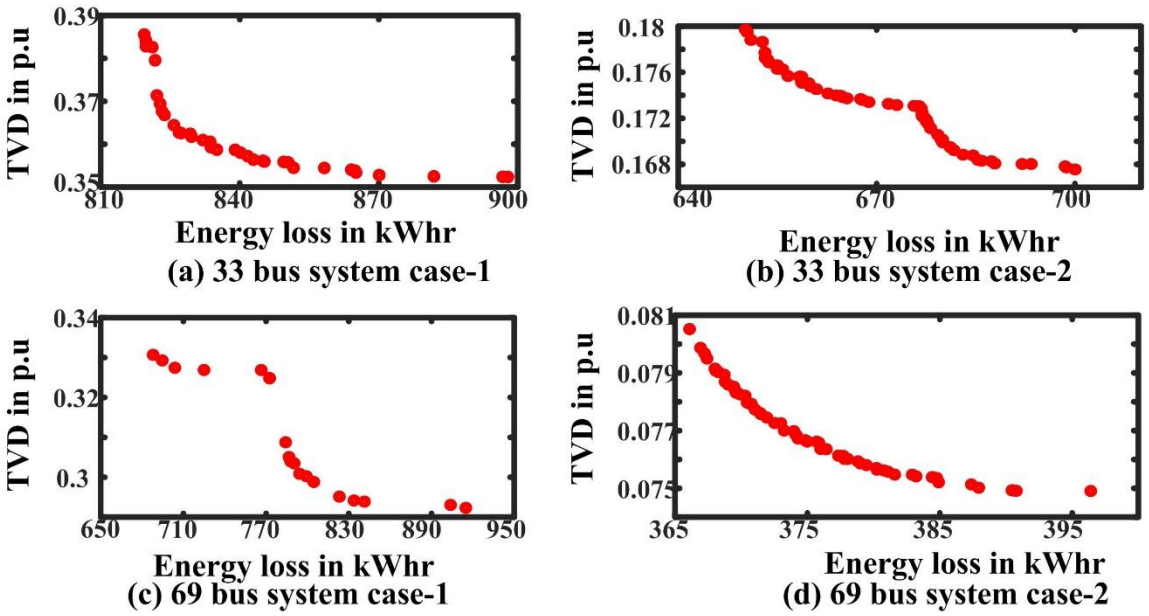

Figure 3.4 Optimal pareto fronts given by MOVBOA for scenario-1 cases

Figure 3.5 depicts the hourly power output of PV and WT units in 33 & 69 bus for the scenario-1 cases. Figure 3.6 illustrates the hourly power taken from the substation, hourly active power loss & average voltage profile of the system for both cases of the third scenario.

From Figure 3.6, it can be observed that the optimal integration of PV & WT units in the system improves the voltage profile and reduces power loss. And also, from Figure 3.6, it can be noticed that there is a significant reduction in substation power between the 5th hour and 17th hour because of the considerable injection of power by PV & WT units into the system due to the availability of an abundance of solar radiance and wind speed.

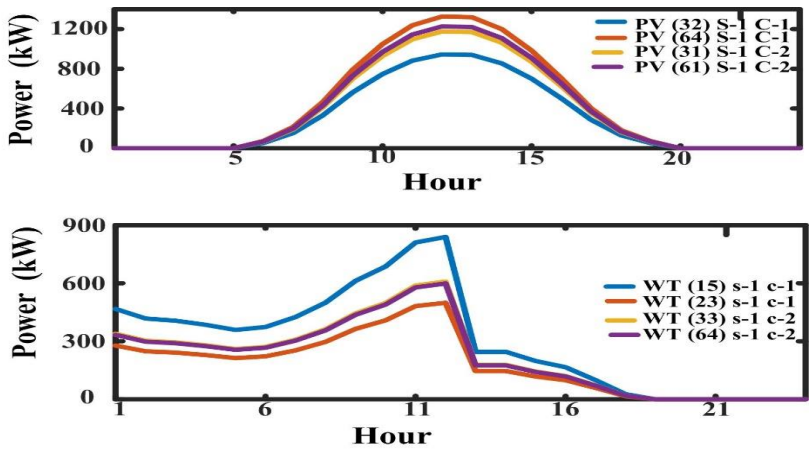

Figure 3.5 Hourly power output curves of PV, WT, units for scenario-1 cases

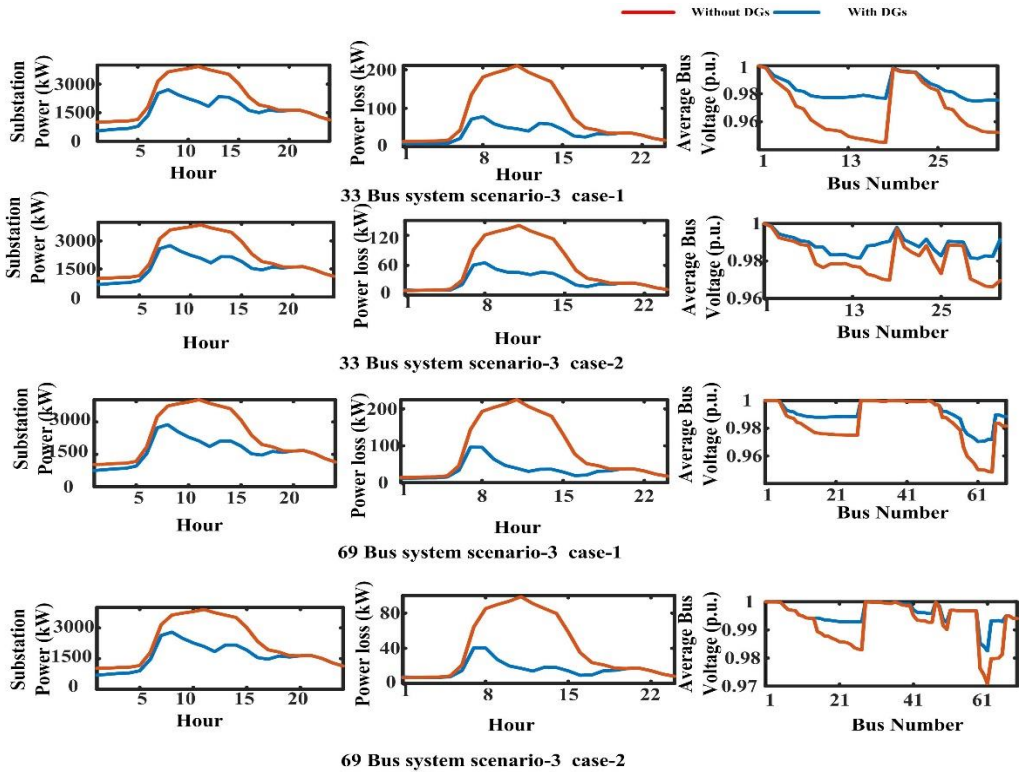

Figure 3.6 Daily substation power, power loss and average voltage profile curves for scenario-1 cases

However, in the remaining period, there is an insignificant reduction in substation power due to the absence of solar radiance and wind speed. Hence, in scenario 2, the minimization of E_{loss} & TVD by optimal integration of dispatchable DGs units in the distribution system is addressed. Table 3.4 & Table 3.5 shows the best-compromised solution and the corresponding DDGs sizes given by the MOCVBOA algorithm for scenarios 2-4 outcomes of the 33 & 69 bus test systems, respectively.

Table 3.4 Simulation outcomes of 33 bus system for scenarios 2,3 & 4

Parameters	**Without Network restructuring**			**With network restructuring**		
	Scenario-2	**Scenario-3**	**Scenario-4**	**Scenario-2**	**Scenario-3**	**Scenario-4**
Energy Loss in kWh	**406**	**461**	**453**	**358**	**424.70**	**398**
Annual Economic Cost in $	878249	**671493**	**704118**	793596	**649676**	**701699**
TVD in p.u	**0.045**	0.1337	**0.1075**	**0.0609**	0.0951	**0.0754**
Minimum Voltage during peak load in p.u	0.9787	0.9725	0.9728	0.974	0.9712	0.9717
$P_{PV-BESS_{max}}$ in kW/Bus No	826/14	541/15	500/17	630/16	500/16	522/33
$P_{WT-Biomas_{max}}$ in kW/Bus No	1027/31	1062/30	1214/30	1223/30	1017/30	1173/30
$P_{PV,Max}$ in kW	1702	1116	1030	1300	1030	1075
$P_{WT,max}$ in kW	487	502	584	583	488	563
$P_{Biomass,Max}$ in kW	815	843	961	969	806	929
P_{PV} in kW	2808	1842	1700	2145	1700	1774
P_{WT} in kW	716	738	859	857	717	828
E_{BES} in kWh	5359	3515	3244	4093	3244	3387
P_{BES} in kW	922	605	558	704	558	583

Table 3.5 Simulation outcomes of 69 bus system for scenarios 2,3 & 4

Parameters	Without Network restructuring			With Network restructuring		
	Scenario-2	**Scenario-3**	**Scenario-4**	**Scenario-2**	**Scenario-3**	**Scenario-4**
Energy Loss in kWh	**260**	**352**	**297**	**152**	**207**	**196**
Annual Economic Cost in $	725646	**651827**	**707359**	781098	**637932**	**647000**
TVD in p.u	**0.056**	0.1809	**0.0734**	**0.0199**	0.0352	**0.0284**
Minimum Voltage during peak load in p.u	0.9794	0.9692	0.9731	0.9883	0.9812	0.9811
$P_{PV-BESS_{max}}$ in kW/Bus No	500/23	500/64	500/21	618/27	500/27	536/64
$P_{WT-Biomas_{max}}$ in kW/Bus No	1400/63	1057/61	1291/62	1282/61	1040/61	1038/61
$P_{PV,Max}$ in kW	1031	1030	1030	1273	1030	1103
$P_{WT,max}$ in kW	670	507	621	613	500	499
$P_{Biomass,Max}$ in kW	1109	837	1022	1016	823	822
P_{PV} in kW	1701	1700	1700	2101	1700	1821
P_{WT} in kW	986	746	913	901	736	734
E_{BES} in kWh	3247	3244	3244	4010	3244	3475
P_{BES} in kW	559	558	558	690	558	598

3.5.2 Scenario-2: Minimization of E_{loss} & TVD (PV-BESS & WT-BIOMASS units)

In scenario 2, the minimization of E_{loss} & TVD of the test systems by optimal integration of dispatchable WT-BIOMASS and PV-BESS units are addressed. Figure 3.7 depicts the optimal Pareto front given by the MOCVBOA technique for case-1 & case-2 of 33 & 69 bus test systems, respectively. For case-1 of the 33 bus system, the system's energy loss is reduced to 406 kWh (accounts for 80% loss reduction), TVD is reduced to 0.045 & for case-2, energy loss is reduced to 358 kWh (accounts for 82.4 % loss reduction), TVD is reduced to 0.0609. For case-1 of 69 bus system, energy loss is reduced to 260 kWh (accounts for 88% loss

reduction) & TVD reduced to 0.05 and for case-2, energy loss is reduced to 152 kWh (accounts 93% loss reduction) & TVD reduced to 0.0199.

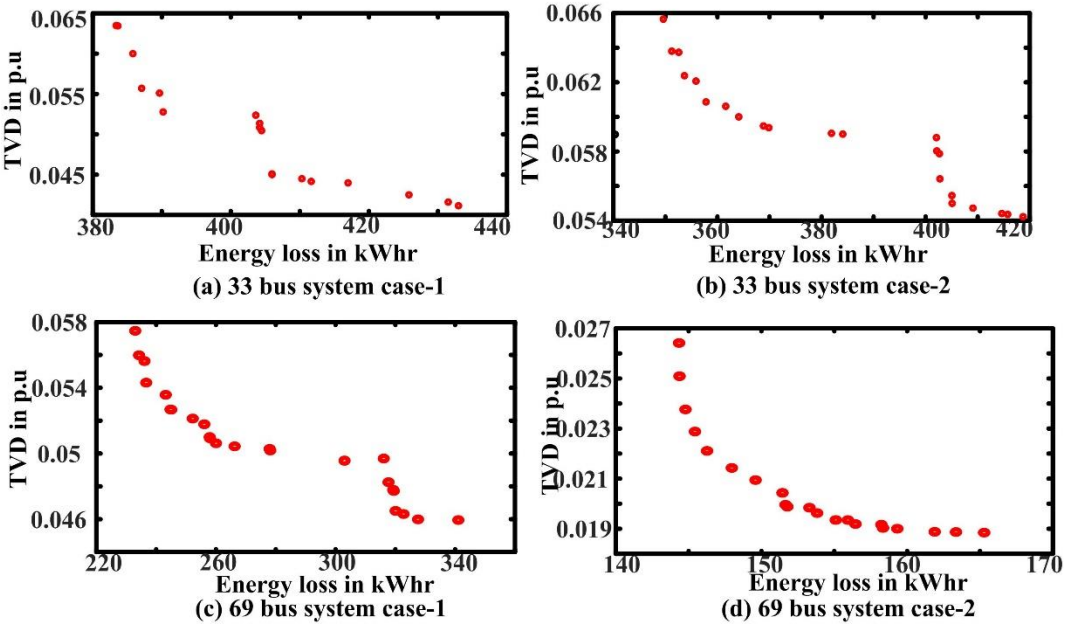

Figure 3.7 Optimal pareto fronts given by MOCVBOA for scenario-2 cases

Figure 3.8 depicts the comparison between outcomes (E_{loss} & TVD) for scenario-1 & 2 cases. From the Figure-3.8, it can be noticed that improvement in the reduction of both the objectives E_{loss} & TVD are comparably higher in scenario-2 than in scenario-1.

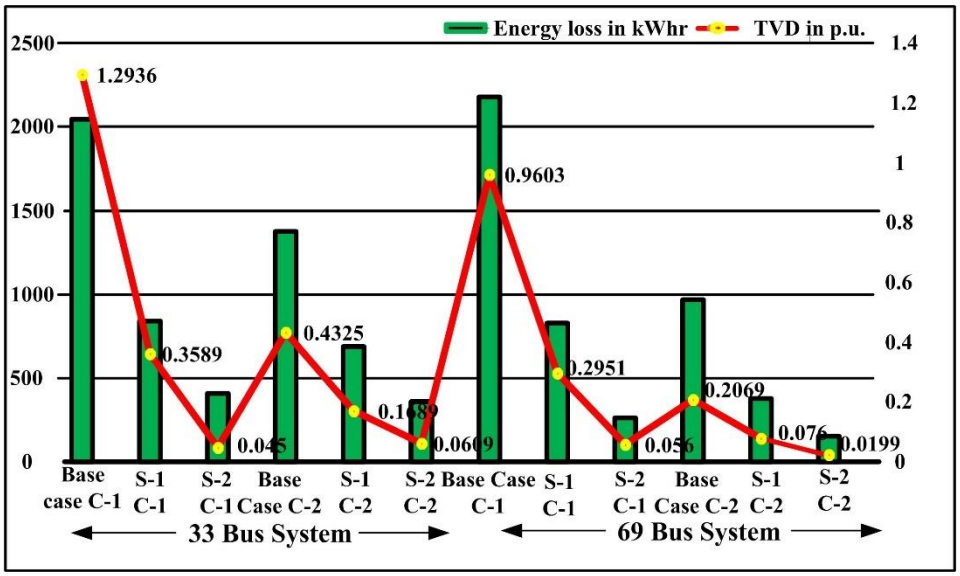

Figure 3.8 Comparison between the outcomes of scenario-1 & 2 cases

This is a result of the fact that optimal dispatch of power by DDGs (WT-BIOMASS, PV-BESS) follows the hourly load demand. And also, it is observed that due to the consideration of only technical aspects in this scenario, the percentage injection of real power by the DDGs into the 33 & 69 bus systems at any time during the day stood at a maximum injection consideration level of 50 % for all the solutions in the Pareto front. However, due to the consideration of all the DG units (PV, WT, BESS, BIOMASS), there is a need to study the AEC along with E_{loss} & TVD.

3.5.3 Scenario-3: Minimization of E_{loss} & AEC (PV-BESS & WT-BIOMASS units)

In scenario 3, the minimization of E_{loss} & AEC of the test systems by optimal integration of dispatchable WT-BIOMASS and PV-BESS units are addressed. Figure 3.9 depicts the optimal Pareto front given by the MOVBOA technique for scenario-3 cases.

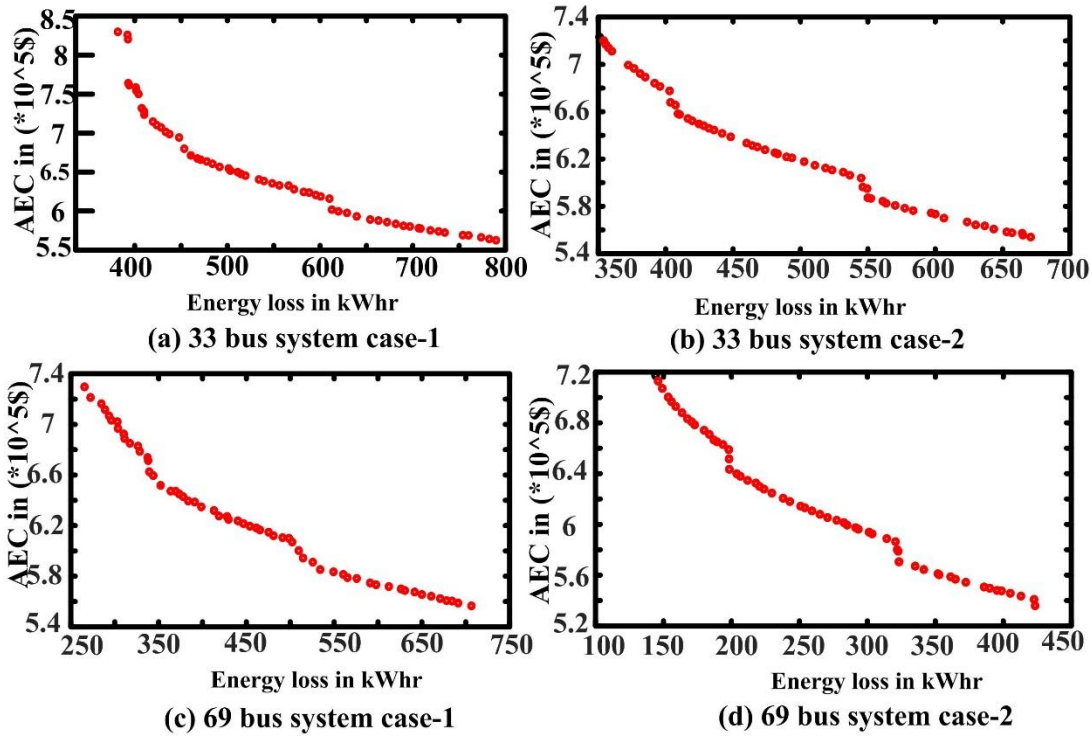

Figure 3.9 Optimal pareto fronts given by MOVBOA for scenario-3 cases

For case-1 of the 33-bus system, energy loss is lessened to 461 kWh, the annual economic cost is reduced to $ 671493 and for case-2, energy loss is lessened to 424 kWh, the annual economic cost is reduced to $ 649676. For case-1 of the 69-bus system, energy loss is mitigated to 352 kWh, the annual economic cost is reduced to $ 651827 and for case-2 energy, the loss is mitigated to 207 kWh, and annual economic cost is reduced to $ 637932. From the

outcomes, it can be noticed that there is a tremendous improvement in both objectives by optimal integration of DDGs in both test systems. And also, it is noticed that both objectives are well improved by optimal integration of DDGs in the optimal reconfigured case, i.e., in case-2. It can also be observed that the percentage of real power injection by the DDGs into the 33 & 69 bus systems at any time during the day stood at around 50% for the left-most solution in the Pareto front, (41-43) % for the compromised solution in the Pareto front, (28-30) % for the rightmost solutions in the Pareto front in both the cases against maximum injection consideration level of 50 %. This is because AEC is considered as one of the objectives in this scenario. In scenario 4, all the objectives (E_{loss} , TVD & AEC) are considered for the balanced optimized solution between three goals.

3.5.4 Scenario-4: Minimization of E_{loss} , TVD & AEC (PV-BESS & WT-BIOMASS units)

In scenario 4, the minimization of E_{loss} , AEC & TVD are considered as main objectives. Figure 3.10 depicts the optimal Pareto front given by MOCVBOA, MOBOA & NSGA-II techniques for case-1 & case-2 of 33 & 69 bus test systems, respectively.

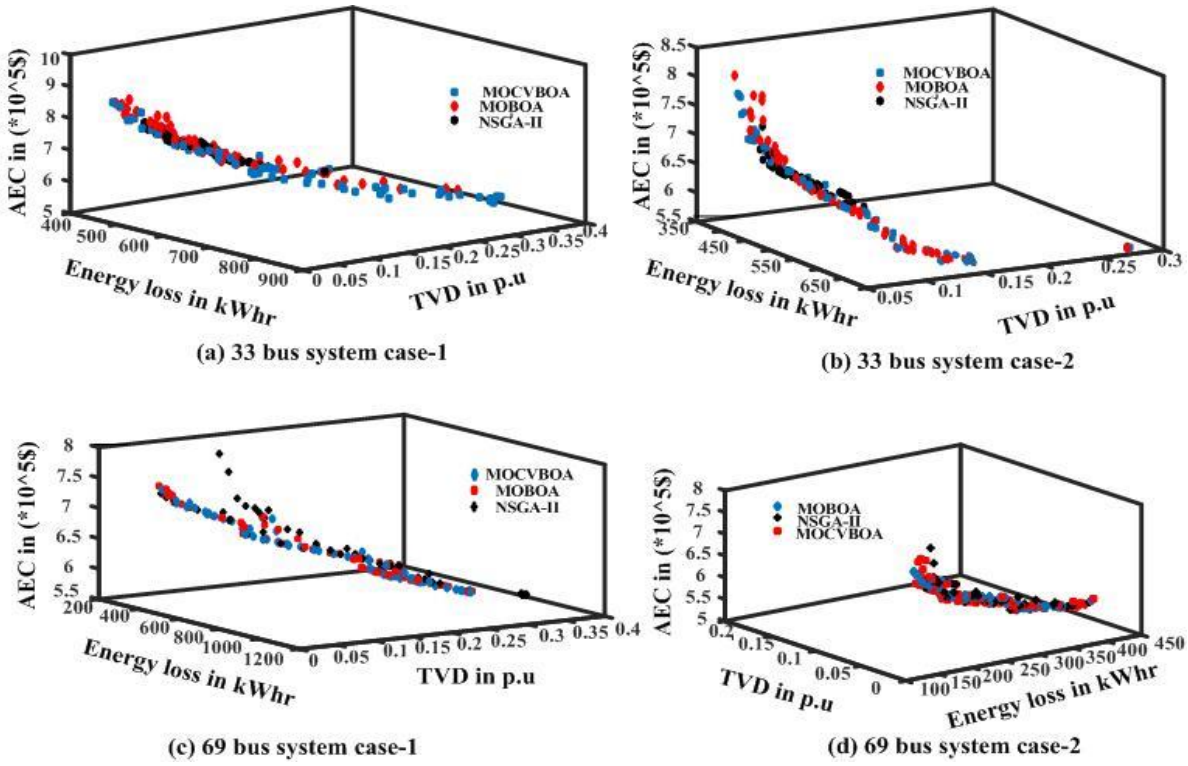

Figure 3.10 Optimal pareto fronts given by MOCVBOA, MOBOA & NSGA-II for scenario-4 cases

In the case of optimal integration of DDGs in the initial configured network, E_{loss} , TVD & AEC of 33 bus system are reduced to 453 kWh, (accounts 77 % loss reduction) 0.1075 p.u & $ 704118 respectively and E_{loss} , TVD & AEC of 69 bus system are reduced to 297 kWh (accounts 86.3 % loss reduction), 0.0734 p.u & $ 707359 respectively. In case of optimal integration of DDGs in the optimal reconfigured network, E_{loss} , TVD & AEC of 33 bus system are reduced to 398 kWh (accounts for 80.5 % loss reduction), 0.0754 p.u & $ 701699 respectively and E_{loss} , TVD & AEC of 69 bus system are reduced to 196 kWh (accounts 91 % loss reduction), 0.0284 p.u & $ 647000 respectively. From the outcomes of scenario 4, it can also be seen that the percentage injection of real power by the DDGs into the 33 & 69 bus systems at any time during the day stood at (42-45) %. From Tables 3.4 & 3.5, it is observed that the objectives are considerably enhanced when DDGs are optimally integrated into the optimally reconstructed network. Furthermore, during the optimization of all three objectives, i.e., in scenario 4, the negotiated solution among all three objectives is attained. Figure 3.11 depicts the hourly power output of PV-BES, PV, BESS, WT-BIOMASS, WT, and BIOMASS units in 33 & 69 bus for the scenario-4 cases.

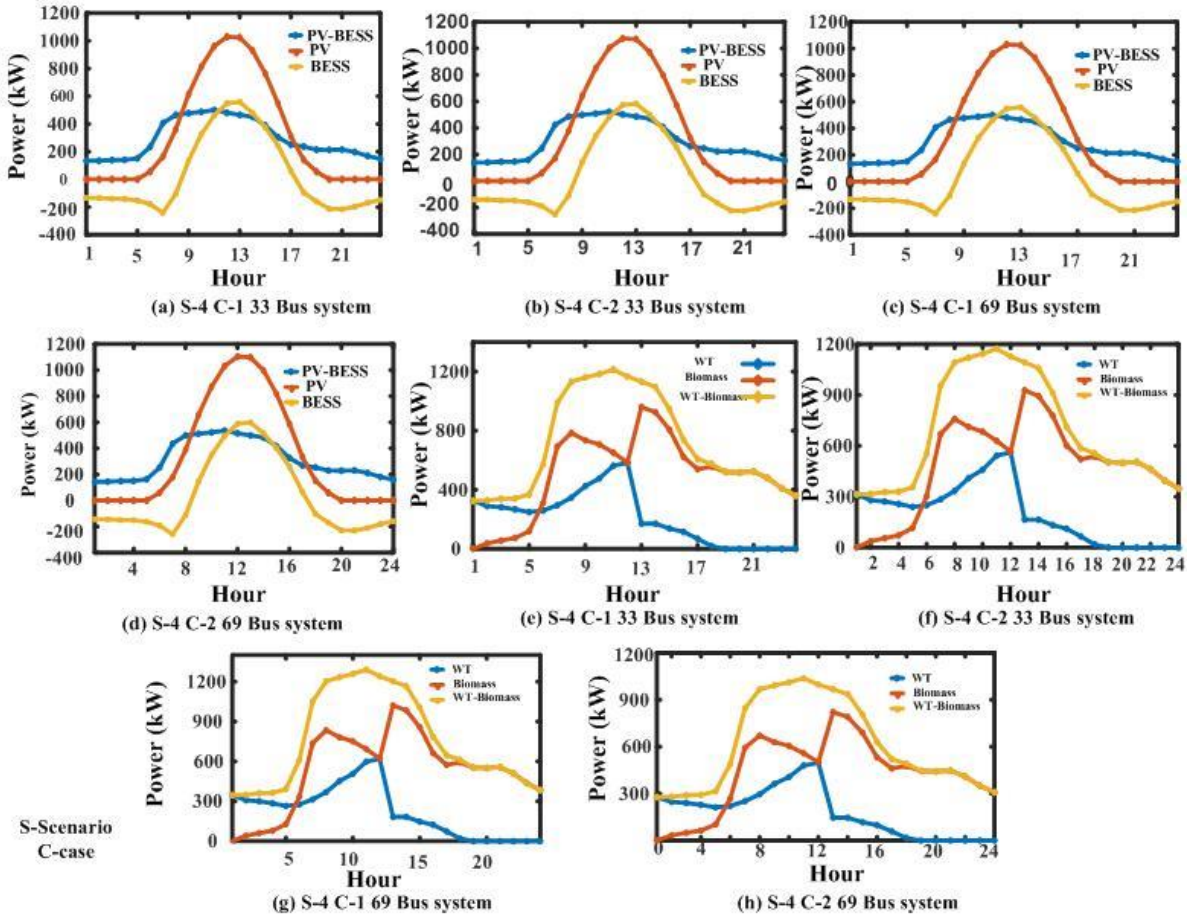

Figure 3.11 Hourly power output curves of PV, BESS, PV-BESS, WT, BIOMASS, WT-BIOMASS units for scenario-4 cases

In Figure 3.11, the negative value of BESS power indicates discharging mode of the BESS, supplying power to the grid & positive value of BESS power indicates the charging mode of the BESS, drawing power from the PV unit. To regulate the output power of the BESS unit in accordance with the curves depicted in Figure 3.11, a converter with advanced controlling mechanisms is necessary. Figure 3.12 illustrates the hourly power taken from the substation, hourly active power loss & average voltage profile of the system's/network's for both cases of the fourth scenario. From Figure 3.12, it can be observed that optimal integration of DDGs in the system improves the voltage profile and reduces power loss.

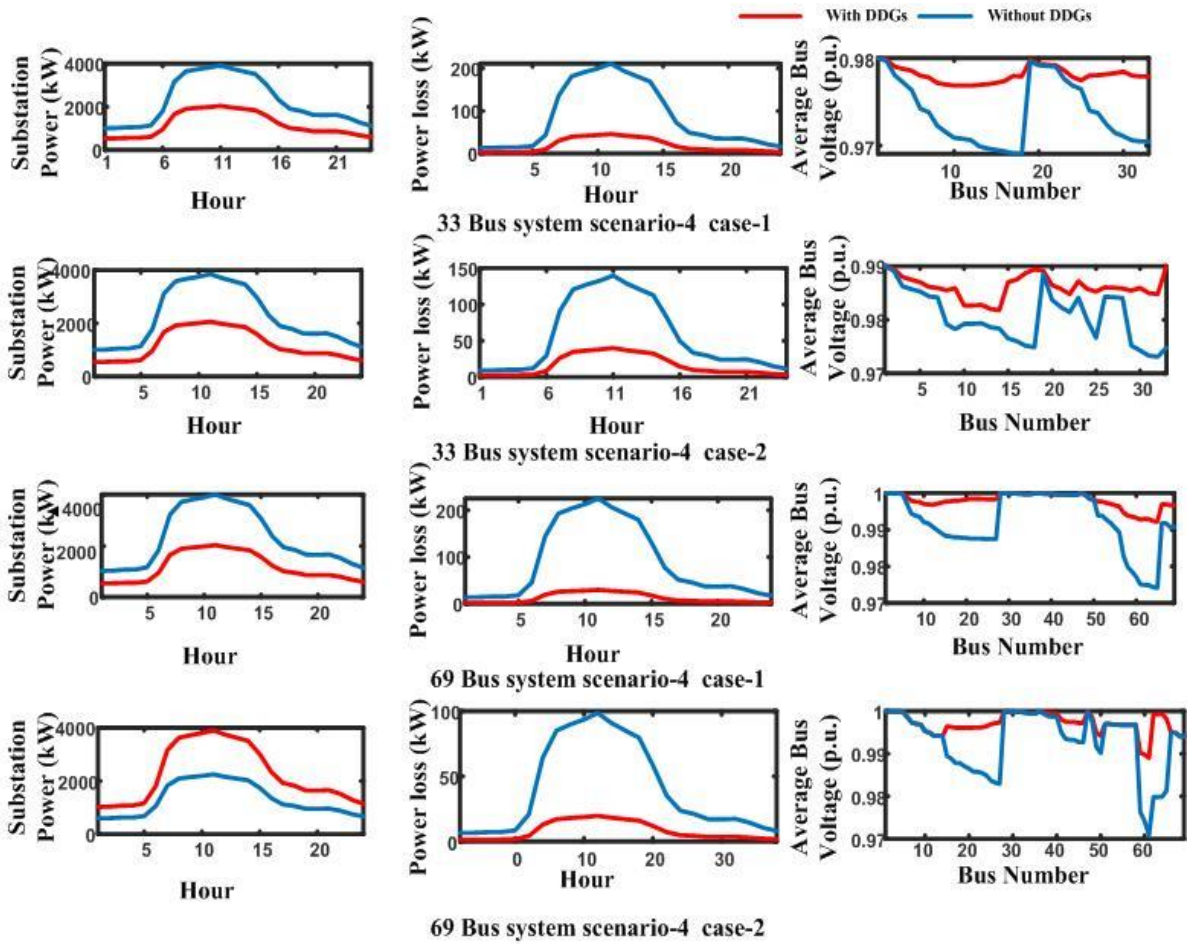

Figure 3.12 Daily substation power, power loss and average voltage profile curves for scenario-4 cases

From the above discussions, it can be concluded that better improvement in technical metrics of the distribution system is observed during optimal planning of dispatchable DGs units (i.e., PV-BESS, WT-BIOMASS). However, in the case of PV-BESS unit, a converter with sophisticated controlling techniques is required to regulate the BESS unit's output power in

line with the optimal curves. And also, from the outcomes of the WT-BIOMASS unit, it is observed that almost an equal size of BIOMASS unit on par with the WT unit is required while making the WT-BIOMASS unit as dispatchable DG. Since biomass units are also deployable, they can be used in place of PV-BESS & WT-BIOMASS units. The optimal power output curves of DDGs can be used to determine the size of BIOMASS units.

To check the efficacy of the MOCVBOA, the outcomes of MOCVBOA are contrasted with the MOBOA & NSGA-II algorithms. From Figure 3.10, it's clear that the dominance of optimal Pareto given by the MOCVBOA algorithm over MOBOA and NSGA-II. Table 3.6 shows the comparison of outcomes between MOCVBOA, MOBOA and NSGA-II algorithms. From this table, it can be noticed that the compromised solutions given by the MOCVBOA algorithm dominate the MOBOA and NSGA-II solutions.

Table 3.6 Comparative study of the MOCVBOA, MOBOA & NSGA-II algorithms' outputs

Algorithms	Energy Loss in kWh	Annual Economic Cost in $	TVD in p.u
33 Bus system, Scenario-4, Case-1			
MOCVBOA	453	704118	0.1075
MOBOA	457	704236	0.1101
NSGA-II	462	704484	0.1112
33 Bus system, Scenario-4, Case-2			
MOCVBOA	398	701699	0.0754
MOBOA	403	701873	0.0763
NSGA-II	408	701927	0.0781
69 Bus system, Scenario-4, Case-1			
MOCVBOA	297	707359	0.0734
MOBOA	299	707396	0.0743
NSGA-II	306	707498	0.0824
69 Bus system, Scenario-4, Case-2			
MOCVBOA	196	647000	0.0284
MOBOA	201	647098	0.0310
NSGA-II	210	647226	0.0356

3.6 Summary and Comments

The optimal integration of PV-BESS and WT-BIOMASS dispatchable DDG units into the 33 & 69 distribution systems in the presence of network restructuring is dealt with in this work. MOCVBOA is used to determine the ideal sizes of PV, BESS, WT, and biomass units in minimising energy loss, total voltage deviation, and annual economic cost. Four scenarios are

considered to fulfil the objectives. For the 33 & 69 bus test systems, improvement in energy loss reduction and voltage profile enhancement is observed in both cases: Optimal integration of non-dispatchable DGs (scenario-1) and dispatchable DGs (scenario-2). However, when dispatchable DGs are connected with the system, better enhancement in objectives is seen. The negotiated solution for the 33 & 69 bus test systems among all three objectives is attained during the optimization of all three objectives in scenario 4. The 33-bus system energy loss is reduced to (77-80) %, 69-bus system energy loss is reduced to (86-91) % in scenario-4 by the injection of a maximum of (42-45) % load demand into the system via DDGs. The objectives are considerably enhanced when DDGs are optimally integrated with the optimally reconstructed network. However, a converter with sophisticated controlling techniques is required to regulate the BESS unit's output power in line with the optimal curves. Since biomass units are also deployable, they can be used in place of PV-BESS units & WT-BIOMASS units. The optimal power output curves of DDGs can be used to determine the size of biomass units. MOCVBOA performs better in achieving the results than MOBOA and NSGA-II optimization algorithms. In chapter 2 & 3, improvement of distribution system metrics by optimal planning of DGs is addressed without considering PHEVs load demand on the system. As PHEVs load demand deteriorates the distribution system performance, in the next chapter, optimal planning of DGs in the distribution system by considering conventional load demand and PHEVs load demand is addressed.

Chapter 4

Optimal integration of DGs into radial distribution network in the presence of plug-in electric vehicles to minimize energy loss and to improve the voltage profile of the system using a pareto-based multi-objective chaotic velocity-based butterfly optimization algorithm

4.1 Introduction

The increase in plug-in hybrid electric vehicles (PHEVs) is likely to see a noteworthy impact on the distribution system due to high electric power consumption during charging and uncertainty in charging behavior. This chapter mainly focuses on the improvement of distribution technical metrics energy loss reduction and voltage profile by optimal integration of distributed generators (DGs) into radial distribution system considering PHEVs load demand. In this work, charging of PHEVs under a private charging scenario, i.e., charging of electric vehicles at residential houses, is considered. Therefore, in this chapter, a distribution system with residential, commercial and industrial buses is considered. 24-hour load demand of the buses is generated with the help of typical p.u daily load curves of different types of buses. The daily electric demand raised due to the charging of PHEVs is generated using the charging time probability distribution functions developed in the literature and imposed on the residential buses of the distribution system. As PHEVs load demand deteriorates the distribution system performance, a pareto-based chaotic velocity-based butterfly optimization algorithm is employed for generating the optimal pareto front between the cited objective functions and then the TOPSIS method is employed for finding the optimal locations and optimal sizes of DGs.

4.2 Modelling of DGs

For load flow studies, DGs can be modelled as either PV mode or PQ mode. In this work, DG is modelled as PQ mode. In this type of modelling, DG is modelled as generating source (negative load model) with constant active power (P_{DG}) and reactive power output Q_{DG}. In this type of modelling, the active power and power factor (PF) of the DG is mentioned. The reactive power of the DG is calculated by using Eq. 4.1.

$$Q_{DG} = P_{DG} * (\tan(\cos^{-1} PF)) \quad (4.1)$$

The effective load at any bus with the integration of DG unit can be expressed as

$$P_{load} = P_{load} - P_{DG} \quad (4.2)$$

$$Q_{load} = Q_{load} - Q_{DG} \quad (4.3)$$

Where P_{load}, Q_{load} are active and reactive power demands at the bus.

4.3. Objective functions

4.3.1 Energy Loss

Optimal integration of DDGs in the system improves the system's efficiency by reducing the system's energy loss (E_{loss}). Energy loss of the system for a 24-hour daily load pattern is obtained by adding all the distribution system active power losses in each hour of that day. The mathematical formulation of the system's energy loss is given below.

$$Minimize \ f_1 = E_{loss} = \sum_{t=1}^{24} \sum_{j=1}^{nb-1} J_{t,j}^2 * R_j \quad (4.4)$$

where $nb, J_{t,j}, R_j$ are the number of buses, branch current and branch resistance, respectively.

4.3.2 Total Voltage Deviation

Optimal integration of DDGs in the network improves its voltage profile. Better enhancement in the voltage profile of the system/network is achieved by taking a mathematically formulated function named Total Voltage Deviation (TVD) as one of the objectives. Mathematical formulations of the VD and TVD are given below

$$VD_t = \sum_{i=1}^{Nbus} (1 - V_{t,i}) \quad t = 1,2,\ldots 24 \quad (4.5)$$

$$Minimize \ f_2 = TVD = \sum_{t=1}^{24} VD_t \quad (4.6)$$

4.3.3 Constraints

1. Active power and reactive power balance constraints.

$$P_{j,sub} + P_{j,T,DG} = P_{j,D} + P_{jloss} \quad (4.7)$$

$$Q_{j,sub} + Q_{j,T,DG} = Q_{j,D} + Q_{jloss}^{DG} \quad (4.8)$$

Where $P_{j,D} = \sum_{i=1}^{nb} (P_{bus\ j,i} + P_{PEV\ j,i})$ (4.9)

$$Q_{j,D} = \sum_{i=1}^{nb} (Q_{bus\ j,i}) \quad (4.10)$$

Where $P_{j,sub}$ is the j^{th} hour active power demand supplied by the sub-station in kW, $P_{j,D}$ is j^{th} hour total active power demand of the system with *PHEV*s in kW, $Q_{j,sub}$ is the j^{th} hour reactive power supplied by the sub-station in kVar, $Q_{j,D}$ is the jth hour total

reactive power demand of the system with *PHEV*s in kVar, , $P_{bus\ j,i}$ is the i^{th} bus active power demand during j^{th} hour, $P_{PEV\ j,i}$ is the ith bus active power demand due to *PHEV*s in j^{th} hour.

2. Voltage magnitude of each bus should be within minimum and maximum voltage limits.

$$|V_{min}| < |V_i| < |V_{max}| \qquad i = 1,2 \dots \dots \dots nb \tag{4.11}$$

3. Sizes of DGs to be placed should be within minimum and maximum kW limit.

$$P_{DGmin} < P_{k,DG} < P_{DGmax} \qquad k = 1,2 \dots \dots . ndg \tag{4.12}$$

4. Total active power compensation by DGs should be less than or equal to the maximum total capacity of DGs ($P_{T,DG}^{max}$) which is user-defined variable and minimum total active power demand throughout the day.

$$P_{T,DG} \leq P_{T,DG}^{max} < min(P_{j,D}) \tag{4.13}$$

4.3 Optimization Algorithm

Section 3.4 of Chapter 3 provides a detailed discussion of the chaotic velocity-based optimization algorithm, Pareto-based multi-objective optimization technique and TOPSIS method.

4.5 PHEVs charging scenario

Based on the charging behaviour of *PHEV*s, various researchers modelled different types of charging scenarios. They are peak charging scenario (PCS), off-peak charging scenario (OPCS) and stochastic charging scenario (SCS). In the peak charging scenario case, all the PHEVs come home after working hours and go for charging as soon as they return from the working place. This charging behaviour of *PHEV*s leads to an increase in peak demand of the system because the load on the system is already peaky during those hours. In the case of OPCS, due to electricity prices implemented by the system operator, the active power demand due to PHEVs shift towards the light demand hours, generally at midnight. In SCS, *PHEV*s go for charging at any time in the day. In this work, PCS is considered for inclusion of *PHEV*s electric demand in the system. The charging time probability distribution of PCS is taken from [112] and given in Figure 4.1. The PCS charging time probability functions are measured with a certain number of *PHEV*s to obtain $P_{PEV\ j,i}$ and then integrated into daily load pattern of the distribution system which consists of residential, commercial, and industrial buses.

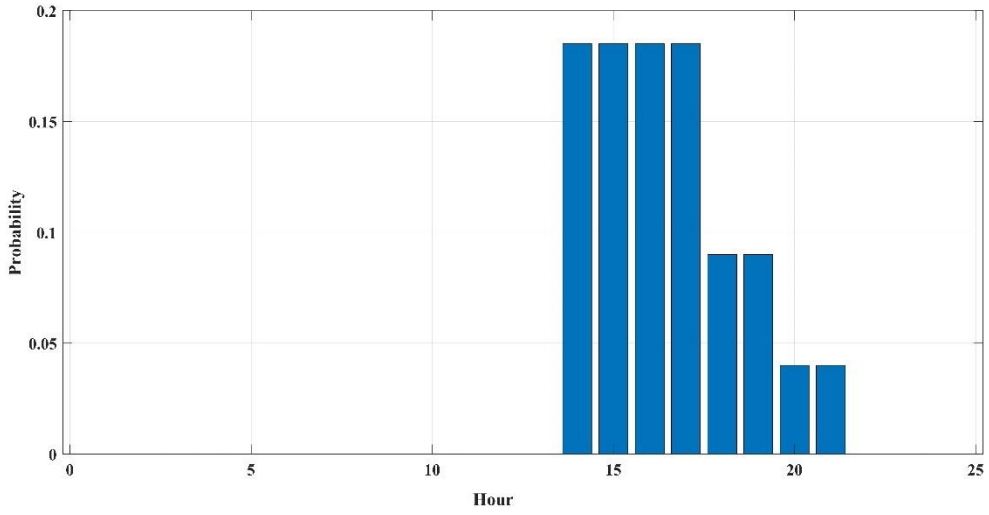

Figure 4.1 PHEVs probability distribution of PCS scenario

4.6 Results and Discussion

An IEEE 33 bus system has been taken for the analysis of the proposed method. The base values of the system are 100 MVA and 12.66 kV. Out of the 33 buses: 17 buses are residential buses, 5 buses are commercial buses, and 9 buses are industrial buses. The data of the grouping of buses is given in Table 4.1. Active and reactive power demands of the buses taken from bus data are considered as peak demands of the respective buses. Hourly active and reactive power demands for a day for each bus is obtained from typical daily load pattern of different type of buses in p.u with respect to peak demand 1 p.u is shown in Figure 4.2 [113]. From Figure 4.2 it has been observed that for a residential bus load demand requirement is high during the period 15.00-20.00 hr.

Table 4.1 Grouping of Buses data

Bus Type	Bus Numbers
Residential buses	2,3,5,6,7,8,9,10,13,14,15,16,17,20,21,23,24
Commercial buses	4,11,12,18,19
Industrial buses	22,25,26,27,28,29,30,31,32,33

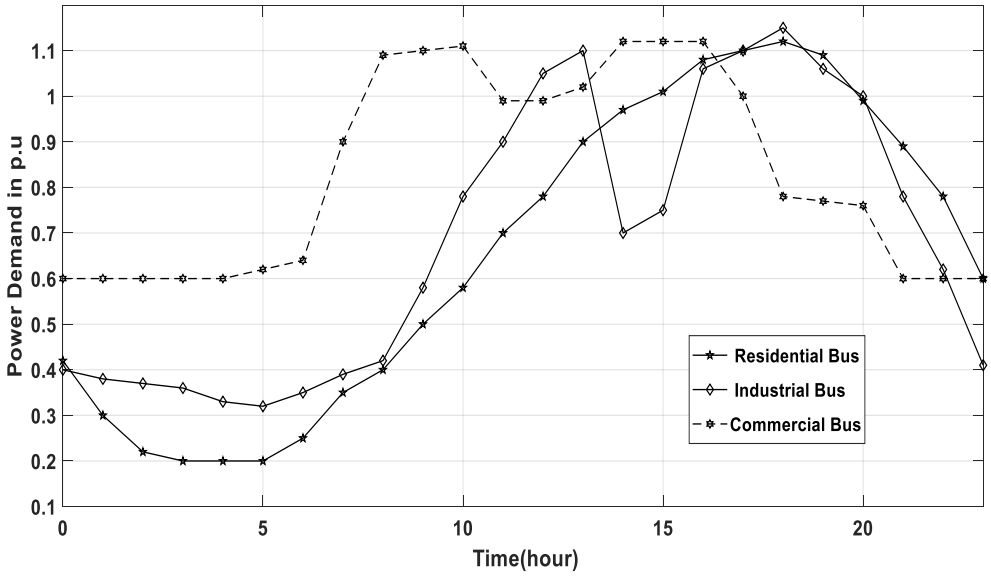

Figure 4.2 Daily load pattern of different types of buses

4.6.1 Analysis of the system without PHEVs load and without DGs

After the initial load flow run, i.e., before load due to electric vehicles, the following points has been observed. Daily active power demand from all the buses is 64510 kW. The daily energy loss of the system is 3053 kWh, total voltage deviation of the system is 31.21 p.u. The lowest voltage of the system is 0.8945 p.u at 18^{th} bus occurred during 17^{th} hour of the day.

4.6.2 Analysis of the system with PHEV load and without DGs

To study the effect of additional electric power demand duo to PHEVs in the electric distribution system, it has been assumed that 50 PHEVs per residential bus with a total of 17*50=850 PHEVs have been considered, where 45% of these PHEVs are low hybrid vehicles equipped with 15 kWh batteries, 25% PHEVs are medium hybrid vehicles with 25kwh batteries and 30% PHEVs are pure battery vehicles with 40 kWh batteries [112]. It is also assumed that all electric vehicles return to the home with a SOC of 50%. Therefore, the total electric demand due to PHEVs per residential bus per day is 50*(15*45%+25*25%+40*30%) *0.5= 625 kW and the total electric demand needed per day due to PHEVs is 625*17 = 10625 kW.

4.6.3 Analysis of the system with PHEVs charging under PCS

The electric demand of 625 kW due to 50 PHEVs for each residential bus has been consumed from the slack bus (bus-1) as per the probability distribution of the charging scenario of PCS depicted in Figure 4.1. Figure 4.3 shows the hourly active power demand of the distribution

system for a day without PHEVs and with PHEVs under PCS case obtained from the daily load pattern of buses and charging scenario.

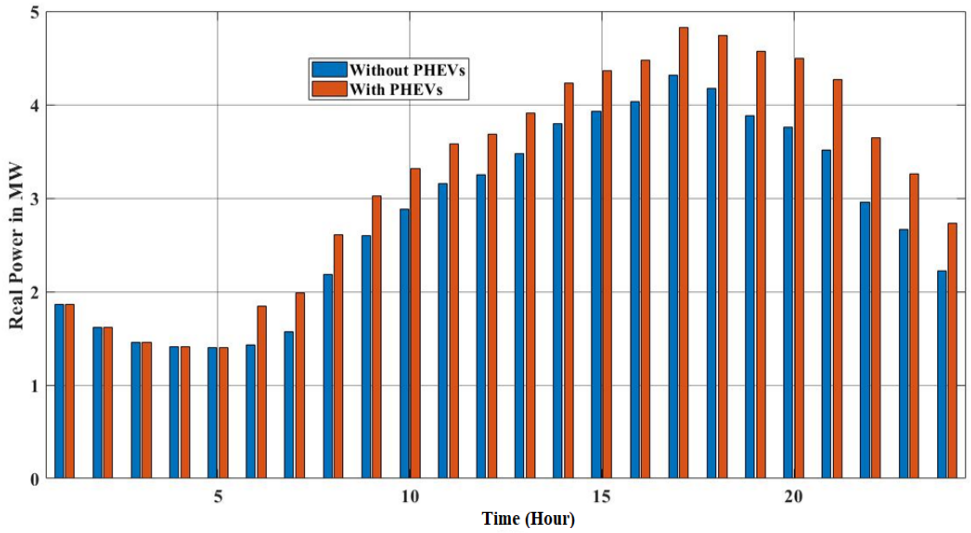

Figure 4.3 Hourly active power demand of the system without and with PHEVs load

Table 4.2 shows the comparison between various parameters between without PHEVs load and with PHEVs load on the distribution system. From the Table 4.2, it has been observed that due to PHEV's electric active power demand of 10625 kW, the distribution system is overloaded by 16.47% with respect to the daily active power demand requirement. In the case of PCS due to extra PHEVs active power demand, energy loss of the system is increased to 4346 kWh from 3053 kWh, which shows a 42.35% increase in daily active power loss. Also, the total voltage deviation index is increased to 36.07 p.u. The system's lowest voltage is 0.8398 p.u occurred at 18^{th} bus during 16^{th} hour of the day.

Table 4.2 Comparison between without and with PHEVs load on test system

Parameters	Without PHEV load	With PHEV load
Energy loss (in kWh)	3053	4346
Total Voltage Deviation (in p.u)	31.21	36.07
Lowest voltage magnitude (in p.u)	0.8945 (18^{th} bus, 17^{th} hour)	0.8398 (18^{th} bus, 16^{th} hour)
Active power demand from the buses for a day (in kW)	64510	75135

4.6.4 Optimal placement of DGs in distribution system with consideration of PHEVs

As it was found in the previous part that PHEVs have a negative impact on the efficiency and voltage profile of the distribution system, this section addresses the optimal planning of DGs operating at 0.9 pf for enhancing the distribution system performance. From Figure 4.3, it is also observed that the lowest active power demand with PHEVs load under PCS case is around 1500 kW occurred during 6^{th} hour of the day; therefore, maximum active power injection by DGs into the distribution system is fixed to 1500 kW. Figure 4.4 depicts the optimal Pareto front given by MOCVBOA & MOBOA techniques.

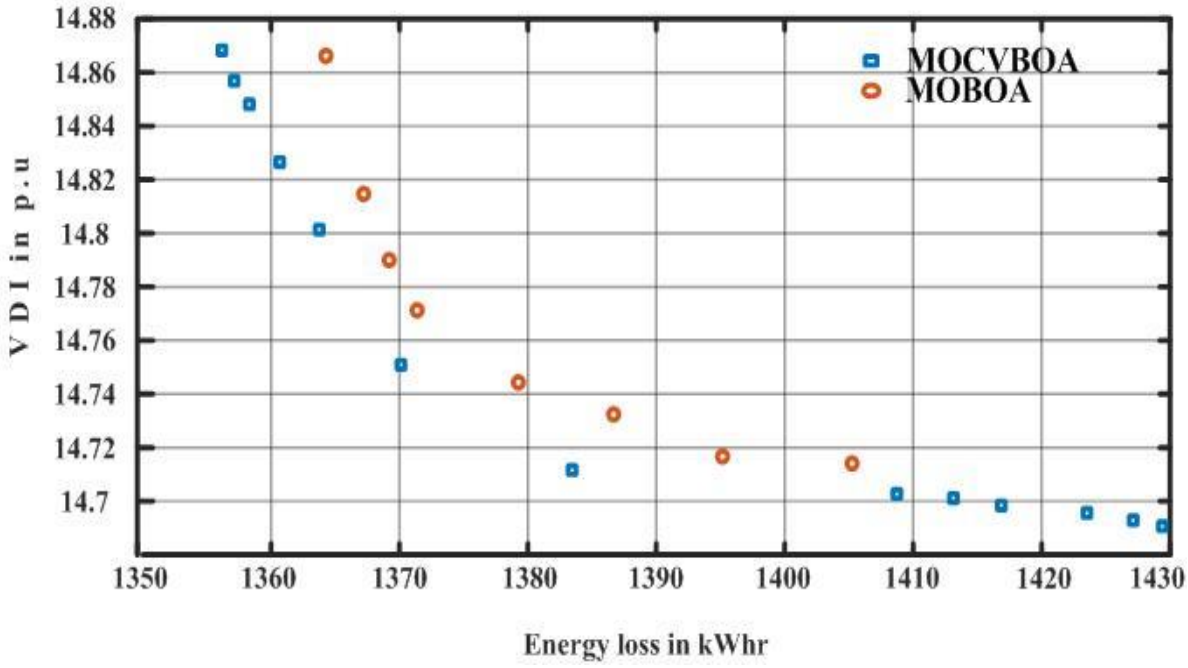

Figure 4.4 Optimal Pareto fronts given by MOCVBOA, MOBOA techniques

Table 4.3 shows the optimal locations, DGs (0.9 pf) sizes and various technical parameters of the best-compromised solution yielded by the TOPSIS-MOCVBOA technique. From Table 4.3, it is observed that the energy loss of the system is reduced to 1383 kWh accounts 58.39% loss reduction, and the voltage deviation index is reduced to approximately 14.71 p.u. The system lowest voltage improved to 0.9249 p.u.

Table 4.3 Simulation outcomes yielded by TOPSIS-MOCVBOA technique

Scenarios	DG size (kW) & Bus number	Energy loss (in kWh)	Total voltage Deviation (in p.u)	Lowest voltage of the system (in p.u)
Base Case	-------	4346	36.07	0.8398 (18th bus, 16th hour)
DGs sizes (in kW)/DGs locations	473 /14 204 /18 713 /32	1383	14.71	0.9249 (18th bus, 16th hour))

Voltage profile characteristics of the system without DGs & with DGs is shown in Figure 4.5. From Figure 4.5 it is observed that obtained optimal locations and sizes of DGs results fairly good voltage improvement at each and every bus of the system.

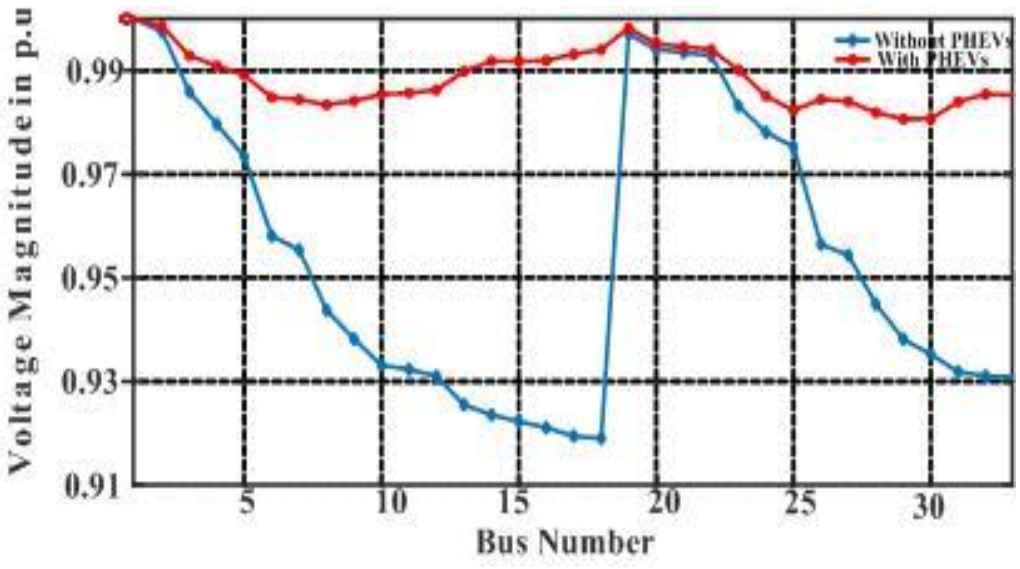

Figure 4.5 Mean voltage profile of the system without PHEVs & with PHEVs load demand

To check the efficacy of the MOCVBOA, the outcomes of the MOCVBOA are contrasted with the MOBOA algorithm. From Figure 4.3, it's clear that the dominance of optimal Pareto is given by the MOCVBOA algorithm over MOBOA.

4.7 Summary and Comments

In this chapter, 33 bus test system consisting of residential buses, commercial buses and industrial buses is considered. The 24-hour load pattern of the whole test system is obtained from the load pattern of different types of buses. PCS charging scenarios had taken for the inclusion of PHEVs load demand on the system. The impact of PHEVs load demand on the system's technical parameters is analysed. A combined 24-hour load pattern of the system, including PHEVs load demand with PCS charging scenario, has been considered for the optimal placement of the DGs in the system. Pareto-based chaotic velocity-based butterfly optimization algorithm has been applied to produce the optimal Pareto front between the mentioned energy loss and voltage deviation objective functions, and the TOPSIS approach has been subsequently applied to determine the optimal positions and sizes of DGs. From the obtained results, it can be concluded that the radial distribution system performance (reduction in system energy loss and improvement in system voltage profile) in the presence of PHEVs loads has improved with the optimal integration of DGs by the proposed approach. However, in this chapter, optimal planning of DGs is addressed without considering their uncertainties and dispatchable nature. And charging of PHEVs charging under only private charging scenario is only considered. Therefore, in the next chapter, optimal planning of DGs (considering their uncertainties & dispatchable nature) in the distribution system considering PHEVs load demand charging under both private & public charging scenario is addressed.

Chapter 5

Probabilistic optimal allocation of Solar PV units and Battery Energy Storage System in the distribution system in the presence of plug-in electric vehicles using a multi-objective chaotic velocity-based butterfly optimization algorithm

5.1 Introduction

This work investigates the combined effect of PHEVs' private and public charging behaviour on the technical metrics of the distribution system. The private charging behaviour of PHEVs is taken from the method developed in [76] and imposed on the residential buses of the distribution system. Additionally, the public charging behaviour is imposed on the few buses on the distribution system using a methodology established in [86]. To improve the efficiency of the distribution system, optimal planning of PV and PV-BESS units is considered. Pareto-based MOCVBOA multi-objective meta-heuristic optimization algorithm is considered to obtain the desired objectives.

5.2 Modelling of DGs and PHEV charging scenarios

5.2.1 Modelling of PV units and BESS units

Section 3.2 of Chapter 3 provides a detailed discussion about the modelling of solar radiance uncertainty using Beta PDF, modelling of PV unit output power and modelling of Battery energy storage system (BESS) output power.

5.2.2 Sizing of PV and BESS units

Section 3.3.2 of Chapter 3 provides a detailed discussion about the sizing of PV and BESS units.

5.2.3 Modelling of PHEVs private charging scenario

Numerous studies have predicted various charging scenarios based on the charging behaviour of PHEVs [76]. In particular, there are two charging scenarios for private charging of electric

vehicles: peak and off-peak charging scenarios. In the case of a peak charging scenario, all PHEVs arrive at their homes after office hours and immediately start charging. Because the system is already under peak load during those hours, this type of PHEVs charging behaviour increases peak demand. In the case of the off-peak charging scenario, the active power demand caused by PHEVs shifts towards the light demand hours, typically at midnight, as a result of electricity tariffs put in place by the system operator. For any type of charging scenario, it is initially necessary to model various PHEV parameters to estimate the electrical demand caused by PHEV charging when linked to the distribution system. As noted in the introduction, the variables arrival time and distance travelled of PHEVs are stochastic in nature. The mathematical modelling of PHEV characteristics, represented by equations 5.1 to 5.4, includes arrival time, trip distance, initial soc, and the amount of energy needed each day to charge the PHEV to 100% SOC.

The arrival time of a PHEV is represented as a random variable with a normal probability distribution function and the corresponding mathematical formulation for estimating the probability of the arrival of n^{th} PHEV at time 't' is calculated using

$$f_n^t(T_a) = \frac{1}{\sqrt{2\pi} * \sigma_{T_a}^t} * e^{-\left[\frac{(T_a - \mu_{T_a}^t)^2}{2*(\sigma_{T_a}^t)^2}\right]} \tag{5.1}$$

Where $\mu_{T_a}^t$ and $\sigma_{T_a}^t$ are the mean and standard deviation of the daily arrival instant of PHEV.

The random nature of distance travelled by PHEV is modelled using the log-normal probability distribution function

$$f_n(d_n) = \frac{1}{\sqrt{2\pi} * \sigma_{d_n} * d_n} * e^{-\left[\frac{(\ln d_n - \mu_{d_n})^2}{2*(\sigma_{d_n})^2}\right]} \tag{5.2}$$

Where $\mu_{d_n} sw$ & σ_{d_n} are the mean & standard deviation of the daily distance travel of PHEV.

The initial SOC of the battery in a PHEV before the beginning of the trip depends on the daily distance covered, all-electric range of that PHEV.

$$SOC = \begin{cases} 1 - \frac{d_n}{AER_n} & d_n < AER_n \\ 0 & d_n > AER_n \end{cases} \tag{5.3}$$

The total energy required to charge a battery from initial soc to fully charged condition is estimated as

$$E_g = \left(\frac{1-\frac{SOC}{100}}{\eta_{Batt}}\right) * C_{Batt} \quad (5.4)$$

Where η_{Batt} and C_{Batt} are the efficacy and capacity of the battery.

In this study, only PHEVs charging under peak charging scenario is considered. And also, it is assumed that the electric vehicles will charge at their homes with a constant charging power rate of 3.3 kW or 6.6 kW. The battery capacity of the PHEVs used in this study ranges from 7.8 kWh to 27.6 kWh [76]. The average distance driven by electric vehicles is 28.556 miles, with a standard variation of 12.524 miles. The detailed process for calculating the 24-hour electric consumption caused by PHEV charging is provided below.

1. With the use of the PDFs outlined above, the arrival time and distance travelled for all-electric vehicles are generated. Additionally, each electric vehicle is randomly assigned a battery rating from the ranges mentioned above.
2. From the outcomes of step 1, the SOC and E_g of all the vehicles is determined.
3. The 24-hour electrical power consumption necessary for charging electric vehicles is calculated using the arrival times, charging rate, and E_g.
4. The total daily electric power demand from all-electric vehicles is then calculated by summing all individual electric vehicles' daily electric power demand.
5. A 1000-time Monte Carlo simulation is performed on the steps mentioned above.
6. The mean of the previous simulation results provides the final electric power consumption profile owing to all-electric vehicles.
7. The distribution system's residential buses are all given an equal share of the final electric power demand profile.

5.2.4 Modelling of PFCS

The rating of PFCS depends on the number of connectors ($NC(j)$) at the station. The mathematical modelling for the capacity of PFCS ($CPFCS(j)$) [87] is given below

$$NC(j) = NPHEV(j) * \max(CPEV) \quad (5.5)$$

$$CPFCS(j) = NC(j) * PC \quad (5.6)$$

Where $NPHEV(j)$ represents the total number of electric vehicles charging through station j, CPHEV(h) represents the vector having probabilities of electric vehicles coming for charging

in the hour h of a day, PC represents the power rating of the connector. The power rating of the connector typically ranges from 50 to 250 kW and depends on the technology being used.

5.3 Modelling of DGs in load flows

Section 4.4.2 of Chapter 4 provides a detailed discussion about the sizing of PV and BESS units.

5.4 Objective Functions

5.4.1 Energy Loss

Through a reduction in energy loss (E_{loss}), optimal RDG integration increases system efficiency. The system's energy loss for the day is calculated by adding up all the real power losses experienced by the distribution system throughout that day's hours. The system's energy loss is mathematically formulated as follows.

$$Minimize\ \ f_1 = E_{loss} = \sum_{t=1}^{24} \sum_{j=1}^{nb-1} J_{t,j}^2 * R_j \quad (5.7)$$

where $R_j, nb, J_{t,j}$ are the j[th] branch resistance, number of buses in distribution system and j[th] branch current in time interval 't' respectively.

5.4.2 Total Voltage Deviation

The goal of voltage profile enhancement is to align all the bus voltage magnitudes as closely as possible to offer uniform voltage profiles for the customers. To achieve this, Total Voltage Deviation (TVD), a mathematically formulated function, is used as one of the objectives. Voltage Deviation (VD) is initially calculated for each hour of the day by adding the voltage deviations of all buses with respect to one p.u. The Total Voltage Deviation (TVD) is then calculated by combining all of the VDs. To improve the system voltage profile, the TVD must be reduced. Below are the mathematical formulations for the TVD and VD.

$$VD_t = \sum_{i=1}^{Nbus} (1 - V_{t,i})\ \ t = 1,2,\ldots 24 \quad (5.8)$$

$$Minimize\ \ f_2 = TVD = \sum_{t=1}^{24} VD_t \quad (5.9)$$

5.4.3 Annual Economic Cost (AEC)

The annual installation and maintenance expenditures of both units are involved in integrating PV-BESS RDGs units into the distribution grid. Thus, a mathematically constructed objective function called Annual Economic Cost (AEC) is developed to find a balance between annual

PV-BESS installation and operational expenses and the improvement in technical metrics, as shown below.

$$Minimize\ f_3 = AEC = k_e * (E_{loss}) * 365 + (AI_{DDG} + OM_{DDG}) \quad (5.10)$$

where AI_{DDG}, OM_{DDG} & k_e are, respectively, the annual installation expenses and maintenance costs in $ and the price of electricity in $/kW-hr.

where k_e, OM_{DDG}, AI_{DDG} are the electricity price in $/kW-hr, annual maintenance & istallation costs in $ respectively.

$$AI_{RDG} = \left(N_{pv} * INC_{pv} * P_{r,PV}\right) * CRF_{DG} + (N_{BESS} * INC_{BESS}) * CRF_{BESS} \quad (5.11)$$

$$OM_{RDG} = 365 * \sum_{i=1}^{24}(OMC_{pv} * P_{t,PV} + OMC_{bess} * N_{BESS}) \quad (5.12)$$

$$CRF_{DG} = \frac{k*(1+k)^{nDG}}{(1+k)^{nDG}-1} \quad (5.13)$$

$$CRF_{BESS} = \frac{k*(1+k)^{nBESS}}{(1+k)^{nBESS}-1} \quad (5.14)$$

Where the respective RDG unit numbers are denoted by N_{pv}, & N_{BESS}, INC_{pv}, INC_{BESS} are installation expenses of individual RDG units, $P_{r,PV}$, are rated power of PV units, the operations & maintenance cost is represented by OMC., $P_{t,PV}$, represents the power dispatched by PV units in the t[th] hour, k denotes the rate of interest, nBESS & nDG denotes the number of years.

5.4.4 Constraints

i) Active power and reactive power balance constraints.

$$P_{t,sub} + P_{t,T,RDG} = P_{t,D} + \sum_{t=1}^{24}\sum_{j=1}^{Nbus-1} J_{t,j}^2 * R_j \quad (5.15)$$

$$Q_{t,sub} + Q_{t,T,RDG} = Q_{t,D} + \sum_{t=1}^{24}\sum_{j=1}^{Nbus-1} J_{t,j}^2 * X_j \quad (5.16)$$

Where $P_{t,D} = \sum_{i=1}^{nb}\left(P_{Bus\ t,i} + P_{PHEV\ t,i}\right)$ (5.17)

$$Q_{t,D} = \sum_{i=1}^{nb}\left(Q_{Bus\ t,i}\right) \quad (5.18)$$

Where $P_{t,sub}$ is the substation's t^{th} hour active power demand supplied in kW, $P_{t,D}$ is the system's hourly active power demand expressed in kW, $Q_{t,sub}$ is the substation's t^{th} hour reactive power demand supplied in kVar, $Q_{t,D}$ is the system's hourly active power demand expressed in kVar, $P_{Bus\ t,i}$ is the i[th] bus active during the t[th] hour, $P_{PHEV\ t,i}$ is the hour's active power demand for the i[th] bus caused by PHEVs..

ii) The system's buses' voltage levels must fall between the permitted minimum and maximum ranges during any time in the day.

$$|V_{min}| < |V_{t,j}| < |V_{max}| \qquad j = 1,2 \ldots\ldots Nbus \quad (5.19)$$

iii) At any point during the day, the total current drawn by each branch must be less than the maximum current rating of that branch.

$$J_{t,j} \leq J_{t,j}^{max} \qquad j = 1,2 \ldots \ldots . Nbus - 1 \tag{5.20}$$

5.5 Optimization Algorithm

Section 3.4 of Chapter 3 provides a detailed discussion of the chaotic velocity-based optimization algorithm, Pareto-based multi-objective optimization technique and TOPSIS method.

5.5.1 Implementation of MOCVBOA

The procedure for finding the optimal sizes and locations of PV and PV-BESS units in the distribution system for the enhancement of the objectives using the MOCVBOA algorithm are given below

1. In this step, with the help of methods developed in section 5.2.1, p.u $P_{t,PV}$ vector values are obtained by reading the historical solar irradiance data and necessary PV unit data such as $N_{PV\,mod}, V_{MPP}, I_{MPP}, FF, V_{OC}, I_{SC}$, k_V, k_i, T_c, T_{cg}, T_A, N_{OT}.
2. Read the distribution network load & line data and data of a typical p.u, twenty - four - hour electrical load for different bus types.
3. Initialization of algorithm parameters such as N, Maxiter & REP_{max} etc.
4. Generation of the initial set of solutions between the minimum and maximum limits.

   For optimal planning of PV units, the decision matrix for the planning of one PV unit is shown below

$$X_{ini} = \begin{bmatrix} L_{1,PV} & P_{1,PV} \\ L_{2,PV} & P_{2,PV} \\ & \cdot \\ & \cdot \\ L_{N,PV} & P_{N,PV} \end{bmatrix} \tag{5.21}$$

   Where $L_{N,PV}$ & $P_{N,PV}$ are the location and PV unit size of Nth agent. The hourly power output from $L_{N,PV}$ is obtained by multiplying $P_{N,PV}$ size is with p.u PV curve

   For optimal planning of PV-BESS units, the decision matrix for the planning of one PV-BESS unit is shown below

$$X_{ini} = \begin{bmatrix} L_{1,PV-BESS} & P_{1,1,PV-BESS} \cdots & P_{t,1,PV-BESS} \cdots & P_{24,1,PV-BESS} \\ L_{2,PV-BESS} & P_{1,2,PV-BESS} \cdots & P_{t,2,PV-BESS} \cdots & P_{24,2,PV-BESS} \\ & & \cdot & \\ & & \cdot & \\ L_{N,PV-BESS} & P_{1,N,PV-BESS} \cdots & P_{t,N,PV-BESS} \cdots & P_{24,N,PV-BESS} \end{bmatrix} \tag{5.22}$$

Where $L_{N,PV-BESS}$ is the location of Nth agent, $P_{t,N,PV-BESS}$ is the Nth agent output power from PV-BESS unit during tth hour of the day.

5. Finding objective function values for each agent.

   By using the above initial data, the values of objective functions are evaluated by the load-flow simulations.
6. Set the iteration count to zero.
7. Update the butterfly's fragrance.
8. Update each agent's positions.
9. The sequential method used in Step 5 should be used to calculate the objective function values for each updated agent.
10. Combine updated agents with agents from prior iterations, then use the methods described in sections 5.5 to identify the non-dominated solutions and use the technique outlined in section 5.5 to update the repository set's solutions.
11. By Utilizing the TOPSIS technique, find the gbest solution from the repository set.
12. If the number of iterations is less than the maximum, repeat steps 6–11; if not, output outcomes such as the global best solution and objective function values.

5.6 Results and Discussion

In this work, an IEEE-33 bus radial distribution system has been used to verify the suggested method. Base values for the system are 100 MVA and 12.66 kV. The 33 buses are grouped into 17 residential buses, 5 commercial buses, and 9 industrial buses. The active and reactive power demands mentioned in the system's bus data are considered as the peak demands of the respective buses. Hourly reactive and active power demands of the buses for a day are obtained by multiplying the peak demand of the respective buses with the p.u daily load curves. An initial load flow is carried out to obtain the distribution system technical metrics without PHEVs load. For load flow investigations, backward/forward sweep-based load flow [114] has been employed. The system's energy loss and voltage deviation index are 3053 kW and 31.2158 p.u. The total daily active electricity requirement from the buses is 64510 kW. The system's lowest voltage of 0.8945 p.u. at bus number 18 occurred during the day's seventeenth hour.

To investigate the impact of increased electric power consumption due to PHEVs on the electrical distribution system technical metrics, it has assumed that 200 PHEVs will charge their vehicles at homes and 300 PHEVs will charge in the PFCS's connected to the buses 12,

19, 24, 27 & 33. The daily charging profile of the PHEVs are generated using the methodologies developed in section 2.5 & 2.6 and imposed on the abovementioned buses of the distribution system. The following points are observed from the load flow results. The total daily active electricity requirement from the buses is increased to 73556 kW, the energy loss and voltage deviation index are increased to 3777 kW and 34.88 p.u. The system's lowest voltage is 0.8839 p.u. The distribution system's hourly active power consumption for a day from the slack bus without PHEVs and with PHEVs is shown in Figure 5.1 for comparison.

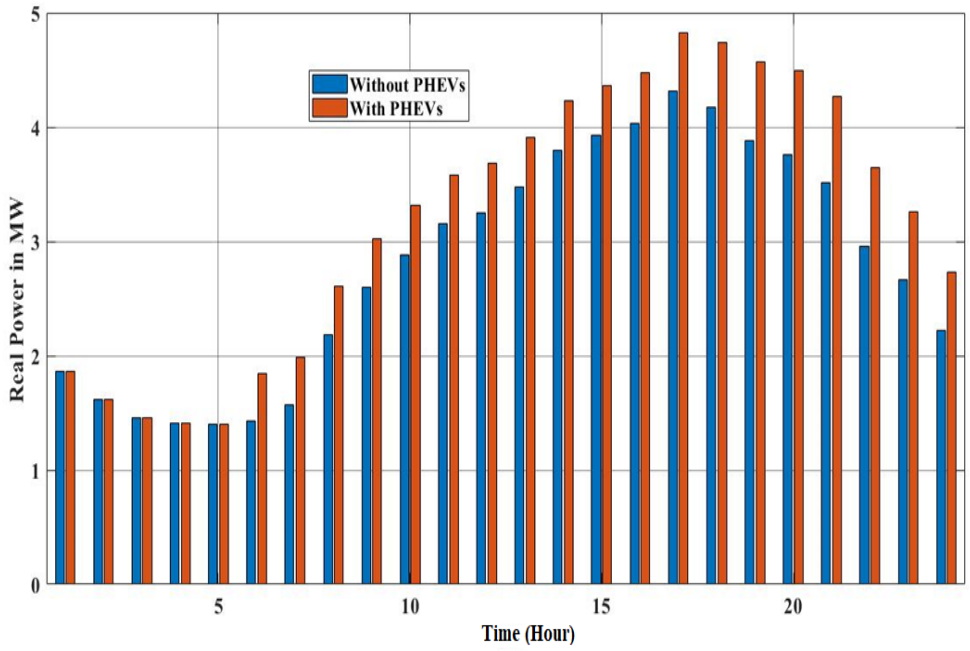

Figure 5.1 Hourly active power demand of the system without and with PHEVs load

From Figure 5.1, it is observed that peak power demand of the system occurred during the 17th hour of the day is increased by 11% due to the PHEVs load. From the discussions above, it is certain that the distribution network's technical parameters worsen due to PHEVs' electrical demand. Therefore, to improve the distribution system's technical metrics, optimal planning of PV and PV-BESS units are considered in this work. The data about the solar radiance is taken from [31]. This study considered a PV module with the following specifications: V_{MPP}=28.36 V, I_{MPP} =7.76 A, V_{OC}=36.96 V, I_{SC}=8.38 A, N_{OT}=43 ^{o}C, k_V=0.1278 V/^{o}C, k_i=0.00545 A/^{o}C and PV unit with $N_{PV\,mod} = 600$, 132 kW rated capacity. Table 5.1 provides operational and installation expenses for PV and BESS units[110], [111]. Figure 5.2 (a) & (b) depicts PDF curves of solar radiance & the p.u PV output curve derived from the methodology discussed in section 5.2.

Table 5.1 Installation and operational expenses for PV and BESS units

Parameters	**Value**
Installation cost of PV unit (INC_{pv}) in \$/kW	1100
Maintenance & Operational cost of PV unit (OMC_{pv}) in \$/kWhr	0.01
Installation cost of 400 kWhr BESS unit (INC_{BESS}) in \$	128000
Maintenance & Operational cost of BESS unit (OMC_{bess}) in \$/year	10666.67
Number of years for DG planning (nDG)	20
Number of years for BESS planning (nBESS)	8
Rate of interest in % (k)	10
Electricity price in \$/kWhr (k_e)	0.2

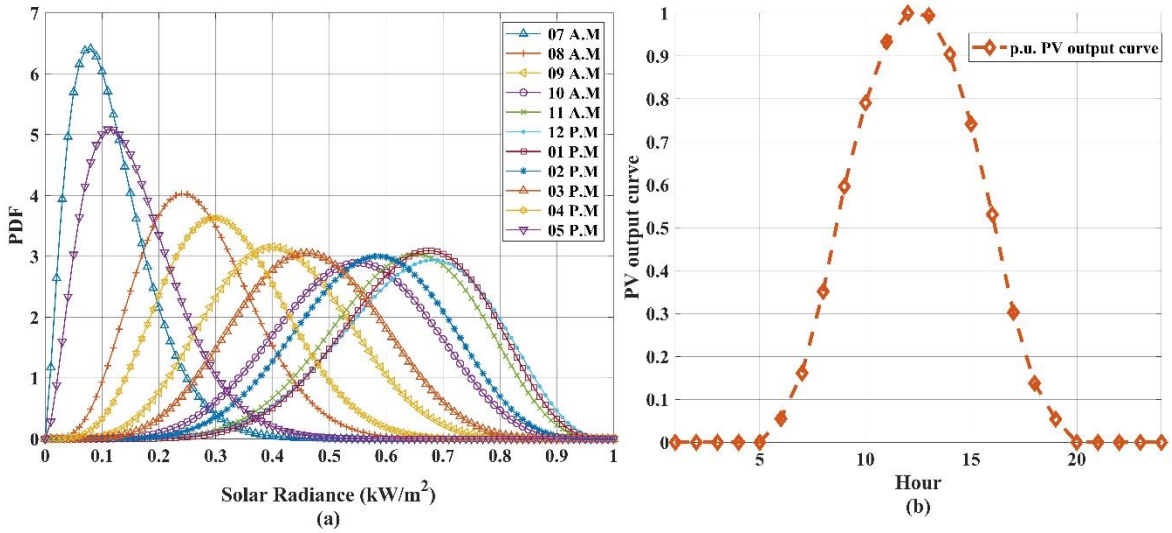

Figure 5.2 PDF curves of solar radiance and p.u unit curve of PV unit

In this work, the following two scenarios to improve the proposed objectives.

1) Optimal planning of PV units.
2) Optimal planning of PV-BESS units.

In scenario 1, the minimization of the distribution system's energy loss and voltage deviation is considered. Due to the consideration of both PV and BESS units in scenario 2, mitigation of the distribution system's total voltage deviation, energy loss and AEC are considered. By oversizing inverter ratings relative to the ratings of RDGs units, it is assumed

in scenarios 1 and 2 that PV and PV-BESS units will operate at a constant 0.9 pf. In this work, the total number of RDGs to be optimally placed in the distribution system is fixed at three. Figure 5.3 (a) & (b) depicts the optimal Pareto front provided by the MOCVBOA algorithm for scenarios 1 & 2, respectively. In the TOPSIS method, by following the restriction that the sum of all weights equals one, all objectives are assigned equal values for picking one solution from the optimal Pareto front. Table 5.2 shows the optimal sizes of PV units, BESS units and distribution system parameters for all scenarios outcomes.

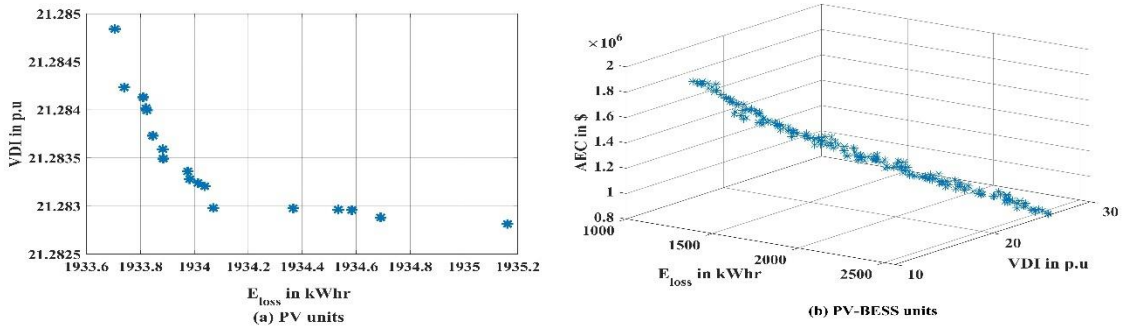

Figure 5.3 Optimal pareto fronts of two scenarios

Table 5.2 Simulation outcomes of all scenarios

Parameters	Scenario-1	Scenario-2
E_{loss} in kWhr	1934	1332
TVD in p.u	21.2	16.188
AEC in $	----------	1511549
Lowest magnitude of bus voltage in p.u	0.8839	0.95
PV units' sizes in kW & locations	1458/13 2943/30 1412/25	802/16 2407/18 2382/33
BESS units' sizes in kWh & locations	--------	1983/16 5948/18 5888/33

From Table 5.2, the following points are observed. In scenario-1, the network's energy loss is mitigated to 1934 kW (accounts 49% loss mitigation), and VDI is reduced to 21.28 p.u. The hourly slack bus power & power output of the PV units in scenarios 1 is shown in Figure 5.4

(a) & (b), respectively. From Figure 5.4 (a), it has been observed that system's slack bus power is zero. This is because output power from PV units is maximum during midday. However, in scenarios 1 & 2, there was no improvement in the distribution system's lowest voltage and reduction in the system's peak power. This is because, during the 17th hour of the day, when system demand is at its highest, the output power from PV units is zero.

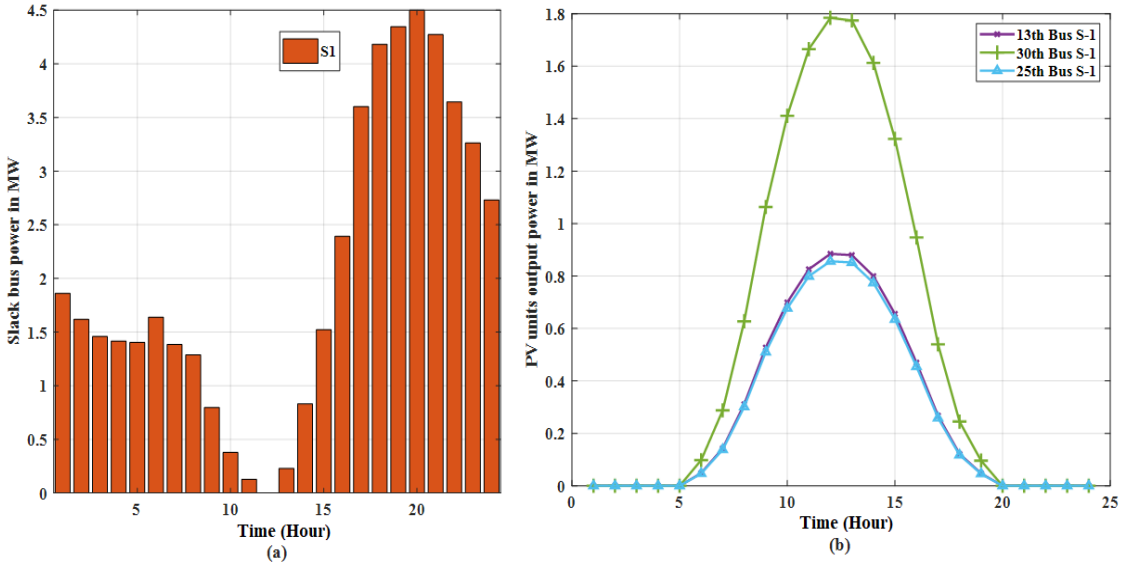

Figure 5.4 Daily slack bus power & PV units output power curves in scenario 1

In scenario 2, the system's energy loss and VDI are mitigated to 1332 kW (accounts for 44.69 % loss mitigation) & 16.188 p.u, respectively. The system's lowest voltage is enhanced to 0.95 p.u in scenario 2. The hourly dispatch of the PV unit's output power, BESS unit's output power, and PV-BESS unit's output power for scenarios 3 & 4 cases are depicted in Figure 5.5. The -ve sign of the BESS unit's output power indicates discharging mode (i.e., supplying power to the grid), +ve sign indicates the charging mode of BESS units. The combined PV-BESS units will inject power at the respective buses as per the PV-BESS units' output power curves, as seen from Figure 5.5, provided the output from BESS units is controlled in accordance with their curves. To regulate the output power of the BESS unit in accordance with the curves depicted in Figure 5.5, a converter with advanced controlling mechanisms is necessary. Figure 5.6 illustrates the power drawn from the substation in scenario's 3 & 4, respectively. And from Figure 5.6 slack bus powers, it is also observed that there is a significant reduction in the distribution system's peak power. The discussions have led to the conclusion that when PV-BESS units are located optimally, the distribution system performance improves in all respects

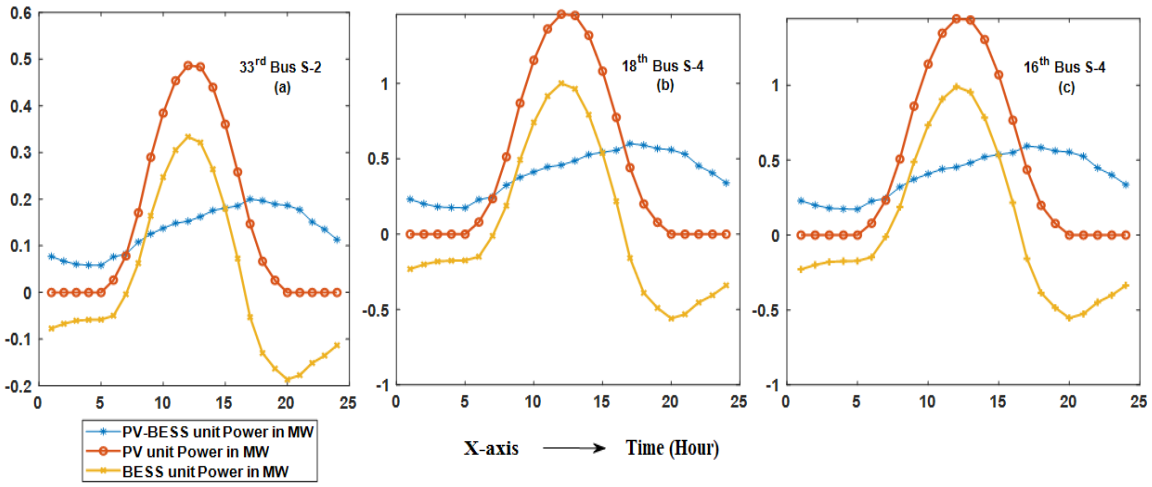

Figure 5.5 output curves of PV-BESS units in scenarios 2 case

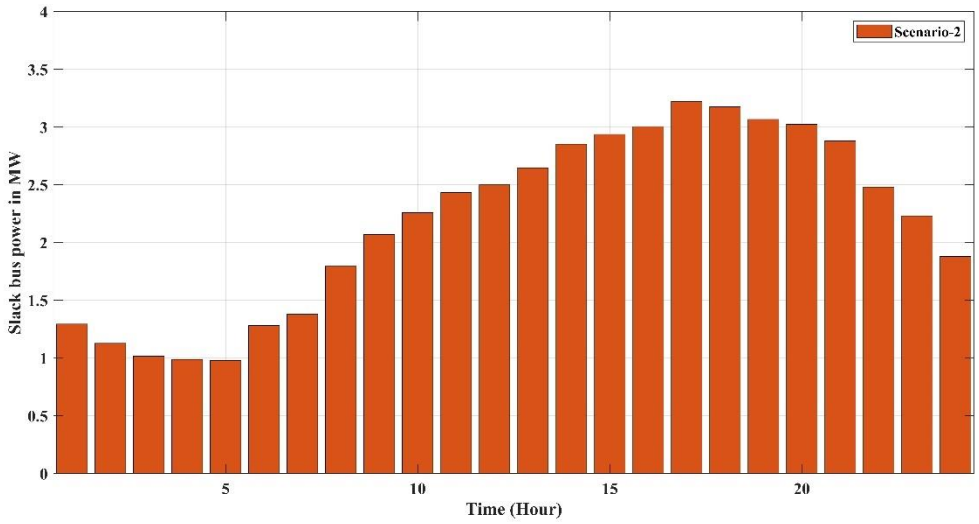

Figure 5.6 Daily slack bus power curves in scenarios 3 case

In substitution of PV-BESS units, dispatchable biomass units can also be deployed. The PV-BESS unit curves shown in Figure 5.5 are used to calculate the maximum optimal sizes of the biomass units. Then, identical system performance can be attained if the biomass units' output is regulated in accordance with the ideal PV-BESS unit curves shown in Figure 5.5.

5.7 Summary and Comments

This work has analysed the effect of PHEVs' electric load on the distribution system's technical parameters. The 33-bus system, which comprises residential, commercial, and

industrial buses, is considered in this study. Two charging scenarios are considered: charging of PHEVs at home during night-time of the day and charging of PHEVs in PFCS. Using the probabilistic methodologies and Monte-Carlo simulation, the daily electric power requirement caused by charging PHEVs in two scenarios is determined. The electrical demand generated in scenario 1 is imposed on the residential buses on the 33-bus distribution system. The PFCSs connected to the few buses in the distribution system are subject to the electrical demand generated in scenario 2. Based on the results of the load flow studies, the system's technical metrics, such as energy loss and voltage profile, have gotten worse as a result of the PHEVs' load demand. The system has also seen an increase in peak power demand. To mitigate the effect on above metrics, optimal planning of PV units operating with is addressed at first. Results shows that the system's energy loss and voltage deviation index have decreased. But there was no improvement in the reduction of system’s peak power and improvement in the system’s lowest voltage magnitude. This is as a result of the PV units' non-dispatchable nature i.e., dependency of PV units output power on solar irradiance. To address the improvement in all aspects of technical parameters and to overcome the non-dispatchable nature of units, optimal planning of PV-BESS units is addressed in the later stage. The optimum PV-BESS units planning results have shown an improvement in every technical metric related to the distribution system. However, a converter with sophisticated controlling techniques is required to regulate the BESS unit's output power in line with the optimal curves. Since biomass units are also deployable, they can be used in place of PV-BESS units. The optimal power output curves of RDGs can be used to determine the size of biomass units.

Chapter 6

Conclusions and Future Scope

6.1 Conclusions

Numerous issues challenge distribution networks, including increasing load needs, environmental concerns, operating limitations, infrastructure development restrictions, and poor efficiency. The optimal integration and planning of distributed generation in distribution networks can result in several advantages, including improved power quality, supply security, voltage stability, reliability, and loss reduction. However, the above-mentioned distribution networks metrics might suffer from improper distributed generation planning. Furthermore, optimal planning of distributed generation in the distribution network gives a viable solution for the increased load demand due to plug-in hybrid electric vehicles. The thesis's objectives are i) Optimal planning of distributed generation and optimal reconfigured network for improving system's efficiency and loadabilty (ii) Optimal planning of non-dispatchable PV & WT units, dispatchable PV-BESS, WT-BIOMASS units by considering solar radiance, wind speed and load uncertainties for mitigating system's energy loss and enhancing voltage profile. (iii) Optimal planning of distributed generation in the presence of PHEVs load demand charging under private charging scenario (iv) Optimal planning of PV & PV- BESS units in the presence of PHEVs load demand charging under private and public charging scenarios.

In Chapter 2, the improvement of two distribution system metrics: enhancement of loadability and minimization of power loss reduction, is addressed. Mitigation of the system's power loss improves its efficiency, and an increase in future load can be effectively met by enhancement in loadability, which enhances the system's voltage stability margin & loading marginal factor. The enhancement in the above two metrics is addressed at the system's peak load level without considering load uncertainties. The idea behind the above assumption is DGs have to inject how much active and reactive power into the system at optimal locations by satisfying operational limits for the improvement of the above-cited metrics to the maximum extent. 33-Bus and 69-Bus radial distribution test systems are considered in this study. At first, the optimization of individual objective functions using the latest butterfly optimizer is addressed. From the outcomes of single objective optimization, it is observed that there exists a conflicting nature between the two objectives. Then a Ɛ-constraint multi-objective technique using the butterfly optimizer technique is developed to bring the compromised solution between the two objectives. From the outcomes of the Ɛ-constraint multi-objective approach, the

succeeding points are observed. The most significant improvement in both objectives is achieved when DGs are optimally placed in the reconfigured distribution network. The optimal percentage injection of total kVA by the DGs into the system is around 85 % for getting the benefits mentioned above, which are only possible with the enormous sizes of the combination of multiple DG types. Similar system performance is achieved if DGs inject power into the system in accordance with load changes, provided that DGs are dispatchable in nature.

In Chapter 3, optimal planning of non-dispatchable PV & WT units, dispatchable PV-BESS & WT-BIOMASS units for the enhancement of distribution system efficiency and voltage profile by considering solar radiance, wind speed and load uncertainties are addressed. Two theoretically objective functions, energy loss and total voltage deviation, are taken for the improvement of the two metrics mentioned above. 33-Bus and 69-Bus radial distribution test systems are considered in this study. In contrast to other multi-objective techniques: the weighted sum method, weighted product method, max-min method, Fuzzy method & Ɛ-constraint method (used in Chapter 2), which reduce multi-objective optimization into a single optimization strategy, the Pareto-based multi-objective approach produces a collection of optimal non-dominant solutions between the competing objectives. Due to the above-cited advantage, we used a Pareto-based multi-objective velocity-based butterfly optimization algorithm (MOVBOA) to bring the optimal Pareto front between the competing objectives and a TOPSIS method was chosen for selecting the most compromised solution. The most significant improvement in both objectives is observed when dispatchable DGs are placed optimally in the optimal reconfigured distribution system. However, a converter with sophisticated controlling techniques is required to regulate the BESS unit's output power in line with the optimal curves. Due to the consideration of all the DGs: PV, BESS, WT & BIOMASS, minimization of the distribution system's energy loss, voltage deviation and AEC are considered, and the final compromised solution is determined.

In Chapter 4, the effect of PHEVs electric load on the distribution system's technical parameters due to charging of PHEVs at home during night-time of the day is studied first. The 33-bus system, which comprises residential, commercial, and industrial buses, is considered in this study. Using the probabilistic curves taken from the literature, the 24-hour electrical demand was generated using the probabilistic curve and imposed on the residential buses on the 33-bus distribution system. Based on the results of the load flow studies, the system's technical metrics, such as energy loss and voltage profile, have gotten worse as a result of the PHEVs' load demand. The system has also seen an increase in peak power demand. To mitigate

the effect on above metrics, optimal planning of DG units is addressed. MOVBOA is used for deriving the final optimal Pareto front between the competing objectives. Results show that the system's energy loss and voltage deviation index have decreased.

In Chapter 5, the effect of PHEV's electric load on the distribution system's technical parameters due to two charging scenarios: charging of PHEVs at home during night-time of the day and charging of PHEVs in PFCS is studied first. The 33-bus system, which comprises residential, commercial, and industrial buses, is considered in this study. Using the probabilistic methodologies and Monte-Carlo simulation, the daily electric power requirement caused by charging PHEVs in two scenarios is determined. The electrical demand generated in scenario-1 is imposed on the residential buses on the 33-bus distribution system. The PFCSs connected to the few buses in the distribution system are subject to the electrical demand generated in scenario 2. Based on the results of the load flow studies, the system's technical metrics, such as energy loss and voltage profile, have gotten worse as a result of the PHEVs' load demand. The system has also seen an increase in peak power demand. To mitigate the effect on above metrics, optimal planning of PV units is addressed first. Results show that the system's energy loss and voltage deviation index have decreased. But there was no improvement in the reduction of the system’s peak power and improvement in the system’s lowest voltage magnitude. This is due to the PV units' non-dispatchable nature i.e., dependency of PV units' output power on solar irradiance. To address the improvement in all aspects of technical parameters and to overcome the non-dispatchable nature of units, optimal planning of PV-BESS units is addressed in the later stage. The optimum PV-BESS unit planning results have shown an improvement in every technical metric related to the distribution system. However, a converter with sophisticated controlling techniques is required for the regulation of the BESS unit's output power in line with the optimal curves.

6.2 Future Scope

- Optimal Planning of PV, WT and distributed BESS units in a distribution network for improving metrics like maximization of DGs power penetration, power loss reduction, and voltage profile improvement.

- Determination of Optimal sizing of BESS in a distribution network with pre-installed PV and WT units for the improvement of metrics like operating cost minimization,

power loss minimization, voltage profile improvement, peak load shaving, and load balancing.

- Simultaneous Optimal planning of Public Fast Charging Stations (PFCS), and DGs in a distribution network by considering uncertainties of DGs and transportation network of PHEVs.

Publications

Journals Published

1. **V. K. Thunuguntla** and S. K. Injeti, "Ɛ-constraint multiobjective approach for optimal network reconfiguration and optimal allocation of DGs in radial distribution systems using the butterfly optimizer," ***Int. Trans. Electr. Energy Syst.*****, vol. 30, no. 11, pp. 1–20, 2020.John Wiley (SCIE Indexed), Impact factor:2.639.**

2. S. K. Injeti and **V. K. Thunuguntla**, "Optimal integration of DGs into radial distribution network in the presence of plug-in electric vehicles to minimize daily active power losses and to improve the voltage profile of the system using bio-inspired optimization algorithms," ***Prot. Control Mod. Power Syst.*****, vol. 5, no. 3, 2020.Springer (SCIE Indexed), Impact factor: 10.5.**

3. **T. Vinod Kumar** and S. Kumar Injeti, "Probabilistic optimal planning of dispatchable distributed generator units in distribution systems using a multi-objective velocity-based butterfly optimization algorithm," ***Renew. Energy Focus*****, vol. 43, pp. 191–209, 2022.Elsevier, (ESCI Indexed).**

4. **V. K. Thunuguntla** and S. K. Injeti, "Butterfly optimizer assisted Max–Min based multi-objective approach for optimal connection of DGs and optimal network reconfiguration of distribution networks," ***J. Electr. Syst. Inf. Technol.*****, vol. 9, no. 1, 2022.**

Journals Under Review

1. **Thunuguntla Vinod Kumar** and Satish Kumar Injeti "Probabilistic optimal allocation of Inverter based Solar PV units and Battery Energy Storage System in the distribution system in presence of plug-in electric vehicles using a multi-objective chaotic velocity-based butterfly optimization algorithm" **Energy Systems, Springer (Under Review).**

Bibliography

[1] A. Ehsan and Q. Yang, "Optimal integration and planning of renewable distributed generation in the power distribution networks: A review of analytical techniques," *Appl. Energy*, vol. 210, no. July 2017, pp. 44–59, 2018.

[2] R. H. A. Zubo, G. Mokryani, H. S. Rajamani, J. Aghaei, T. Niknam, and P. Pillai, "Operation and planning of distribution networks with integration of renewable distributed generators considering uncertainties: A review," *Renew. Sustain. Energy Rev.*, vol. 72, no. May 2016, pp. 1177–1198, 2017.

[3] B. Yang *et al.*, "Modelling, applications, and evaluations of optimal sizing and placement of distributed generations: A critical state-of-the-art survey," *Int. J. Energy Res.*, vol. 45, no. 3, pp. 3615–3642, 2021.

[4] R. H. A. Zubo, G. Mokryani, H. S. Rajamani, J. Aghaei, T. Niknam, and P. Pillai, "Operation and planning of distribution networks with integration of renewable distributed generators considering uncertainties: A review," *Renew. Sustain. Energy Rev.*, vol. 72, no. September 2016, pp. 1177–1198, 2017.

[5] O. Badran, S. Mekhilef, H. Mokhlis, and W. Dahalan, "Optimal reconfiguration of distribution system connected with distributed generations: A review of different methodologies," *Renew. Sustain. Energy Rev.*, vol. 73, no. August 2015, pp. 854–867, 2017.

[6] R. C. Green, L. Wang, and M. Alam, "The impact of plug-in hybrid electric vehicles on distribution networks: A review and outlook," *Renew. Sustain. Energy Rev.*, vol. 15, no. 1, pp. 544–553, 2011.

[7] H. Ma, Z. Yang, P. You, and M. Fei, "Multi-objective biogeography-based optimization for dynamic economic emission load dispatch considering plug-in electric vehicles charging," *Energy*, vol. 135, pp. 101–111, 2017.

[8] Z. YANG, K. LI, Q. NIU, Y. XUE, and A. FOLEY, "A self-learning TLBO based dynamic economic/environmental dispatch considering multiple plug-in electric vehicle loads," *J. Mod. Power Syst. Clean Energy*, vol. 2, no. 4, pp. 298–307, 2014.

[9] R. K. Avvari and V. Kumar D M, “A Novel Hybrid Multi-Objective Evolutionary Algorithm for Optimal Power Flow in Wind, PV, and PEV Systems,” *J. Oper. Autom. Power Eng.*, vol. 11, no. 2, pp. 130–143, 2023.

[10] A. Ehsan and Q. Yang, “Optimal integration and planning of renewable distributed generation in the power distribution networks: A review of analytical techniques,” *Appl. Energy*, vol. 210, no. October 2017, pp. 44–59, 2018.

[11] N. Acharya, P. Mahat, and N. Mithulananthan, “An analytical approach for DG allocation in primary distribution network,” *Int. J. Electr. Power Energy Syst.*, vol. 28, no. 10, pp. 669–678, 2006.

[12] P. Mahat, “Optimal placement of wind turbine DG in primary distribution systems for real loss reduction,” *Proc. Energy …*, no. 4, 2006.

[13] D. Q. Hung, N. Mithulananthan, and R. C. Bansal, “Analytical expressions for DG allocation in primary distribution networks,” *IEEE Trans. Energy Convers.*, vol. 25, no. 3, pp. 814–820, 2010.

[14] D. Q. Hung and N. Mithulananthan, “Multiple distributed generator placement in primary distribution networks for loss reduction,” *IEEE Trans. Ind. Electron.*, vol. 60, no. 4, pp. 1700–1708, 2013.

[15] D. Q. Hung and N. Mithulananthan, “Alternative analytical approaches for renewable DG allocation for energy loss minimization,” *IEEE Power Energy Soc. Gen. Meet.*, pp. 1–10, 2012.

[16] D. Q. Hung, S. Member, N. Mithulananthan, and S. Member, “Determining PV Penetration for Distribution Determining PV Penetration for Distribution Systems With Time-Varying Load Models,” *Power Syst. IEEE Trans.*, vol. 29, no. July, pp. 3048–3057, 2016.

[17] D. Quoc, N. Mithulananthan, and R. C. Bansal, “Integration of PV and BES units in commercial distribution systems considering energy loss and voltage stability,” *Appl. Energy*, vol. 113, pp. 1162–1170, 2014.

[18] V. V. S. N. Murthy and A. Kumar, “Comparison of optimal DG allocation methods in radial distribution systems based on sensitivity approaches,” *Int. J. Electr. Power*

Energy Syst., vol. 53, no. 1, pp. 450–467, 2013.

[19] S. Gopiya Naik, D. K. Khatod, and M. P. Sharma, "Optimal allocation of combined DG and capacitor for real power loss minimization in distribution networks," *Int. J. Electr. Power Energy Syst.*, vol. 53, pp. 967–973, 2013.

[20] S. Elsaiah, M. Benidris, and J. Mitra, "Analytical approach for placement and sizing of distributed generation on distribution systems," *IET Gener. Transm. Distrib.*, vol. 8, no. 6, pp. 1039–1049, 2014.

[21] M. Mirzaei, J. Jasni, H. Hizam, N. I. A. Wahab, and S. E. G. Mohamed, "An analytical method for optimal sizing of different types of DG in a power distribution system," *Conf. Proceeding - 2014 IEEE Int. Conf. Power Energy, PECon 2014*, pp. 309–314, 2014.

[22] Salem Elsaiah; Mohammed Benidris; Joydeep Mitra, "An analytical method for placement and sizing of distributed generation on distribution systems," in *2014 Clemson University Power Systems Conference*, 2014.

[23] P. V. Prasad and S. Satyanarayana, "A Novel Method for Optimal Distributed Generator Placement in Radial Distribution Systems," *Distrib. Gener. Altern. Energy J.*, vol. 26, no. 1, pp. 7–19, 2011.

[24] D. Q. Hung, N. Mithulananthan, and R. C. Bansal, "Analytical strategies for renewable distributed generation integration considering energy loss minimization," *Appl. Energy*, vol. 105, pp. 75–85, 2013.

[25] T. Gözel and M. H. Hocaoglu, "An analytical method for the sizing and siting of distributed generators in radial systems," *Electr. Power Syst. Res.*, vol. 79, no. 6, pp. 912–918, 2009.

[26] G. Dhiman and A. Kaur, "Optimizing the design of airfoil and optical buffer problems using spotted hyena optimizer," *Designs*, vol. 2, no. 3, pp. 1–16, 2018.

[27] S. K. Injeti and N. Prema Kumar, "A novel approach to identify optimal access point and capacity of multiple DGs in a small, medium and large scale radial distribution systems," *Int. J. Electr. Power Energy Syst.*, vol. 45, no. 1, pp. 142–151, 2013.

[28] F. S. Abu-Mouti and M. E. El-Hawary, "Optimal distributed generation allocation and

sizing in distribution systems via artificial bee colony algorithm," *IEEE Trans. Power Deliv.*, vol. 26, no. 4, pp. 2090–2101, 2011.

[29] S. Kumar Injeti, S. M. Shareef, and T. V. Kumar, "Optimal Allocation of DGs and Capacitor Banks in Radial Distribution Systems," *Distrib. Gener. Altern. Energy J.*, vol. 33, no. 3, pp. 6–34, 2018.

[30] P. Phonrattanasak and A. Objectives, "Optimal Placement of DG Using Multiobjective particle Swarm Optimization," *Electr. Technol.*, no. Icmet, pp. 342–346, 2010.

[31] M. M. Aman, G. B. Jasmon, A. H. A. Bakar, and H. Mokhlis, "A new approach for optimum simultaneous multi-DG distributed generation Units placement and sizing based on maximization of system loadability using HPSO (hybrid particle swarm optimization) algorithm," *Energy*, vol. 66, pp. 202–215, 2014.

[32] V. Veeramsetty, C. Venkaiah, and D. M. V. Kumar, *Hybrid genetic dragonfly algorithm based optimal power flow for computing LMP at DG buses for reliability improvement*, vol. 9, no. 3. Springer Berlin Heidelberg, 2018.

[33] B. H. MERLIN A, "Search for a minimal-loss operating spanning tree configuration in an urban power distribution system.," in *Power Syst Comput Conf (Proceedings. Power Systems Computation Conference 5th 750901 Vol.1-2)*, 1975, pp. 1,2/6,1-1,2/6,18.

[34] N. D. R. Sarma and K. S. Prakasa Rao, "A new 0-1 integer programming method of feeder reconfiguration for loss minimization in distribution systems," *Electr. Power Syst. Res.*, vol. 33, no. 2, pp. 125–131, 1995.

[35] H. M. Khodr, J. Martinez-Crespo, M. A. Matos, and J. Pereira, "Distribution systems reconfiguration based on OPF using benders decomposition," *IEEE Trans. Power Deliv.*, vol. 24, no. 4, pp. 2166–2176, 2009.

[36] H. Haghighat and B. Zeng, "Distribution System Reconfiguration under Uncertain Load and Renewable Generation," *IEEE Trans. Power Syst.*, vol. 31, no. 4, pp. 2666–2675, 2016.

[37] M e w E. Baran Felix F. Wu, "NETWORK RECONFIGURATION IN DISTRIBUTION SYSTEMS FOR LOSS REDUCTION AND LOAD BALANCING," *IEEE Trans. Power Deliv.*, vol. 4, no. 2, 1989.

[38] R. J. Sârfi and M. M. A. Salama, “Distribution system reconfiguration for loss reduction: an algorithm based on network partitioning theory,” *IEEE Trans. Power Syst.*, vol. 11, no. 1, pp. 504–510, 1996.

[39] F. V. Gomes, S. Carneiro, J. L. R. Pereira, M. P. Vinagre, P. A. N. Garcia, and L. A. Ramos, “A new heuristic reconfiguration algorithm for large distribution systems,” *IEEE Trans. Power Syst.*, vol. 20, no. 3, pp. 1373–1378, 2005.

[40] G. K. Viswanadha Raju and P. R. Bijwe, “Efficient reconfiguration of balanced and unbalanced distribution systems for loss minimisation,” *IET Gener. Transm. Distrib.*, vol. 2, no. 1, pp. 7–12, 2008.

[41] A. K. Ferdavani, A. A. M. Zin, A. Khairuddin, and M. M. Naeini, “Reconfiguration of distribution system through two minimum-current neighbour-chain updating methods,” *IET Gener. Transm. Distrib.*, vol. 7, no. 12, pp. 1492–1497, 2013.

[42] K. Nara, A. Shiose, M. Kitagawa, and T. Ishihara, “Implementation of Genetic Algorithm for Distribution Systems Loss Minimum Re-Configuration,” *IEEE Trans. Power Syst.*, vol. 7, no. 3, pp. 1044–1051, 1992.

[43] A. C. B. Delbem, A. C. P. de Leon Ferreira de Carvalho, and N. G. Bretas, “Main chain representation for evolutionary algorithms applied to distribution system reconfiguration,” *IEEE Trans. Power Syst.*, vol. 20, no. 1, pp. 425–436, 2005.

[44] R. Pegado, Z. Ñaupari, Y. Molina, and C. Castillo, “Radial distribution network reconfiguration for power losses reduction based on improved selective BPSO,” *Electr. Power Syst. Res.*, vol. 169, no. September 2018, pp. 206–213, 2019.

[45] T. T. Nguyen and A. V. Truong, “Distribution network reconfiguration for power loss minimization and voltage profile improvement using cuckoo search algorithm,” *Int. J. Electr. Power Energy Syst.*, vol. 68, pp. 233–242, 2015.

[46] T. T. Nguyen, T. T. Nguyen, A. V. Truong, Q. T. Nguyen, and T. A. Phung, “Multi-objective electric distribution network reconfiguration solution using runner-root algorithm,” *Appl. Soft Comput. J.*, vol. 52, pp. 93–108, 2017.

[47] B. Venkatesh, R. Ranjan, and H. B. Gooi, “Optimal Reconfiguration of Radial Distribution Systems to Maximize Loadability,” *IEEE Trans. Power Syst.*, vol. 19, no.

1, pp. 260–266, 2004.

[48] M. M. Aman, G. B. Jasmon, A. H. A. Bakar, and H. Mokhlis, “Optimum network reconfiguration based on maximization of system loadability using continuation power flow theorem,” *Int. J. Electr. Power Energy Syst.*, vol. 54, pp. 123–133, 2014.

[49] A. Tyagi, A. Verma, and P. R. Bijwe, “Reconfiguration for loadability limit enhancement of distribution systems,” *IET Gener. Transm. Distrib.*, vol. 12, no. 1, pp. 88–93, 2018.

[50] R. S. Rao, K. Ravindra, K. Satish, and S. V. L. Narasimham, “Power loss minimization in distribution system using network reconfiguration in the presence of distributed generation,” *IEEE Trans. Power Syst.*, vol. 28, no. 1, pp. 317–325, 2013.

[51] T. T. Nguyen, A. V. Truong, and T. A. Phung, “A novel method based on adaptive cuckoo search for optimal network reconfiguration and distributed generation allocation in distribution network,” *Int. J. Electr. Power Energy Syst.*, vol. 78, pp. 801–815, 2016.

[52] A. Bayat, A. Bagheri, and R. Noroozian, “Optimal siting and sizing of distributed generation accompanied by reconfiguration of distribution networks for maximum loss reduction by using a new UVDA-based heuristic method,” *Int. J. Electr. Power Energy Syst.*, vol. 77, pp. 360–371, 2016.

[53] A. Parizad, A. H. Khazali, and M. Kalantar, “SITTING AND SIZING OF DISTRIBUTED GENERATION THROUGH HARMONY SEARCH ALGORITHM FOR IMPROVE VOLTAGE PROFILE AND REDUCUCTION OF THD AND LOSSES The Center of Excellence for Power System Automation and Operation , Department of Electrical Engineering , Iran Un,” 2010.

[54] A. Aref *et al.*, “PSO Based multi objective approach for optimal sizing and placement of distributed generation,” *Res. J. Appl. Sci. Eng. Technol.*, vol. 4, no. 22, pp. 4617–4624, 2012.

[55] Mojtaba Nuri; Mohammad Reza Miveh; Sohrab Mirsaeidi; Mohammad Reza Gharibdoost, “Distributed generation placement to maximize the loadability of distribution system using genetic algorithm,” in *Proceedings of 17th Conference on Electrical Power Distribution*, 2012.

[56] P. K. N and M. R. K, “IPSO Algorithm for Maximization of System Loadability, Voltage Stability and Loss Minimisation by Optimal DG Placement,” *Ijireeice*, vol. 3, no. 11, pp. 73–77, 2015.

[57] R. Yousefian and H. Monsef, “DG-allocation based on reliability indices by means of Monte Carlo simulation and AHP,” *2011 10th Int. Conf. Environ. Electr. Eng. EEEIC.EU 2011 - Conf. Proc.*, pp. 1–4, 2011.

[58] H. Doagou-Mojarrad, G. B. Gharehpetian, H. Rastegar, and J. Olamaei, “Optimal placement and sizing of DG (distributed generation) units in distribution networks by novel hybrid evolutionary algorithm,” *Energy*, vol. 54, pp. 129–138, 2013.

[59] S. Sultana and P. K. Roy, “Multi-objective quasi-oppositional teaching learning based optimization for optimal location of distributed generator in radial distribution systems,” *Int. J. Electr. Power Energy Syst.*, vol. 63, pp. 534–545, 2014.

[60] M. M. Aman, G. B. Jasmon, H. Mokhlis, and A. H. Abu Bakar, “Optimum tie switches allocation and DG placement based on maximisation of system loadability using discrete artificial bee colony algorithm,” *IET Gener. Transm. Distrib.*, vol. 10, no. 10, pp. 2277–2284, 2016.

[61] B. Kiran Babu and S. Maheswarapu, “New hybrid multiverse optimisation approach for optimal accommodation of DGs in power distribution networks,” *IET Gener. Transm. Distrib.*, vol. 13, no. 13, pp. 2673–2685, 2019.

[62] S. Arabi Nowdeh *et al.*, “Fuzzy multi-objective placement of renewable energy sources in distribution system with objective of loss reduction and reliability improvement using a novel hybrid method,” *Appl. Soft Comput. J.*, vol. 77, pp. 761–779, 2019.

[63] A. Selim, S. Kamel, A. S. Alghamdi, and F. Jurado, “Optimal Placement of DGs in Distribution System Using an Improved Harris Hawks Optimizer Based on Single- And Multi-Objective Approaches,” *IEEE Access*, vol. 8, pp. 52815–52829, 2020.

[64] S. K. Injeti, “A Pareto optimal approach for allocation of distributed generators in radial distribution systems using improved differential search algorithm,” *J. Electr. Syst. Inf. Technol.*, vol. 5, no. 3, pp. 908–927, 2018.

[65] Z. M. Salameh, B. S. Borowy, and A. R. A. Amin, “Photovoltaic Module-Site

Matching Based on the Capacity Factors," *IEEE Trans. Energy Convers.*, vol. 10, no. 2, pp. 326–332, 1995.

[66] Y. M. Atwa, E. F. El-Saadany, M. M. A. Salama, and R. Seethapathy, "Optimal renewable resources mix for distribution system energy loss minimization," *IEEE Trans. Power Syst.*, vol. 25, no. 1, pp. 360–370, 2010.

[67] A. Ali, K. Mahmoud, and M. Lehtonen, "Multiobjective Photovoltaic Sizing with Diverse Inverter Control Schemes in Distribution Systems Hosting EVs," *IEEE Trans. Ind. Informatics*, vol. 17, no. 9, pp. 5982–5992, 2021.

[68] J. H. Teng, S. W. Luan, D. J. Lee, and Y. Q. Huang, "Optimal charging/discharging scheduling of battery storage systems for distribution systems interconnected with sizeable PV generation systems," *IEEE Trans. Power Syst.*, vol. 28, no. 2, pp. 1425–1433, 2013.

[69] A. Ali, D. Raisz, and K. Mahmoud, "Optimal oversizing of utility-owned renewable DG inverter for voltage rise prevention in MV distribution systems," *Int. J. Electr. Power Energy Syst.*, vol. 105, no. August 2018, pp. 500–513, 2019.

[70] M. Khasanov, S. Kamel, C. Rahmann, H. M. Hasanien, and A. Al-Durra, "Optimal distributed generation and battery energy storage units integration in distribution systems considering power generation uncertainty," *IET Gener. Transm. Distrib.*, vol. 15, no. 24, pp. 3400–3422, 2021.

[71] J. Radosavljevic, N. Arsic, M. Milovanovic, and A. Ktena, "Optimal Placement and Sizing of Renewable Distributed Generation Using Hybrid Metaheuristic Algorithm," *J. Mod. Power Syst. Clean Energy*, vol. 8, no. 3, pp. 499–510, 2020.

[72] D. Q. Hung, N. Mithulananthan, and R. C. Bansal, "Integration of PV and BES units in commercial distribution systems considering energy loss and voltage stability," *Appl. Energy*, vol. 113, pp. 1162–1170, 2014.

[73] H. Abdel-Mawgoud, S. Kamel, M. Khasanov, and T. Khurshaid, "A strategy for PV and BESS allocation considering uncertainty based on a modified Henry gas solubility optimizer," *Electr. Power Syst. Res.*, vol. 191, no. October 2020, p. 106886, 2021.

[74] M. Khasanov, S. Kamel, A. Awad, and F. Jurado, "Optimal planning DG and BES

units in distribution system considering uncertainty of power generation and time-varying load," *Turkish J. Electr. Eng. Comput. Sci.*, vol. 29, no. 2, pp. 773–795, 2021.

[75] S. Velamuri, S. H. C. Cherukuri, S. K. Sudabattula, N. Prabaharan, and E. Hossain, "Combined Approach for Power Loss Minimization in Distribution Networks in the Presence of Gridable Electric Vehicles and Dispersed Generation," *IEEE Syst. J.*, vol. 16, no. 2, pp. 3284–3295, 2022.

[76] B. K. Jha, "Coordinated effect of PHEVs with DGs on distribution network," no. October, pp. 1–24, 2018.

[77] Z. Liu, F. Wen, and G. Ledwich, "Optimal planning of electric-vehicle charging stations in distribution systems," *IEEE Trans. Power Deliv.*, vol. 28, no. 1, pp. 102–110, 2013.

[78] P. Sadeghi-barzani, A. Rajabi-ghahnavieh, and H. Kazemi-karegar, "Optimal fast charging station placing and sizing," *Appl. Energy*, vol. 125, pp. 289–299, 2014.

[79] Z. H. Zhu, Z. Y. Gao, J. F. Zheng, and H. M. Du, "Charging station location problem of plug-in electric vehicles," *J. Transp. Geogr.*, vol. 52, pp. 11–22, 2016.

[80] S. R. Gampa, K. Jasthi, P. Goli, D. Das, and R. C. Bansal, "Grasshopper optimization algorithm based two stage fuzzy multiobjective approach for optimum sizing and placement of distributed generations, shunt capacitors and electric vehicle charging stations," *J. Energy Storage*, vol. 27, no. December 2019, p. 101117, 2020.

[81] F. Ahmad, A. Iqbal, I. Ashraf, M. Marzband, and I. Khan, "Placement of electric vehicle fast charging stations in distribution network considering power loss, land cost, and electric vehicle population," *Energy Sources, Part A Recover. Util. Environ. Eff.*, vol. 44, no. 1, pp. 1693–1709, 2022.

[82] A. Mohsenzadeh, S. Pazouki, S. Ardalan, and M. R. Haghifam, "Optimal placing and sizing of parking lots including different levels of charging stations in electric distribution networks," *Int. J. Ambient Energy*, vol. 39, no. 7, pp. 743–750, 2018.

[83] A. Awasthi, K. Venkitusamy, S. Padmanaban, R. Selvamuthukumaran, F. Blaabjerg, and A. K. Singh, "Optimal planning of electric vehicle charging station at the distribution system using hybrid optimization algorithm," *Energy*, vol. 133, pp. 70–78,

2017.

[84] H. Zhang, Z. Hu, Z. Xu, and Y. Song, “An Integrated Planning Framework for Different Types of PEV Charging Facilities in Urban Area,” *IEEE Trans. Smart Grid*, vol. 7, no. 5, pp. 2273–2284, 2016.

[85] A. Eid, “Allocation of distributed generations in radial distribution systems using adaptive PSO and modified GSA multi-objective optimizations,” *Alexandria Eng. J.*, vol. 59, no. 6, pp. 4771–4786, 2020.

[86] G. Battapothula, C. Yammani, and S. Maheswarapu, “Multi-objective optimal planning of FCSs and DGs in distribution system with future EV load enhancement,” *IET Electr. Syst. Transp.*, vol. 9, no. 3, pp. 128–139, 2019.

[87] G. Battapothula, C. Yammani, and S. Maheswarapu, “Multi-objective simultaneous optimal planning of electrical vehicle fast charging stations and DGs in distribution system,” *J. Mod. Power Syst. Clean Energy*, vol. 7, no. 4, pp. 923–934, 2019.

[88] K. E. Adetunji, I. W. Hofsajer, A. M. Abu-Mahfouz, and L. Cheng, “An optimization planning framework for allocating multiple distributed energy resources and electric vehicle charging stations in distribution networks,” *Appl. Energy*, vol. 322, no. December 2021, p. 119513, 2022.

[89] I. A. Quadri, S. Bhowmick, and D. Joshi, “Multi-objective approach to maximise loadability of distribution networks by simultaneous reconfiguration and allocation of distributed energy resources,” *IET Gener. Transm. Distrib.*, vol. 12, no. 21, pp. 5700–5712, 2018.

[90] Kalyanmoy Deb, *Multi-Objective Optimization using Evolutionary Algorithms*. WILEY.

[91] D. K. Lal, A. Barisal, and S. D. Madasu, “AGC of a two area nonlinear power system using BOA optimized FOPID+PI multistage controller,” *2019 2nd Int. Conf. Adv. Comput. Commun. Paradig. ICACCP 2019*, pp. 1–6, 2019.

[92] K. Aygül, M. Cikan, T. Demirdelen, and M. Tumay, “Butterfly optimization algorithm based maximum power point tracking of photovoltaic systems under partial shading condition,” *Energy Sources, Part A Recover. Util. Environ. Eff.*, vol. 00, no. 00, pp. 1–

19, 2019.

[93] S. Arora and S. Singh, “Butterfly optimization algorithm: a novel approach for global optimization,” *Soft Comput.*, vol. 23, no. 3, pp. 715–734, 2019.

[94] K. Muthukumar and S. Jayalalitha, “Optimal placement and sizing of distributed generators and shunt capacitors for power loss minimization in radial distribution networks using hybrid heuristic search optimization technique,” *Int. J. Electr. Power Energy Syst.*, vol. 78, pp. 299–319, 2016.

[95] P. Kayal and C. K. Chanda, “Optimal mix of solar and wind distributed generations considering performance improvement of electrical distribution network,” *Renew. Energy*, vol. 75, pp. 173–186, 2015.

[96] Z. M. Salameh, B. S. Borowy, and A. R. A. Amin, “Photovoltaic Module-Site Matching Based on the Capacity Factors,” vol. 10, no. 2, pp. 326–332, 1995.

[97] A. Ali, K. Mahmoud, and M. Lehtonen, “Multiobjective Photovoltaic Sizing With Diverse Inverter Control Schemes in Distribution Systems Hosting EVs,” vol. 17, no. 9, pp. 5982–5992, 2021.

[98] J. Teng, S. Member, S. Luan, D. Lee, and Y. Huang, “Optimal Charging / Discharging Scheduling of Battery Storage Systems for Distribution Systems Interconnected With Sizeable PV Generation Systems,” pp. 1–9, 2012.

[99] A. Ali, D. Raisz, and K. Mahmoud, “Electrical Power and Energy Systems Optimal oversizing of utility-owned renewable DG inverter for voltage rise prevention in MV distribution systems,” *Electr. Power Energy Syst.*, vol. 105, no. August 2018, pp. 500–513, 2019.

[100] E. Dall’Anese, S. V. Dhople, and G. B. Giannakis, “Optimal dispatch of photovoltaic inverters in residential distribution systems,” *IEEE Trans. Sustain. Energy*, vol. 5, no. 2, pp. 487–497, 2014.

[101] A. Ali, D. Raisz, and K. Mahmoud, “Optimal oversizing of utility-owned renewable DG inverter for voltage rise prevention in MV distribution systems,” *Int. J. Electr. Power Energy Syst.*, vol. 105, no. June 2018, pp. 500–513, 2019.

[102] K. Turitsyn, P. Šulc, S. Backhaus, and M. Chertkov, “Options for control of reactive

power by distributed photovoltaic generators," *Proc. IEEE*, vol. 99, no. 6, pp. 1063–1073, 2011.

[103] W. Long, M. Xu, J. Jiao, T. Wu, M. Tang, and S. Cai, "A velocity-based butterfly optimization algorithm for high-dimensional optimization and feature selection," *Expert Syst. Appl.*, vol. 201, no. December 2020, p. 117217, 2022.

[104] G. Chen, L. Liu, P. Song, and Y. Du, "Chaotic improved PSO-based multi-objective optimization for minimization of power losses and L index in power systems," *Energy Convers. Manag.*, vol. 86, pp. 548–560, 2014.

[105] M. Zhang, D. Long, T. Qin, and J. Yang, "A chaotic hybrid butterfly optimization algorithm with particle swarm optimization for high-dimensional optimization problems," *Symmetry (Basel).*, vol. 12, no. 11, pp. 1–27, 2020.

[106] S. Kumar, K. K. Mandal, and N. Chakraborty, "Optimal DG placement by multi-objective opposition based chaotic differential evolution for techno-economic analysis," *Appl. Soft Comput. J.*, vol. 78, pp. 70–83, 2019.

[107] Q. Li, Y. Bai, and W. Gao, "Improved Initialization Method for Metaheuristic Algorithms: A Novel Search Space View," *IEEE Access*, vol. 9, pp. 121366–121384, 2021.

[108] P. Singh, N. K. Meena, J. Yang, E. Vega-Fuentes, and S. K. Bishnoi, "Multi-criteria decision making monarch butterfly optimization for optimal distributed energy resources mix in distribution networks," *Appl. Energy*, vol. 278, no. September, 2020.

[109] A. Valencia, R. A. Hincapie, and R. A. Gallego, "Optimal location, selection, and operation of battery energy storage systems and renewable distributed generation in medium–low voltage distribution networks," *J. Energy Storage*, vol. 34, no. November 2020, p. 102158, 2021.

[110] S. Barik and D. Das, "Determining the Sizes of Renewable DGs Considering Seasonal Variation of Generation and Load and Their Impact onSystem Load Growth Determining the Sizes of Renewable DGs Considering Seasonal Variation of Generation and Load and Their Impact on System Load," no. August, 2018.

[111] A. Valencia, R. A. Hincapie, and R. A. Gallego, "Optimal location, selection, and

operation of battery energy storage systems and renewable distributed generation in medium–low voltage distribution networks," *J. Energy Storage*, vol. 34, no. August 2020, p. 102158, 2021.

[112] Z. Yang, K. Li, and Q. Niu, "A self-learning TLBO based dynamic economic / environmental dispatch considering multiple plug-in electric vehicle loads," vol. 2, pp. 298–307, 2014.

[113] Almoataz Y. Abdelaziz, "A Multi-objective Optimization for Sizing and Placement of Voltage-controlled Distributed Generation Using Supervised Big Bang–Big Crunch MethodNo Title," *Electr. Power Components Syst.*

[114] S. K. Injeti, V. K. Thunuguntla, and M. Shareef, "Electrical Power and Energy Systems Optimal allocation of capacitor banks in radial distribution systems for minimization of real power loss and maximization of network savings using bio-inspired optimization algorithms," *Int. J. Electr. Power Energy Syst.*, vol. 69, pp. 441–455, 2015.

APPENDIX-A

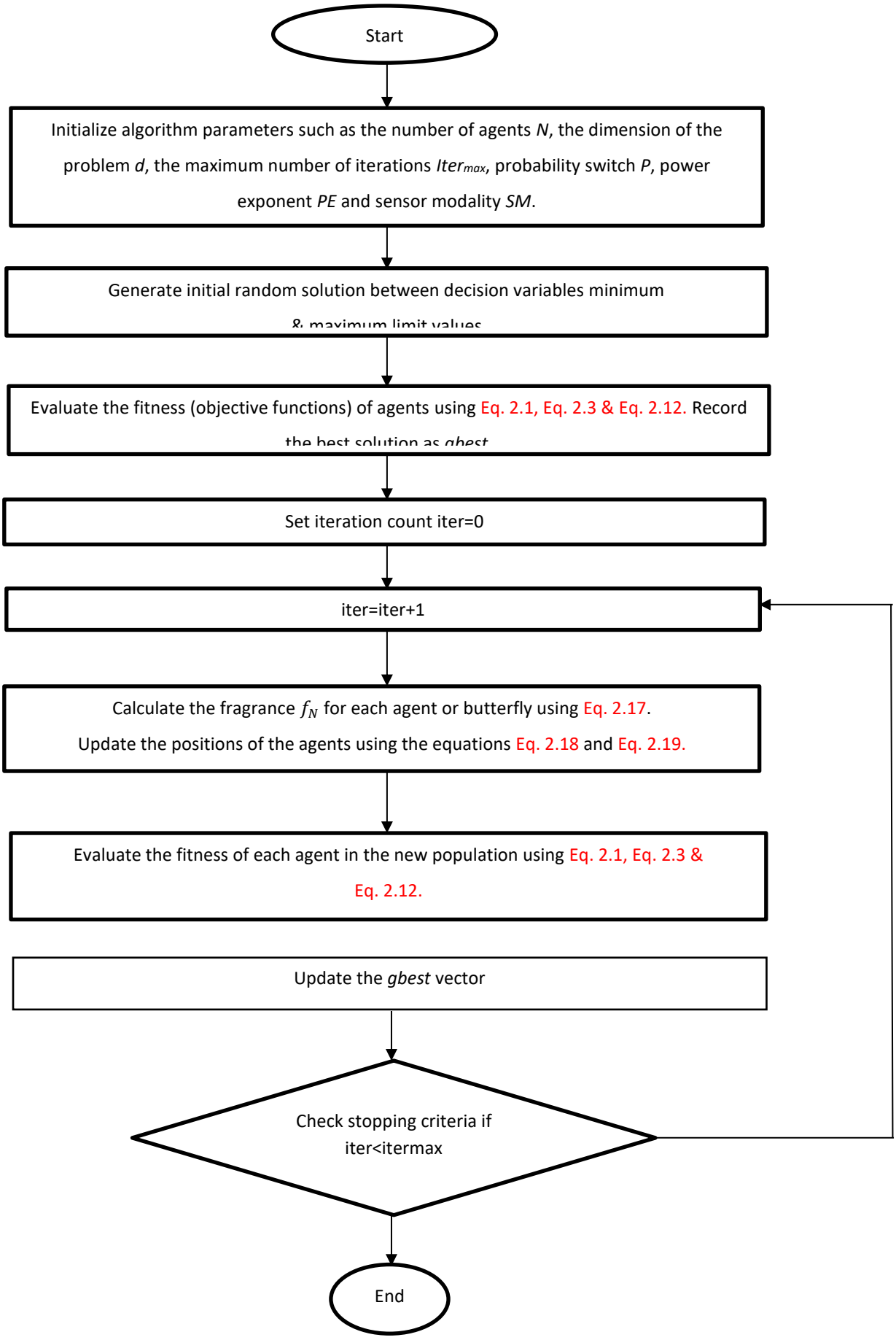
Start
Initialize algorithm parameters such as the number of agents N, the dimension of the problem d, the maximum number of iterations Iter_max, probability switch P, power exponent PE and sensor modality SM.
Generate initial random solution between decision variables minimum & maximum limit values
Evaluate the fitness (objective functions) of agents using Eq. 2.1, Eq. 2.3 & Eq. 2.12. Record the best solution as gbest
Set iteration count iter=0
iter=iter+1
Calculate the fragrance f_N for each agent or butterfly using Eq. 2.17.
Update the positions of the agents using the equations Eq. 2.18 and Eq. 2.19.
Evaluate the fitness of each agent in the new population using Eq. 2.1, Eq. 2.3 & Eq. 2.12.
Update the gbest vector
Check stopping criteria if iter<itermax
End

APPENDIX-B

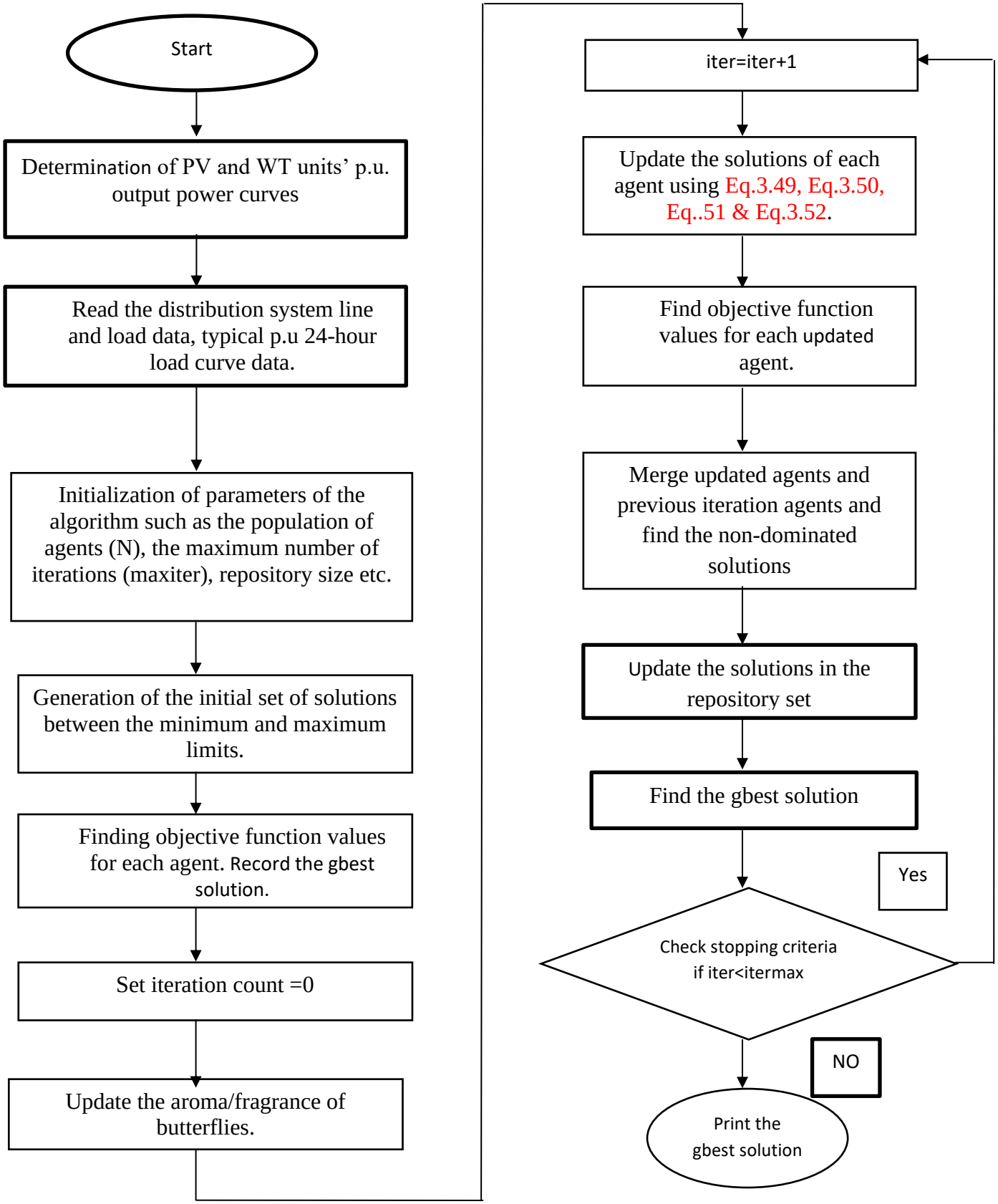
Start
Determination of PV and WT units' p.u. output power curves
Read the distribution system line and load data, typical p.u 24-hour load curve data.
Initialization of parameters of the algorithm such as the population of agents (N), the maximum number of iterations (maxiter), repository size etc.
Generation of the initial set of solutions between the minimum and maximum limits.
Finding objective function values for each agent. Record the gbest solution.
Set iteration count =0
Update the aroma/fragrance of butterflies.
iter=iter+1
Update the solutions of each agent using Eq.3.49, Eq.3.50, Eq..51 & Eq.3.52.
Find objective function values for each updated agent.
Merge updated agents and previous iteration agents and find the non-dominated solutions
Update the solutions in the repository set
Find the gbest solution
Yes
Check stopping criteria if iter<itermax
NO
Print the gbest solution